Monash University, Faculty of engineering
EPFL, Faculté des Sciences et Techniques de l'Ingénieur
IGM-Mechanical Engineering
Department of Chemical Engineering (Monash)
Industrial Energy Systems Laboratory LENI (EPFL)

A Techno Assessment of Different Solvent-based Capture Technologies Within an IGCC-CCS Power-station

2012

Master Project

URECH Jeremy

Professors responsible:	Prof Andrew Hoadley (Monash University) Dr MER François Maréchal (EPFL, LENI)
Engineer responsible:	Laurence Tock (EPFL, LENI)

EIDGENÖ SSISCHE TECHNISCHE HOCHSCHULE LAUSANNE

POLITECNICO FEDERALE DI LOSANNA

SWISS FEDERAL INSTITUTE OF TECHNOLOGY LAUSANNE

ÉCOLE POLYTECHNIQUE FÉDÉRALE DE LAUSANNE

Laboratoire d'Énergétique Industrielle (LENI)

Industrial Energy Systems Laboratory (LENI)

Projet de TdM 30 crédits de Urech Jeremy

A techno-economic assessment of different solvent-based capture technologies within an IGCC-CCS Powerstation

A techno-economic assessment of different solvent-based capture technologies within an IGCC-CCS Powerstation

Context

The CO2CRC is involved in research, development and demonstration of a number of different methods for the large scale capture of carbon dioxide. The Engineering Development Group within the CO2CRC is involved with assessing and optimization the process designs associated with the capture of CO2. The Engineering Development Group recently assessed a number of capture methods for air blown gasification of brown coal.

Objectives

The aim of the project is to assess three different solvent absorption methods for the capture of CO2 from a shifted synthesis gas stream prior to combustion in a gas turbine. The project will build on the framework already developed by Urech for an IGCC powerstation based on black coal. The mass and energy balances will be developed in greater detail with emphasis on the water gas shift reactor and the solvent capture processes. The three solvent capture processes will be:

1. Selexol (glycol-based physical absorbent) generally employed for IGCC
2. MEA (solvent used by Urech in his preliminary study – may be change to MDEA)
3. UNO Mk1 Potassium carbonate solvent

The UNO solvent is an ionic liquid and can operate at much higher temperatures without degradation and thus does not necessarily require the condensation of the H_2O fraction from the synthesis gas. It therefore can be positioned between shift reactors, if a high conversion of H_2 is required.

The CO2CRC economic parameters will be used for the economic assessment. The economic parameters used for optimization will be the Levelised Cost of Electricity and the Cost of CO2 avoided compared to a no capture reference case.

The main project steps are:

- Development and preliminary optimization of Selexol CO2 removal

- Development and preliminary optimization of amine CO2 removal

- Development and preliminary optimization of UNO (post shift) CO2 removal

- Investigation of UNO (between the WGS reactors) for CO2 removal

- Process Integration optimization studies

- Multi-objective economic optimization of best solvent case

- Final economic analysis and oral presentation of results

Lausanne, le 27/07/2012

Validation du projet:

Ingénieur responsable: **Laurence Tock**
laurence.tock@epfl.ch

Enseignant responsable: **Dr. MER F. Maréchal**
(tél: 021/693.35.16) / francois.marechal@epfl.ch

#Project ID: 629

Imprimer cette page Fermer cette page

Abstract

Detailed IGCC coal power-plant thermo models, including different CO_2 capture such as the chemical absorption MDEA and the hot potassium carbonate UNO Mk1, and the physical absorption Selexol are presented in this work. Based on these models, energy integrations are performed and IGCC efficiencies are compared for the cases with and without CO_2 capture. For each CO_2 capture system, different configurations are simulated in order to determine the best solutions in term of efficiency. The IGCC without capture yields an efficiency of 45.02%. The efficiency are closed for the IGCC with the MDEA and Selexol cases with 36.39% for the IGCC with MDEA capture and 36.42% for the IGCC with the Selexol capture system. The IGCC with the UNO process yields the highest efficiency with 37.33%. The UNO absorber can operate at higher temperature than the MDEA and Selexol cases. Therefore the water present in the syngas is not condensed before the absorber, thus the syngas mass-flow sending to the gas turbine is higher and the power produced in the gas turbine is, as well, higher.

An overall Moo optimization is performed on the IGCC with the UNO CO_2 capture system by varying different decision variables in the gasification, WGS, CO_2 capture and gas turbine and cogeneration Rankine steam network units. The air pre-heat in the gas turbine has the most influence on the efficiency. By optimizing the different decision variables, an efficiency of 39.31% is yielded for the IGCC with the UNO CO_2 capture for 90% of capture rate. In the prospect of resolving the best thermo-economic solution, an economic evaluation has to be performed in the future.

Key words: IGCC, CO_2 capture, MDEA, Selexol, UNO Mk1 (hot potassium carbonate), process design, process integration, thermo-modeling

Table of Contents

Abbreviations and Acronyms

Abbreviations

CC	Carbon Capture
CCS	Carbon Capture Storage
CHP	Combined Heat and Power (Cogeneration)
DEPG	Mixture of Dimethyl Ether of Polyethylene Glycol
IGCC	Integrated Gasification Combined Cycle
GCC	Grand Composite Curve
GCL	Gas Cleaning
GHG	Greenhouse Gas
HHV	Higher Heating Value [kJ/kg]
LHV	Lower Heating Value [kJ/kg]
MDEA	N-Methyl diethanolamine (tertiary amine)
MEA	Monoethanolamine
MER	Minimum Energy Requirement
Moo	Multi objectives optimization
ppm	Parts per Million
PSA	Pressure Swing Absorption
S/C	Steam to Carbon ratio
Selexol	Commercially name for DEPG
SG	Syngas: mixture of H_2, CO, CO_2, H_2O, possibly N_2
SNG	Synthetic Natural Gas
PC	Pulverized coal power-plant
UNO	Mk1 hot potassium carbonate solvent
WGS	Water Gas Shift

Roman and Greek Letters

c_p	Specific heat capacity [J/K kg]
d	Diameter [m]
Δh_r^o	Standard molar enthalpy change of reaction [kJ/mol]
$\varepsilon_{chemical}$	Chemical Efficiency
ε	Total Energetic Efficiency
$\dot{E}$	Mechanical Power [kW]
h	Height [m]
Kp	Equilibrium Constant
$\dot{m}$	Mass flow rate [kg/sec]
%mol	Mole Percent
P	Pressure [bar]
T	Temperature [°C or K]
$\dot{Q}$	Thermal Power [kW]
$\dot{V}$	Volumetric flow rate [m^3/sec]
%vol	Volume Percent
%wt	Weight Percent

Chapter 1

Introduction

1.1 Context

The global electricity demand and the greenhouse gas emissions are constantly increasing. Renewable energy is more and more promoted but fossil fuels still supply almost all the energy demand (heat, electricity,…). These fossil resources contribute to more than 80% of the worldwide production. As seen on Figure 1, coal takes an important part with 26.5% of the energy production.

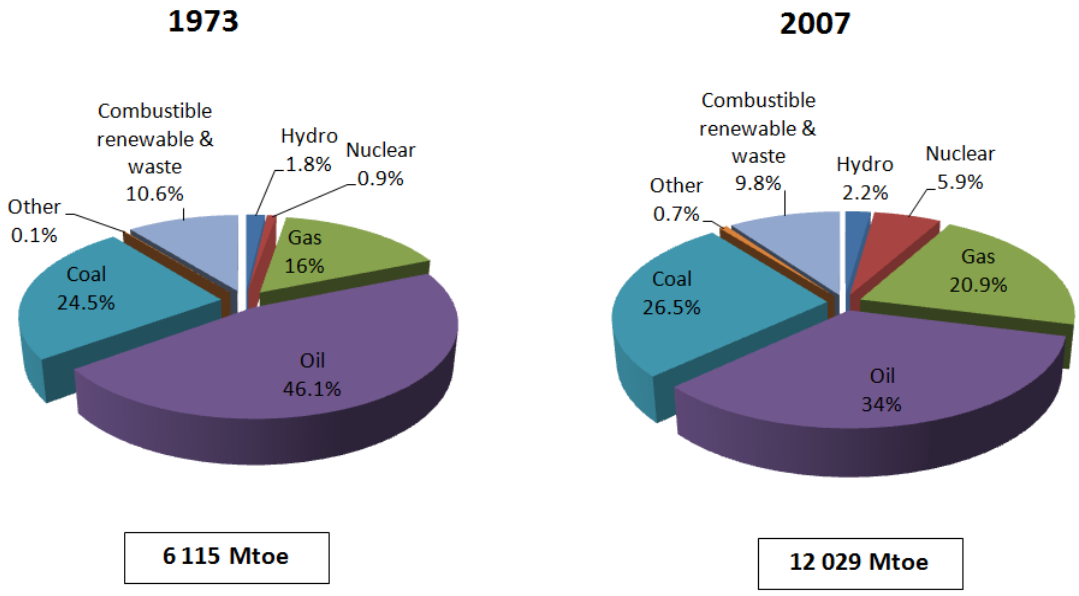

Figure 1: Worldwide energy production [1]

Since fossil fuels are exhausted and emit a lot of greenhouse gases, the world is facing the dual challenge of energy supply security and climate change mitigation. To minimize the impact and reduce the atmospheric CO_2 emissions, engineers are now looking for solutions to retrofit coal power-plants, by increasing the efficiency and reducing the CO_2 emissions.

To reduce the greenhouse gas emissions, engineers are developing several techniques to capture and sequestrate it. But Carbon Capture and Storage (CCS) introduces not only financial penalty by introducing supplementary installations, but also efficiency penalty in term of electricity production. Indeed a high heat demand is required to separate the CO_2 from the gas and power supply to compress the CO_2 for the transport and the sequestration. For this reason, the concept of CCS will become competitive only if new policies limiting the greenhouse gas emissions or

taxing the CO_2 are established. According to the reference [2], the cost of electricity of an IGCC power-plant (Integrated Gasification Combined Cycle) is increased of about 30% and the efficiency is lowered by about 7-12% by adding a CCS unit.

1.2 Objectives

The purpose of this project is to analyze the competitiveness of coal power-plants such as Integrated Gasification Combined Cycle (IGCC) with different solvent techniques to capture the CO_2. An IGCC uses pre-combustion CO_2 capture, which means that the CO_2 is captured before to be burnt in the gas turbine. Simulations are performed to assess the energy penalty of the CO_2 mitigation with different processes.

Three absorption systems are simulated in this study such as the MDEA (monodiethanolamine), the Selexol, and the hot carbonate potassium UNO Mk1 system. The three systems are optimized and compared with conventional power-plants without a CCS system in order to determine the best system for CO_2 capture in term of efficiency.

1.3 Methodology

The methodology that is applied in this project is based on the different models including energy flow and energy integration and performance evaluation following the approach described in [3]. After modeling of the IGCC flowsheet, three different CO_2 capture systems can be simulated separately with the same IGCC basis. For each unit, thermodynamic models are developed and technical performances are analyzed.

The objectives of these thermo-models are to compute the system efficiency as a function of decision variables and to determine the parameters for the process improvement.

The thermodynamic model is divided into two parts. The process flowsheet, representing the transformation from the feedstock to the power production, is developed with the commercial software Aspen Plus [4]. The energy integration, which integrates the results from the process simulation (thermodynamic calculations) such as the minimum energy requirement, the steam network integration or the heat and power integration, uses the software AMPL [5].

The interface for the data transfer between the different models and softwares is managed by the OSMOSE framework developed at the Laboratory of Industrial Energy Systems (LENI) [6]. From the OSMOSE platform, Moo optimization and sensitivity analysis can also be computed. OSMOSE used the MATLAB programming language and allows to pilot all the parameters for different simulation cases without modifying the Aspen files themselves.

1.4 Outline of Report

After introducing the general concepts of CCS and its penalty in Chapter 2, a description of the IGCC coal power-station including the gasification, the Water-Gas-Shift (WGS) and the different solvent CO_2 capture technologies are exposed in chapter 3. Chapter 4 presents the development of the IGCC model on Aspen Plus and the different modeling assumptions. The energy integration principles are discussed in Chapter 5 followed by the definition of the performance indicators. The results of the IGCC simulation with and without CO_2 capture are detailed in Chapter 6, where each capture system results are separately discussed. In Chapter 7, the best cases among each simulation are compared and discussed. Finally, the Chapter 8 presents a Moo optimization performed on the best capture system followed by a final conclusion resuming the whole study in Chapter 9.

Chapter 2

Coal power-plants with CO_2 capture

Before introducing the IGCC coal power-plant, the different CO_2 capture concepts are explained in sub-section 2.1. The penalty and the additional costs introduced by adding CCS are compared with literature references in subsection 2.2.

2.1 CO_2 capture concepts

To capture CO_2 in power-plants and industrial processes, different concepts that are briefly discussed here can be applied. More information can be found in reference [2]. The three main processes for capturing CO_2 described in Figure 2 are:

- Post-combustion CO_2 capture
- Pre-combustion CO_2 capture
- Oxyfuel combustion

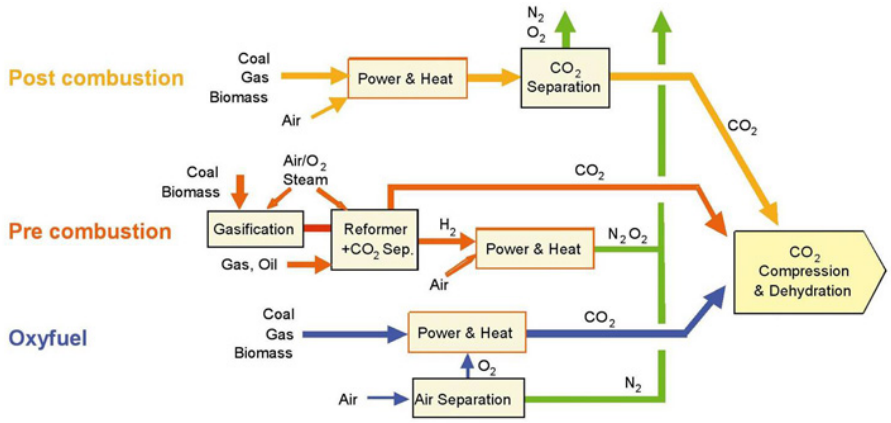

Figure 2: Different types of CCS [2]

Post-combustion CO_2 capture

In the post-combustion concept, the CO_2 is captured from the flue gas after the combustion, by different technologies. In coal power-plants, post-combustion is used typically for pulverized coal systems. An organic solvent like Monoethanolamine (MEA) is used in chemical absorption to capture the low CO_2 partial pressure. Other possible techniques are listed below:

- Absorption process with aqueous alkaline solvent (chemical or physical absorption)
- Adsorption process in which molecular sieves or activated carbons are used in order to adsorb CO_2 (Pressure swing adsorption)
- Membranes, which are used for high CO_2 concentration

Pre-combustion CO_2 capture

In pre-combustion system, the fuel reacts first with oxygen (O_2) or air and/or steam to obtain a synthesis gas (syngas) composed of carbon monoxide (CO) and hydrogen (H_2). The syngas is catalytically shifted by reacting the CO with steam to maximize the H_2 level and to concentrate the carbon species in a Water Gas Shift (WGS) reactor. CO_2 will then get separated by using chemical or physical absorption process. The H_2 rich fuel, which is carbon free, can be combusted in a gas turbine to generate electricity. In coal power-plants, this kind of central is known as an Integrated Gasification Combined Cycle (IGCC).

Oxyfuel combustion

In the oxyfuel combustion process, O_2 is used for the combustion of the primary fuel, in place of air. It produces flue gas with a high CO_2 concentration (>80%) gas, that can be sent to the storage process after H_2O condensation. However, this system requires the upstream separation of O_2 from air, resulting in an O_2 content of 95-99%.

2.2 Energy and cost penalty of CCS

Power-plants with carbon capture system reduce CO_2 emission of 80-90% per kWh. However, carbon capture introduces additional costs with the requirement of new equipments for CO_2 separation and compression. The CO_2 removal requires the addition of two main units: a CO into CO_2 shift conversion unit downstream of the gas dedusting system in case of pre-combustion separation, and a CO_2 separation and compression unit meeting the transport conditions. CO_2 capture increases the cost of electricity by 43-91% for a supercritical PC plant and by 20-78% for an IGCC power-plant [2]. According to the reference [2], the cost of electricity of an IGCC power-plant increases from 0.041-0.061 USD/kWh without CCS to 0.055-0.091 USD/kWh with CCS as illustrated in Table 1. Moreover, the costs of the transport and the storage have to be included. In future, CCS can become competitive only if new policies limiting the greenhouse gas emissions or taxing the CO_2 are established.

Power-plant performances	*Pulverized coal*	*IGCC*
Reference plant without CO_2 capture		
Efficiency	41-45	43.1-47.4
Cost of electricity [US$/kWh]	0.043-0.052	0.041-0.061
Power-plant with CO_2 capture		
Efficiency	30-35	31-40.1
Increased fuel requirement [%]	24-40	14-25
CO_2 captured [kg/kWh]	0.82-0.97	0.67-0.94
CO_2 avoided [kg/kWh]	0.62-0.70	0.59-0.73
% CO_2 avoided	81-88	81-91

Table 1: Performance comparison of CO_2 capture for an IGCC and a pulverized coal power-plant [2]

Chapter 3

Coal power-plants: principles and technologies

Two major technologies exist to produce electricity from coal. The first one is the pulverized coal power-plant (PC power-plant), which burns directly the coal to produce heat and then electricity. The second way consists in the gasification process. The coal is gasified to produce syngas, which is burnt in a gas turbine to produce electricity (IGCC: Integrated gasification combined cycle). Each type of coal power-plant requires a specific CO_2 capture technology.

This work is focused on an IGCC power-plant, which used a pre-combustion carbon capture. The point 3.1 presents the principle of such IGCC power-plants.

3.1 IGCC power-plants

The operating principle of an IGCC is illustrated in Figure 3. First, the crushed coal enters into the gasifier to react with O_2 and steam, leading to the production of the syngas. To obtain pure O_2, an air separation unit (ASU) is required. The syngas leaving the coal gasifier is quenched to 1173 K (900 °C) before being cool down in a convective syngas cooler to produce superheated steam. The syngas is then cleaned up from ashes before sending to the Water Gas Shift (WGS) unit. The syngas is catalytically shifted by reacting the CO with steam to maximize the H_2 level and to concentrate the carbon species (CO_2), which can be later captured.
Then the sulfur (H_2S) is removed in a desulfurization unit and the CO_2 in a CO_2 capture unit. The H_2 rich gas, which is carbon and sulfur free, can be combusted in a gas turbine to generate electricity. The steam generated in the process produces electricity in a Rankine cycle.

The advantages of an IGCC compared to a PC power-plant, regarding the CO_2 capture, are that the CO_2 can be separated at higher partial pressure reducing the amount of required capital. However, this kind of power-plant is more complicated to operate and construct than a PC power-plant [8].

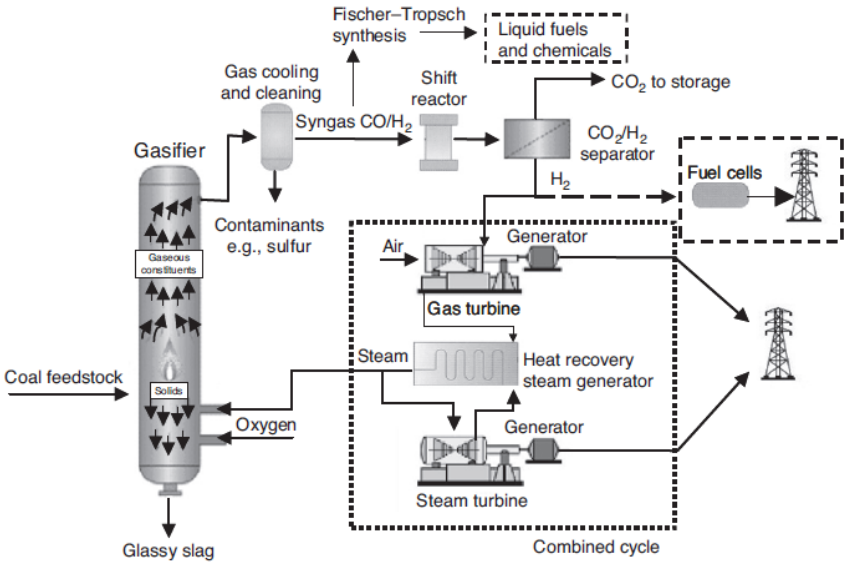

Figure 3: IGCC process [7]

3.2 Coal gasification processes

One important part of the coal power-plant is the gasification process. In this section, the different gasification steps are explained and the reaction equations described.

3.2.1 Gasification process

The coal gasification process is described in Figure 4. After drying, the devolatilization occurs first followed by the gasification.

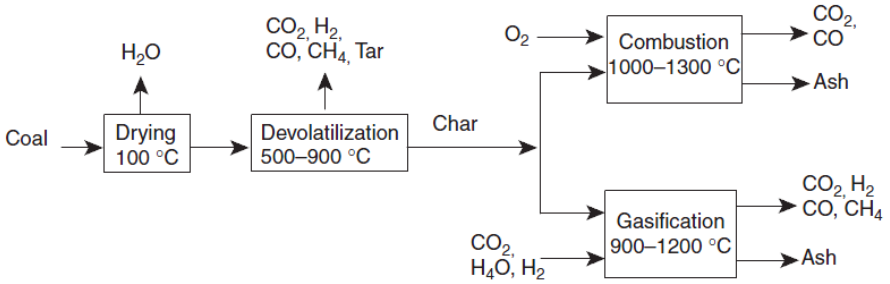

Figure 4: Gasification of the coal [9]

Devolatilization

In a gasifier, the coal undergoes a series of chemical and physical changes. First the coal enters in a step of drying. Afterwards the devolatilization (or pyrolysis) occurs. The labile bounds between the aromatic clusters in coal are cleaved, which creates smaller molecular weight fragments [9].

The light gases and tars are composed of the fragments with low molecular weight, which vaporize and escape from coal particles. The fragments with high molecular weight remain in the coal under typical devolatilization conditions until they reattach to the char lattice.
The heating rate and final temperature affect the volatile yield and its composition. A significant devolatilisation begins at 500°C. The devolatilization gases are composed of CO, CO_2, CH_4, H_2, and H_2O. The amount of tar produced is less if there is a higher coal rank or if the gasifier temperature and pressure are higher.

The solid products leaving the devolatilization state are called char. During the devolatilization process, the porosity of coal changes from 2-20 % to more than 80 % and the reactivity increases according to an increasing nitrogen surface area (10-20 m^2/g -> 200-400 m^2/g).

Combustion and gasification

After the devolatilization stage, char undergoes combustion in an O_2 atmosphere. As shown on Figure 4, a partial combustion occurs in the gasifier. The gasifier needs 30-50 % of O_2 to achieve a complete combustion to CO_2 and H_2O. The principal output products are CO and H_2 but only a fraction of the carbon is completely oxidized to CO_2.

Gasification reaction

The gasification reaction is a conversion of char with CO_2, H_2O, and H_2. The first step in a coal gasification reaction is the exothermic combustion of carbon to CO (eq. 1 and eq. 2) [10]. Then the H_2O reacts with hot carbon to yield CO in an endothermic reaction (eq. 3). These compounds react and produce H_2 and CO or CH_4 and CO_2 (eq. 4). By direct endothermic carbon gasification, H_2 and CO can be produced (eq. 3). In the special case of an entrained-flow gasifier (cf. 3.2.2 gasifier types), the reaction sequence is mostly overlapping and the temperature profile is essentially determined by the mode of the reaction. “The composition of gasification gas is determined by a more or less accurate adjustment of the simultaneous equilibrium among the shift conversion reaction (eq. 4), the methane reforming reaction (eq. 5), and the Boudouard reaction (eq. 6)” [10]. Char properties and the gasification conditions influence the rate of gasification. The coal sulfur content is converted to H_2S under reducing conditions of gasification.

$$C + \frac{1}{2}O_2 \rightleftarrows CO \qquad \Delta h_r^0 = -110.62\left[\frac{kJ}{mol}\right] \qquad \text{(eq. 1)}$$

$$CO + \frac{1}{2}O_2 \rightleftarrows CO_2 \qquad \Delta h_r^0 = -283.15\left[\frac{kJ}{mol}\right] \qquad \text{(eq. 2)}$$

$$C + H_2O \rightleftarrows CO + H_2 \qquad \Delta h_r^0 = +131.38\left[\frac{kJ}{mol}\right] \qquad \text{(eq. 3)}$$

$$CO + H_2O \rightleftarrows CO_2 + H_2 \qquad \Delta h_r^0 = -41.16\left[\frac{kJ}{mol}\right] \qquad \text{(WGS) (eq. 4)}$$

$$CH_4 + H_2O \rightleftarrows CO + 3H_2 \qquad \Delta h_r^0 = +206.28\left[\frac{kJ}{mol}\right] \qquad \text{(eq. 5)}$$

$$C + CO_2 \rightleftarrows 2CO \qquad \Delta h_r^0 = +172.54\left[\frac{kJ}{mol}\right] \qquad \text{(eq. 6)}$$

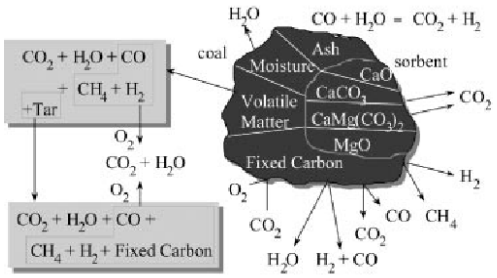

Figure 5: Gasification reactions [10]

3.2.2 Gasifier Types

There are three main gasifier types: *Fixed-bed gasifier, fluidized-bed gasifier and entrained flow gasifier.* Figure 6 illustrates these three gasifier types and detailed explanations follow below.

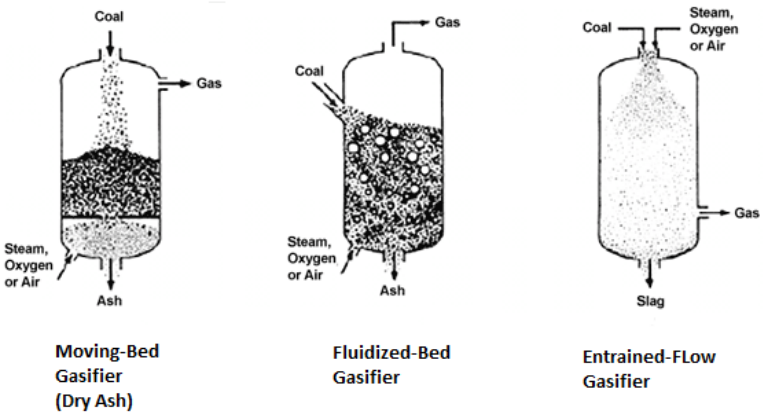

Figure 6: Illustration of different gasifier types [11]

Fixed (moving) bed gasifier

The fixed bed gasifier is a relatively simple technology as illustrated in Figure 6. Coal is introduced at the top of the gasifier and the fuel moves downwards by gravity. Air and steam are introduced at the bottom and move upward through the coal bed. The coal travels downward counter

current to the flow of gases. The flow of hot gases preheats the coal, which yields a heat economy and assures a high carbon conversion.

The coal has to be uniformly sized crushed without tendency to agglomerate to undergo a uniform and stable reaction. Bituminous coal rank, which swells and agglomerates, cannot be used because it produces a bad distribution of both gas and solid flow (failure process).

The process operates typically between 1773 and 2273 K (1500-2000°C) in the combustion zone and between 1 and 3.1 bar [10]. Coal with more than 35 % moisture cannot be used in this type of gasifier.

Fluidized-bed gasifier

The fluidized-bed gasifier was developed to overcome the size limitations and the lack of fuel flexibility of the fixed bed gasifier. In the fluidized reactor, the air and steam flows are sufficient to fluidize the bed of coal, the char and the ashes. “Fluidization occurs when the gas flow velocity lifts the particles causing the gas-solid mixture flow like a fluid” [9].

This gasifier povides a better and more uniform mixing that allows O_2 to react with the devolatilization products. These products undergo thermal craking when reacting with steam and H_2.

This gasifier allows to use caking coal, as well as low quality coals with high ash content. It operates also with a widerange of operating loads without efficiency drop. Fluidized-beds gasifiers also have high heat transfer rates, as well as good solids and gas mixing. The temperature of the fuel gas at the exit of the reaction is high. If cold gas cleaning is used, this high exit temperature consitutes a loss in the heat process. Morever, solids drained by this reactor still have a significant amount of carbon than has to be reused to avoid inefficiencies.

The gasification process occurs typically between 1088 and 1473 K (815 and 1200°C) and between 1 and 40 bars [10].

Entrained flow gasifier

The entrained flow gasifier presented in Figure 6 was developed to improve the gas production flow rate and operates with a wider range of fuel feedstock. Coal is introduced into air or O_2 and steam atmosphere and is heated up to 1300-2000°C (2-3 seconds). Pulverized coal and oxidizing gas flow counter-current at uniformly high temperature, which converts completely all the coal into H_2, CO and CO_2.

A high standard heat recovery system is needed but the product gas is free of methane tars, which simplifies considerably the gas and water treatment. These gasifiers are often applied in conjunction with coal based combined cycle power systems. The gasification process occurs typically between 1523 and 2273 K (1250 and 2000°C) and between 1-40 bar [10].

3.3 Water Gas Shift reaction

IGCC with CO_2 capture requires a shift reaction unit to convert CO into H_2 and CO_2 by adding steam. This step is named Water Gas Shift (WGS). The exothermic reaction, which is catalytic, is described by eq. 7. The catalysts for each temperature are described in point 3.3.1.

$$CO + H_2O \rightleftarrows CO_2 + H_2 \qquad \Delta h_r^0 = -41 \frac{kJ}{mol} \qquad \text{(eq. 7)}$$

The equilibrium conversion is temperature dependent and favored at low temperature for CO conversion, despite a lower reaction rate. For this reason, the reaction is usually divided into two steps. The first one, operating at high temperature between 623 and 823 K (350-550 °C) ([6], [12]), converts the bulk of CO to CO_2 at a relatively fast reaction rate; the second reaction operates at a relatively low temperature between 423 and 623 K (150-350 °C), which increases the conversion. The syngas filters and upstream guard bed protect the catalyst and the temperature is maintained high enough to prevent water condensation.

3.3.1 Water Gas Shift types

In IGCC power-plants, two kinds of WGS designs could be used. Shift converters can be either sour or clean.

Sour Gas Shift

In a sour gas shift reactor, the H_2S removal section is performed with the CO_2 removal unit following the shift reaction unit. Therefore the shift reactor requires to be sulfur tolerant (Co-Mo). Furthermore the COS is directly converted inside the shift reactor (eq. 8).

$$COS + H_2O \rightleftarrows H_2S + CO_2 \qquad \text{(eq. 8)}$$

"The metal oxide in the sour shift catalyst reacts with the sulfur and forms metal sulfide. This sulfide state is the active state of the catalyst" [13]. Figure 7 describes the sour WGS configuration.

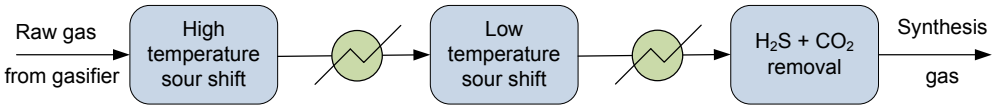

Figure 7: Layout of sour WGS [13]

Clean Gas shift

In clean gas shift reactors, the COS hydrolysis and the H_2S removal have to occur before the WGS reactor. Clean gas shift reactors are cheaper than sour gas shift reactors because they do not have to be sulfur tolerant, but the syngas has to be cooled down before the H_2S removal. This option is not appropriate with quench cooling systems because there is a significant amount of water,

which requires to be condensed, resulting in an energy loss. Figure 8 describes the sour WGS configuration.

Temperature condition: 250-500°C [14].

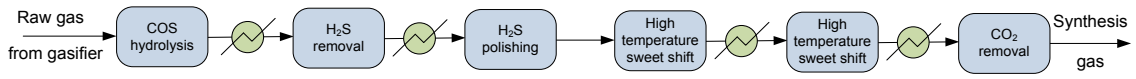

Figure 8: Layout of clean WGS [13]

Catalyst
High Temperature:

- Chromium promoted iron oxide: 613-783 K (340 - 510°C)
- Insensitive to sulfur. Eg Haldor Topsoe SK-201. Sulfur <150 ppm
- Optimal Operation temperature: 593-623 K (320-350°C)

Low Temperature:

- Copper and Zinc: 450-613 K (177-340°C)
- Very sensitive to sulfur

Medium temperature:

- Cobalt-Molybdenum: 563 K (290°C)
- Insensitive to sulfur
- Temperature limit of 1173 K (900°C)

3.3.2 Process description for sour gas shift

The WGS reaction is equilibrium-limited thus the CO concentration in the syngas after the reaction depends on the syngas composition coming from the gasifier and the temperature. The equilibrium constant described below in eq. 9 is a function of temperature. At a given temperature, the higher the conversion for CO is desired the higher amount of steam that has to be added.

$$K_p = \frac{CO_2 * H_2}{CO * H_2O} \qquad \text{(eq. 9)}$$

Steam is added and can be adjusted to reach the desired steam-to-carbon mole ratio (S/C) (between 2 and 3). To achieve a low CO slip, the S/C ratio can be increased or the exit equilibrium decreased by cooling down between two or more sour shift reactors. Figure 9 illustrates the conversion rate with two different S/C ratios. The pressure does not influence the equilibrium constant.

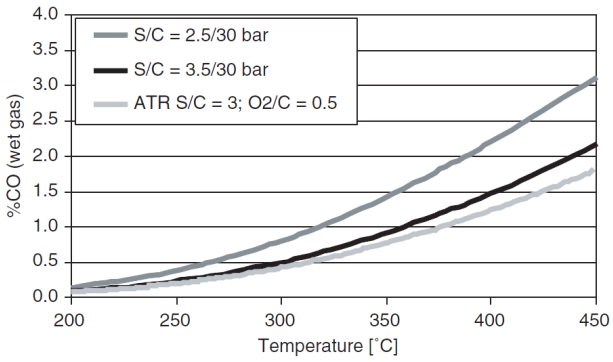

Figure 9: WGS equilibrium curves for different S/C mole ratio [15]

An IGCC power-plant with CO_2 capture requires a high conversion of CO. The WGS is carried out in two reactors in series with a heat exchanger, which cools down the exit gas and recovers the heat.

3.4 CO_2 capture technologies

This section presents the three absorption systems simulated in this study such as the MDEA, the Selexol, and the hot carbonate potassium UNO systems. The differences and advantages of the chemical and physical absorption are described below.

3.4.1 Absorption process

The absorption process consists in using a liquid solvent to remove one or more compounds from a gas stream. In coal power-plants, the absorption process is used to remove sulfur compounds, CO_2 and other impurities such as cyanide or mercury, which are undesirable in the gas turbine and harmful for the environment.

This study will compare three different absorption processes:

- A chemical absorption as the MDEA solvent (Methyl diethanolamine)
- A physical absorption as the Selexol
- A chemical absorption as the hot potassium carbonate solvent UNO Mk1

Process description

The process mainly consists in one absorption and one desorption step as shown in Figure 10. In the absorber, the gas and the liquid interact together counter-currently and the solvent removes one or more components from the syngas (more or less selectively) [10]. Then the solvent laden with the absorbed components is sent in a regeneration system, where the absorbed components are freed of. Finally the lean solvent returns back to the absorber.

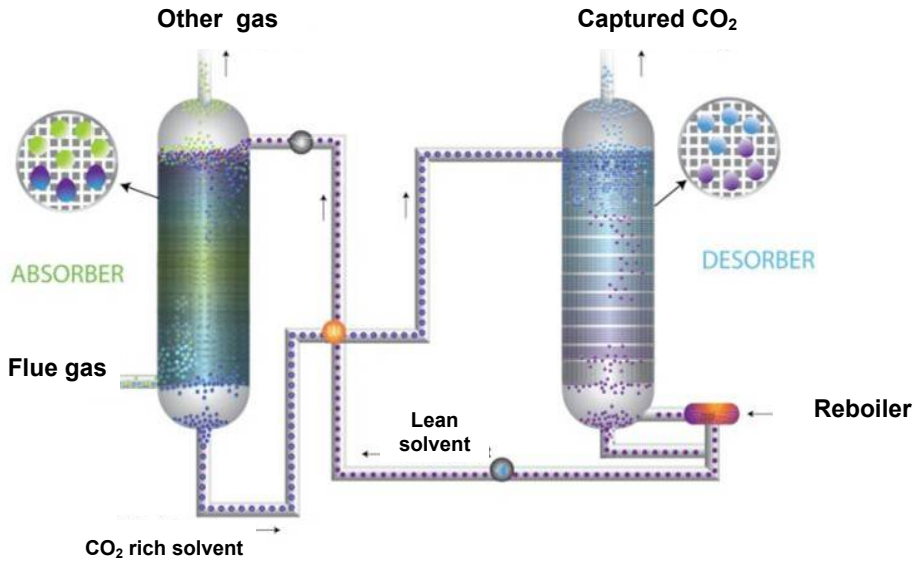

Figure 10: Schematic diagram of solvent CO_2 capture process [16]

Types of regeneration system

Different technologies are available to recover the acid gas and the CO_2 from the rich solvent. The three main methods are listed below:

a. *Flash regeneration*

This method is relatively simple and cheap. The pressurized laden solvent is depressurized in couple of stages to recover the solvent. By reducing the pressure of the solvent, the chemical equilibrium is shifted and the acid gas, as well as the CO_2, could be released. The residual content of the H_2S or CO_2 depends on the pressure of the last stage of flashing. It is often reduced to the vacuum.

b. *Stripping*

The residual content of dissolved components could be removed by inert gas stripping. In case where the residual load of the solvent is very low, the provided inert gas stays completely free of the gas to be removed.

c. *Reboiling*

This method is based on the fact that the solubility of the CO_2 and H_2S decreases sharply by increasing the temperature. A reboiler is used to strip the laden solvent to release the CO_2. The CO_2 gas is then cooled down to condense the water and compressed for the storage. A very high purity could be obtained but the cost is higher because a regeneration column with a reboiler, a condenser and a heat exchanger to heat laden solvent are required.

The principal differences between physical and chemical absorptions are explained below.

Chemical and physical absorption

The two techniques can be distinguished based on the fact that the gas components are dissolved physically or bound chemically to the solvent. As shown in Figure 11, the loading in physical absorption is almost directly proportional to the pressure in the gas phase. For the chemical absorption, the equilibrium line is bowed sharply during the saturation of the chemical active solvent component. For this reason, the absorption capacity is much higher with chemical solvent at low partial pressure and physical absorption shows better result at high partial pressure. Thus less solvent is used to absorb the same amount of CO_2.

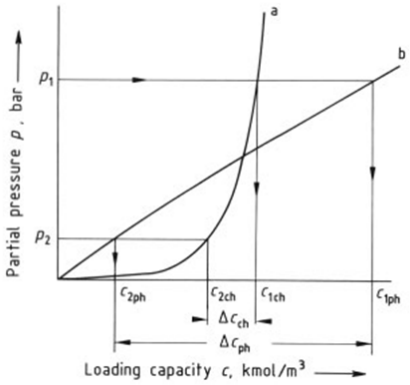

Figure 11: Equilibrium lines for (a) chemical absorption and (b) physical absorption [10]

"Fever trays are generally required for chemical absorption than for physical due to the acceleration of mass transfer by chemical reaction in the liquid phase and the low acid gas equilibrium pressure over the solvent at low loading" [10]. The solvent circulation rate determines the equipment size and thus capital and operating costs.

Chemical absorption is a cheap process but requires low pressure steam or waste heat at sufficiently high temperature. The chemical absorption is also able to reduce the acid gas level to a very low level and shows better result at low partial pressure. In physical absorption, the required electricity amount is relatively low and the cooling water at low temperature is also an advantage. Otherwise the extent of acid gas removal is limited in case of physical absorption.

3.4.2 MDEA capture process

In the MDEA process, the acid components react with an alkanolamine absorption liquid namely MDEA via an exothermic, reversible reaction in a gas/liquid contactor. The acid gas is then stripped from the solvent at low pressure (1-3 bar) or/and high temperature in a regenerator (inlet rich solvent temperature 380-391 K (107-115°C) [17]). A high amine concentration is allowed with MDEA to improve the CO_2 absorption rate and to reduce corrosion potential, because it

contains specific additives. The temperature in desorption column must not be higher than 393-398 K (120-125°C) because of the possible solvent degradation [18].

All amines are reacting with H_2S (hydrogen sulfide) to form sulfide but CO_2 can only react with primary and secondary amines to form carbonate. The reactions with H_2S and CO_2 are described below [10], [19]:

Reaction of amine and water

$$MDEA + H_2O \rightleftarrows MDEAH^+ + OH^- \quad \text{(eq. 10)}$$

Sulfide formation:

$$H_2S + MDEA \rightleftarrows MDEAH^+ + HS^- \quad \text{(eq. 11)}$$

Bicarbonate formation:

$$CO_2 + OH^- \rightleftarrows {HCO_3}^- \quad \text{(eq. 12)}$$

$$MDEA + CO_2 + H_2O \rightleftarrows MDEAH^+ + {HCO_3}^- \quad \text{(eq. 13)}$$

In the sulfide formation equation (Eq. 11), H_2S is thought to react almost instantaneously with the amines by proton transfer [19]. The bicarbonate reaction is slow and the CO_2 reaction can only occur after CO_2 is dissolved in the water via the slow bicarbonate reaction (Eq. 12) [19]. By increasing the temperature and reducing the pressure of the solvent, the chemical equilibrium of the equation is shifted to the left, thus the acid gas is released.

When CO_2 and H_2S are present, the chemical reactions presented below occur in an aqueous solution [19].

$$CO_2 + H_2O \rightleftarrows {HCO_3}^- + H^+ \quad \text{(eq. 14)}$$

$${HCO_3}^- \rightleftarrows {CO_3}^{2-} + H^+ \quad \text{(eq. 15)}$$

$$H_2O \rightleftarrows OH^- + H^+ \quad \text{(eq. 16)}$$

$$MDEAH^+ \rightleftarrows MDEA + H^+ \quad \text{(eq. 17)}$$

$$H_2S \rightleftarrows HS^- + H^+ \quad \text{(eq. 18)}$$

$$HS^- \rightleftarrows S^{2-} + H^+ \quad \text{(eq. 19)}$$

$$CO_2 + H_2O \rightleftarrows H^+ + HCO_3^- \quad \text{(eq. 20)}$$

Two groups of reaction can be distinguished in the liquid phase: the equilibrium reactions and the kinetics reactions. The enhancement of the mass transfer (composition of the different ion species in the liquid phase) is controlled by the chemical reaction. The first kinetics of reaction that has to

be considered are the one of CO_2 hydration (eq. 20); but this reaction may actually be neglected because it is very slow [17].

The second reaction is the bicarbonate reaction (eq. 12). ''This reaction is fast and can enhance mass transfer even when the concentration of the hydroxyl is low and may have significant contribution to observed reaction rate'' [17]. The process operates as described in the point 3.4.1.

3.4.3 Selexol capture process

The Selexol is the commercial name for DEPG, which is a mixture of Dimethyl Ether of Polyethylene Glycol ($CH_3(C_2H_4O)_nCH_3$ (n is between 2 and 9)). This solvent is used to physically absorb H_2S and CO_2. DEPG is non-corrosive, relatively non-toxic, has chemical and thermal stability and requires only carbon steel construction.

Different process configurations are possible depending on the requirement for the level of H_2S-CO_2 selectivity, the depth of H_2S removal and the need of CO_2 capture rate removal. But in all processes, the following steps are occurring (like in the MDEA process) [20]:

- Sour gas absorption
- Solvent regeneration and sour gas recovery
- Solvent recycling

The operating process temperature range from 313 to 253 K (40 to -20°C) covers the most commercial application for the absorber [21]. The pressure and the temperature govern the amount of CO_2 absorbed by the solvent determined by the vapour-liquid equilibrium [22]. The absorption capacity increases with decreasing temperature. ''A decrease in temperature can reduce the circulation rate, thus reducing the operating costs'' [23].

DEPG Characteristics

According to [23], the physical properties for the DEPG are described in Table 2. The difference in solubility of gases in DEPG solvent relative to the CO_2 is described in Table 3.

Solvent	***DEPG***
Process name	Selexol or Coastal AGR
Freezing point [K]	245
Boiling point [K]	548
Maximum operating temperature [K]	448
CO_2 solubility at 298 K (vol CO_2/vol solvent)	3.63

Table 2: DEPG solvent characteristics

	H_2	N_2	O_2	CO	$\mathbf{CO_2}$	H_2S	H_2O
DEPG at 298 K	0.013	-	-	0.028	**1**	8.93	1200

Table 3: Solubilities of different components relative to the CO_2 at 1 atm and 298 K (25°C) in DEPG

Process description

If selective H_2S-CO_2 removal is required, a two-stage process with two absorption and regeneration columns is usually used. As illustrated in Figure 12, the H_2S is selectively absorbed in a first column by a lean solvent and regenerated in a reboiler stripper with steam. The CO_2 is removed in a second absorber, and most usually regenerated by using a series of flashes (until vacuum) or a second reboiler stripper.

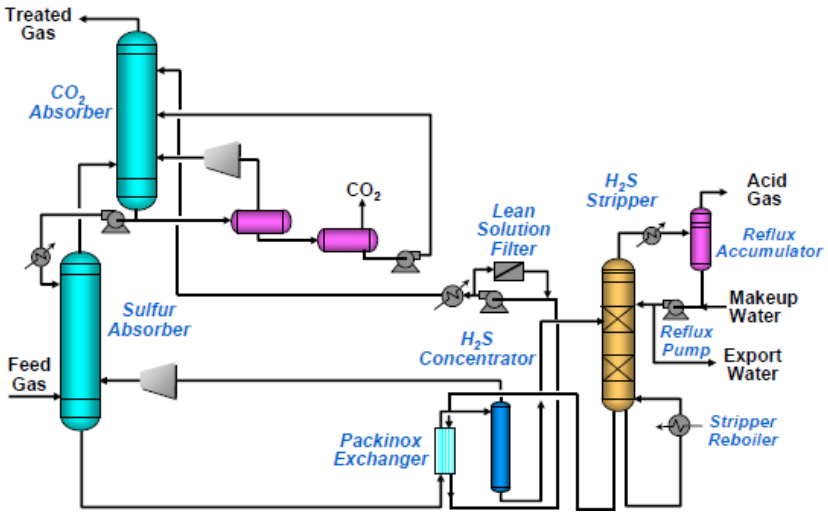

Figure 12: Selexol process for H_2S and CO_2 removal [24]

3.4.4 Hot potassium carbonate capture process

The traditional solvent absorption (MEA-MDEA) operating at low temperature creates thermodynamic inefficiencies and alters the water content in the treated syngas, leading to a reduction of the power production by the gas turbine. With hot potassium carbonate, known internally as the UNO Mk1 process, the process operates at high temperature for the absorption, resulting in improved power output. “The CCS identified potassium carbonate as a strong candidate solvent due to its oxygen and impurity tolerance and low volatility” [16].

The hot potassium carbonate process operates with a potassium carbonate concentration K_2CO_3 varying from 20-30 wt. % in aqueous solution [16]. The CO_2 removal from syngas is one of the

main applications of the process. The CO_2 partial pressure after the conversion process is in the range of 4 -7 bar [10], which is the optimum range for equilibrium behavior of the solution (see curve (e) in Figure 13).

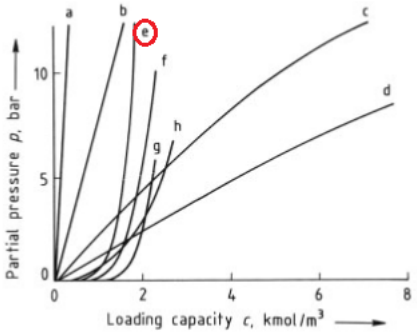

Figure 13: Equilibrium curves of CO_2 in various solvents a) H_2O 303 K (30°C); b) N-methyl-2-pyrrollidone 313 K (40°C); c) Methanol 258 K (- 15°C); d) Methanol 243 K (-30°C); **e) Hot potassium carbonate solution 383 K (110°C);** f) Sulfinol solution 423 K (50°C); g) 2.5 M Diethanolamine solution 423 K (50°C); h) 3 M Amisol DETA solution [10]

Compared to amine based solvents, the used of potassium carbonate has some advantages. The reaction with CO_2 occurring in the process shows an equilibrium behavior. This equilibrium is favorable to absorption even at elevated temperature. Therefore the absorber can process at high temperature and steam is not required to heat the solution until the stripping temperature. Hot potassium carbonate is less toxic and less prone to degradation effects that are commonly seen with amines at high temperature and in presence of O_2 [16]. The investment costs are also lower than with ordinary amine solvent because solvents heat exchangers are not required. On the contrary, the rate of the reaction is low, thus the mass transfer performance is poor. It's one of the biggest challenges to improve the efficiency of this process.

Process description

Figure 14 illustrates the flow diagram of hot potassium process for the absorption of CO_2. The process works like the amine chemical absorption. The single stage process can be modified to reach a higher purity of treated gas by cooling down a part of the solvent to lower the vapor pressure of CO_2. To obtain a CO_2 content of less than 0.5% in the syngas, a two stage design (Figure 14) has to be used. The main solution stream is withdrawn from the stripping column to the reboiler. "Since this portion of solution is regenerated by the total steam supply to the stripping column, it is thoroughly regenerated and is capable of reducing the $C0_2$ content of the gas to a low value. The main solution-stream is fed into the midpoint of the absorber, while the more completely regenerated portion is fed at the top." [25]

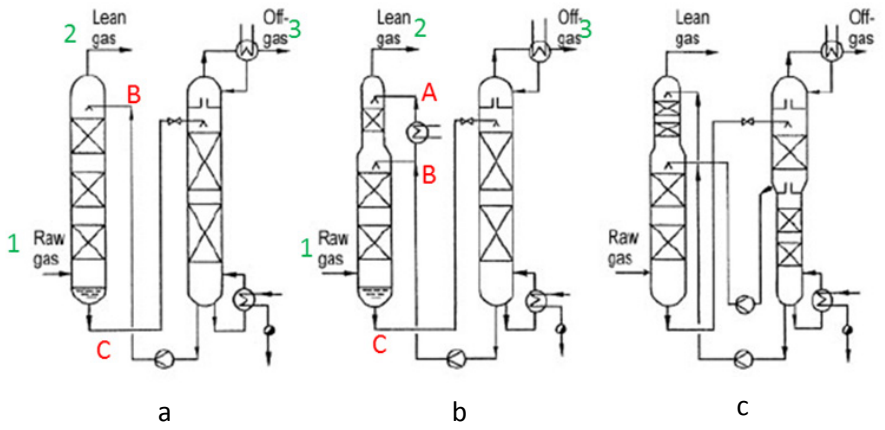

Figure 14: Typical flow diagrams of the hot potassium process for CO_2 removal. a) Single stage; b) Single stage with split flow; c) Two stage process [10]. A) cooled lean solution, B) main lean solution stream, C) rich solution; 1) feed gas, 2) purified gas, 3) acid gas [25]

Hot potassium reaction

The absorption of the CO_2 by the hot potassium follows the next overall reaction:

$$CO_2 + K_2CO_3 + H_2O \rightleftarrows 2KHCO_3 \qquad \text{(eq. 21)}$$

"Since the carbonate and bicarbonate are strong electrolyte, it can be assumed that the metal is present only in the form of reaction K^+ ions and the reaction eq. 21 can be represented as reaction eq. 22" [16].

$$CO_2 + {CO_3}^{2-} + H_2O \rightleftarrows 2{HCO_3}^- \qquad \text{(eq. 22)}$$

Reaction eq. 22 proceeds according to the following sequences of elementary steps [16]:

$$CO_2 + H_2O \rightleftarrows {HCO_3}^- + H^+ \qquad \text{(eq. 23)}$$

$$CO_2 + OH^- \rightleftarrows {HCO_3}^- \qquad \text{(eq. 24)}$$

$$H_2O \rightleftarrows OH^- + H^+ \qquad \text{(eq. 25)}$$

Reactions eq. 23 and eq. 24 are both followed by subsequent instantaneous reactions as follow [16]:

$$H^+ + {CO_3}^{2-} \rightleftarrows {HCO_3}^- \qquad \text{(eq. 26)}$$

$$H_2O + {CO_3}^{2-} \rightleftarrows {HCO_3}^- + OH^- \qquad \text{(eq. 27)}$$

"The reaction sequence eq. 23, eq. 25, eq. 26 are known as the acidic mechanism" [16]. The acidic mechanism can be neglected because it occurs at high pH (pH>8) in industrial absorption. The reactions eq. 25 and eq. 27 are instantaneous then the rate for the absorption of CO_2 into the hot potassium solution is controlled by the reaction eq. 24.

The reactions eq. 28 and eq. 29 show us that the CO_2 concentration, the hydroxyl ion concentration or the temperature influences the rate of the reaction for the CO_2 [25].

$$\text{reaction rate}\left[\frac{\text{g mol}}{(\text{liter})(\text{sec})}\right] = k_{OH}(CO_2)(OH^-) \qquad \text{(eq. 28)}$$

With the value of the second order rate constant K_{OH}:

$$\log_{10} k_{OH} = 13.635 - \frac{2.895}{T} + 0.08\,I \qquad \text{(eq. 29)}$$

Where: T = temperature [K]

I = Ionic strength of the solution

Chapter 4

Process modeling

The IGCC power-plant can be divided in different process units as shown in Figure 15. The crushing part and the ASU are not modeled. It is assumed that pure O_2 is bought. Moreover, the Claus process is not modeled and the H_2S is recovered together with the CO_2.

After the gasification the syngas is quenched, cooled down and ashes are removed in a cyclone inside the cooling unit. In this IGCC modeling, the WGS is placed before the acid gas removal, which means that the WGS has sour WGS reactors. Then three different capture systems are modeled such as the MDEA, the Selexol and the UNO system. Finally the CO_2 free syngas is sent to the gas turbine to produce electricity. The heat available in the process is recovered and sent into a cogeneration Rankine steam cycle. The next sub-section describes in details each unit.

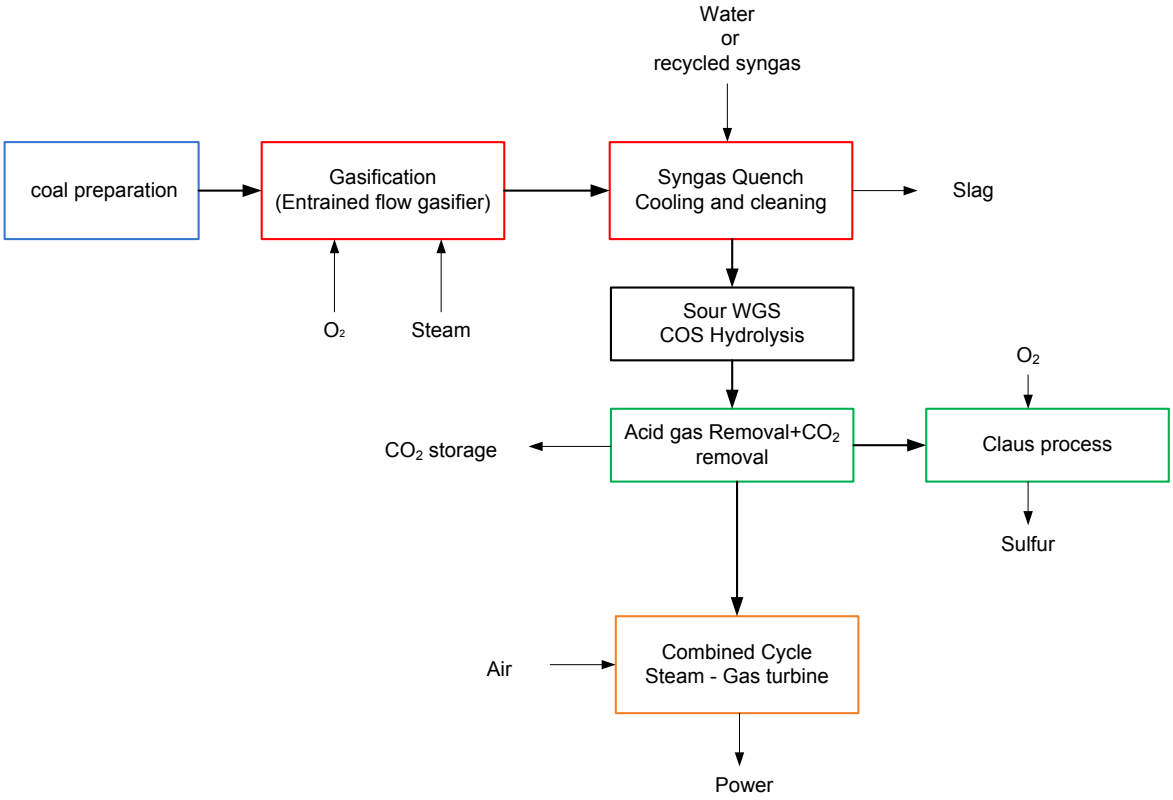

Figure 15: Block flow diagram of an IGCC power-plant

4.1 Feedstock

Coal Illinois#6 is used as feedstock. Table 4 describes the composition of this coal. This study is done based on the lower heating value.

Bituminous Illinois No.6		
Proximate Analysis (wt %) (Note A)		
	As received	**Dry**
Moisture	11.12	0.00
Ash	9.70	10.91
Volatile Matter	34.99	39.37
Fixed Carbon	44.19	49.72
Total	100.00	100.00
Sulfur	2.51	2.82
HHV [MJ/kg]	27.113	30.506
LHV [MJ/kg]	26.151	29.544

Bituminous Illinois No.6		
Ultimate Analysis (wt %)		
	As received	**Dry**
Moisture	11.12	0.00
Carbon	63.75	71.72
Hydrogen	4.05	5.06
Nitrogen	1.25	1.41
Chlorine	0.29	0.33
Sulfur	2.51	2.82
Ash	9.70	10.91
Oxygen	6.88	7.75
Total	100.00	100.00

Table 4: Coal feedstock characteristics [7]

4.2 Gas production

4.2.1 Coal preparation

Usually the coal is simultaneously crushed and dried in the coal mill and then delivered to a surge hopper. The coal is drawn from the surge hoppers and fed through a pressurization lock hopper system to a dense phase pneumatic conveyor and then sent to the gasifier.

In this IGCC power-plant model, the coal is directly sent into the gasifier as received without a drying part. The mass-flow of the coal is 46.05 kg/sec representing a thermal energy of 1200 [MW_{th}] on the lower heating value basis.

4.2.2 Air separation

It is considered that the O_2 is purchased and no on site air separation is included. The required power for importing one kg of O_2 is taken as 1080 kJ/kg O_2 [26] in the efficiency calculation.

One drawback is that the nitrogen, which gets separated, cannot be sent into the turbine like it is shown in Figure 16. The consequence is that the mass-flow (which enters into the turbine) is less important, thus the power production is lower. In this study, more air is sent into the gas turbine to maintain the combustion chamber temperature (detail in sub-section 4.2.7).

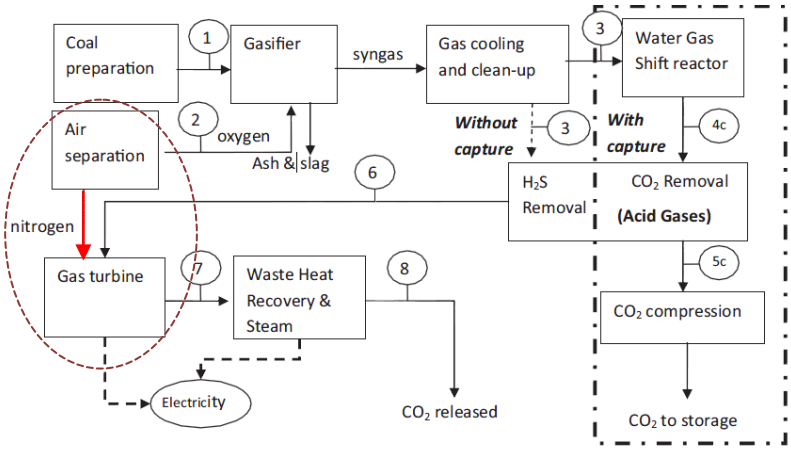

Figure 16: Air separation unit simulated in the study of reference [27]

4.2.3 Gasification

This process is based on an entrained flow gasifier, more especially a shell gasifier which uses dry crushed coal. This kind of gasifier is the most commonly used in coal power-plants. It maximizes the H_2 production potential and facilitates the CO_2 capture.

The reactor is based on equilibrium consideration and atomic balances and all reactions occur at equilibrium. In the Shell gasifier, the gasification occurs at 2273 K (2000°C) and 30 bar.

Model description

The coal is defined as an unconventional component on Aspen Plus (processes with solids). For this reason, it has to be sent first in a Yield reactor assimilated to the pyrolysis. In this yield reactor the splitting of coal into elementary components occurs. Then the C, H, O …, react with the steam and O_2 in the Gibbs reactor to extract the syngas. Figure 17 illustrates this model.

RYield reactor is used to simulate a reactor with a known yield, and does not require reaction stoichiometry and kinetics. Rgibbs reactor minimizes Gibbs free energy, subject to atom balance

constraints. This reactor does not require reaction stoichiometry and can determine phase equilibrium without chemical reaction.

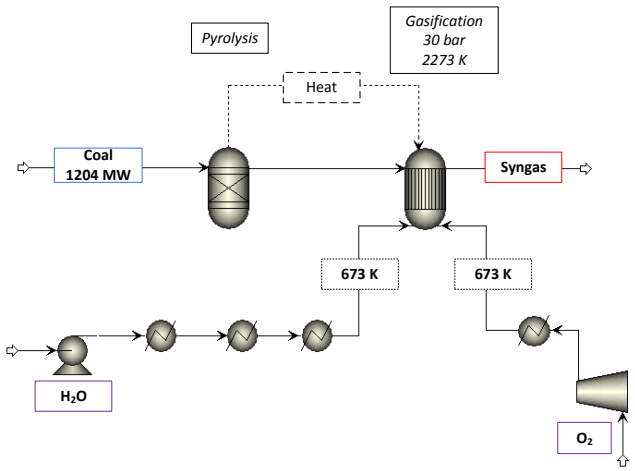

Figure 17: Coal gasifier model in Aspen Plus

4.2.4 Syngas cooling and cleaning

The syngas has first to be quenched before being sent to a convective syngas cooler because of the very high temperature at the outlet of the gasification. Two options can be used in reality:

- Recycle gas quench: the syngas is quenched by a cool recycle gas before entering the convective cooler where superheated steam is generated (see Figure 18).

- Water quench: Water is mixed with the syngas to cool it down. Then the syngas passes through a convective syngas cooler to remove a maximum of energy (see Figure 18).

The syngas is generally quenched to 1173 K (900°C) before the convective cooler. After being cooled down in the convective cooler, it passes through a cyclone and bag filters unit to remove solid particles and tars.

Model description

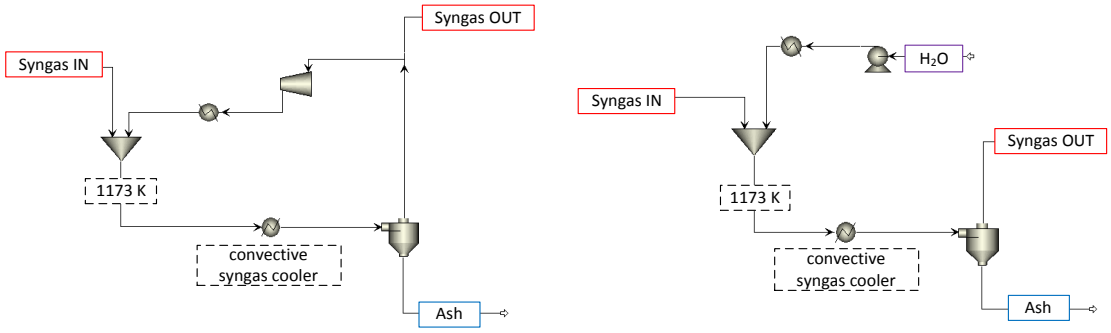

Recycle quench cooling Water quench cooling

Figure 18: Model of recycled quench cooling (left) and water quench cooling (right)

4.2.5 Water gas shift

To enhance the conversion of CO, the reaction takes place in two subsequent reactors. The temperature of the two WGS reactors will be important decision variables and interesting elements. The first reactor has a range of temperatures between 623 and 823 K (350-550 °C) and the second reactor works between 423 and 623 K (150-350 °C). The pressure is the same as the outlet of the gasifier, that is 30 bar. The steam to carbon mole ratio is fixed at 2 but will also constitute a decision variable.

The contribution of the chemical reaction and heat transfer were decoupled in this model. This is done by considering an isothermal reactor rather than an adiabatic one. With this configuration the reaction temperature could be considered as a decision variable. Considering the fact that heat exchange can be performed simultaneously to the reaction, the WGS reactor configuration has been modeled as shown in Figure 19. The WGS heat design is based on reference [28] and more details are explained in Annex I.

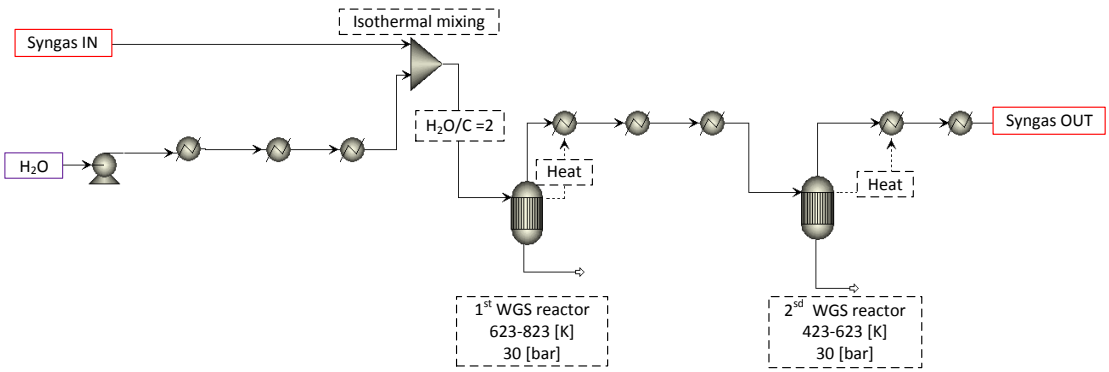

Figure 19: Isothermal WGS reactor model

4.2.6 CO_2 capture

In all three different solvent models (MDEA, Selexol and UNO), the CO_2 and H_2S are removed from the syngas together. According to the reference [23], if the H_2S in the syngas constitutes less than 2-3 % (mole), this flow scheme is usually acceptable. But when H_2S is present in significant amount, thermal regeneration is necessary, which induces supplementary heat demand and increases the cost by adding a second absorber and stripper. To have more rigorous models and simulations, H_2S should be separated in a different unit (absorber and stripper) in a future work.

Modeling a close loop in a flowsheet simulation could be hard work and requires much more time to compute. For this reason, the three solvent units (MDEA, Selexol and UNO) are modeled without solvent recycling (close loop) but integrates a series of calculator and design specifications to match the inlet lean solvent stream with the outlet regenerated solvent stream (mole-flow, temperature, water content, …).

To compress the CO_2 until 100 bar, 4 compression stages (10/30/60/100 bar) are introduced in each CO_2 capture model. Couple of simulations has shown that the efficiency is higher with multiple compressions stages than with only one. After each stage, the stream is cooled down to 313 K (40 °C) and the condensed water is separated and remixed with the lean solvent.

For each solvent model, the capture rate can by imposed by varying the solvent flow rate. For the base case simulation, the capture rate is fixed at 90 %.

MDEA capture process

The syngas coming from the WGS is cooled down and the water is condensed. The syngas is then sent at the bottom of the absorber while the recycle solvent is sprayed at the top. CO_2 and H_2S are removed from the syngas together. The rich solvent is sent to the stripper to be separated from the solvent. Then the condensed water is separated from CO_2 and H_2S and sent back to the stripper. The CO_2 and H_2S are compressed for storage (100 bars) together in this case.

The MDEA model is composed with an absorber operating at 30 bar and around 313 K, and a stripper operating at 2 bar and 380 K (107 °C). The flowsheet is illustrated in Figure 20.

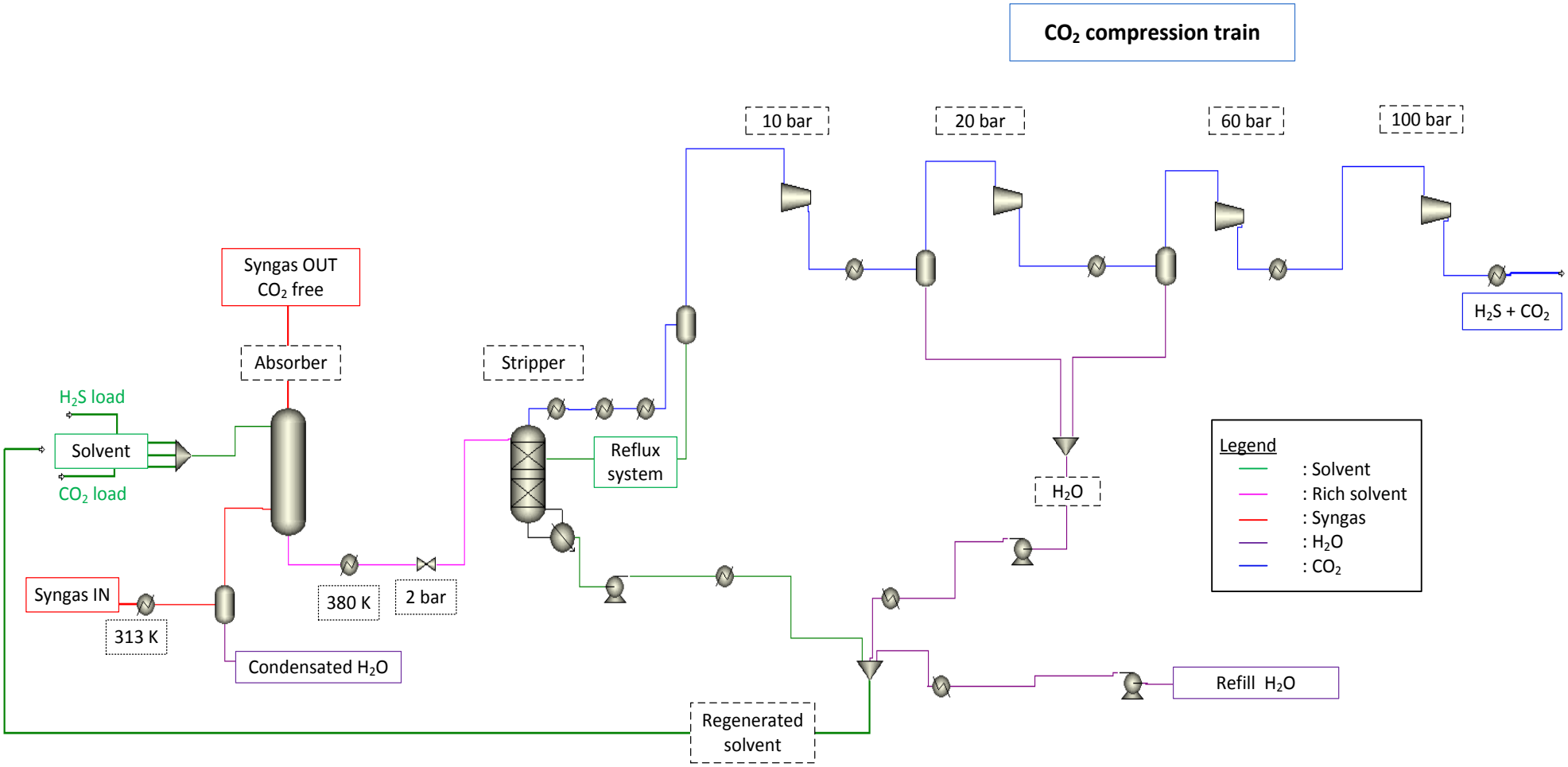

Figure 20: MDEA CO_2 capture model

Three different models are simulated with the MDEA solvent. The first model is operating with 33% wt. fraction of MDEA in aqueous solution, the second with 40 wt. % and the third with 50% wt. MDEA.

Absorber

An equilibrium approach for the absorption is not suitable. Realistic simulations can only be achieved by using a rate-based non-equilibrium model based on the mass and heat transfer between the liquid and the vapour phase. Mass and energy balances are connected by rate-equation across the interface.

The MDEA absorber is based on the reference [29] and received a series of modifications. The ''trays model'' is replaced by a ''packing model'', which is more suitable for high liquid rate, the diameter and the number of stages are adapted.

All the details concerning the modelisation of the absorber and the stripper are attached in Annex II. In this section, only the key parameters are presented.

The main design specifications for the absorber are listed in Table 5 below.

MDEA absorber design parameters	
Type of calculation	Rate-based
Type of column	Packing
Number of stages	14
Diameter [m]	5.5
Height of the absorber column [m]	14
CO_2 lean loading [mole CO_2/mole amine]	0.1
Pressure [bar]	2

Table 5: MDEA (33 wt. %) absorber design parameters

Stripper

The rate-based calculation is more accurate as it takes into account the reaction kinetics. However at the temperature of the stripper, the kinetics don't have a large influence so the equilibrium method is a good approximation. A model was done with rate-based calculation but the simulation was very difficult to converge and the difference on the reboiler heat duty was only 0.2%. For this reason the equilibrium calculation was chosen. Table 6 presents the main stripper characteristic. The mole stripper ratio is defined below in eq.30:

$$mole\ stripper\ ratio = \frac{CO_2}{MDEA} = \frac{HCO_3^-}{MDEA + MDEAH^+} \quad \text{(eq. 30)}$$

MDEA stripper design parameters	
Type of calculation	Equilibrium
Type of column	Packing
Number of stages	10
Diameter [m]	8.1
Height of the stripper column [m]	15
CO_2 lean loading [mole CO_2/mole amine]	0.1
Pressure [bar]	2

Table 6: MDEA stripper design parameters

Solvent with 33%- 40%-50% MDEA

The percentage of MDEA (in wt. %) mixed with water in the solvent mixture has an influence on the capture process. The literature gives a possible operating range between 30-50% wt. MDEA in the lean solvent. The design parameters of the absorber and the stripper have to be adapted for each case. The same approach presented with the first configuration (33% MDEA) is used to design the two other absorbers; the main parameters are listed in Table 7 and Table 8.

Absorber design parameters	*33% MDEA*	*40% MDEA*	*50% MDEA*
Type of calculation	Rate-based	Rate-based	Rate-based
Type of column	Packing	Packing	Packing
Number of stages	14	14	14
Diameter [m]	5.5	5.85	7.25
Height of the absorber column [m]	14	14	14
CO_2 lean loading [mole CO_2/mole amine]	0.1	0.09	0.08
Pressure [bar]	2	2	2

Table 7: Absorber design parameters for different MDEA wt. fraction in the solvent mixture

Stripper design parameters	*33% MDEA*	*40% MDEA*	*50% MDEA*
Type of calculation	Equilibrium	Equilibrium	Equilibrium
Type of column	Packing	Packing	Packing
Number of stages	10	10	10
Diameter [m]	8.1	7.75	7.3
Height of the stripper column [m]	10	10	10
CO_2 lean loading [mole CO_2/mole amine]	0.1	0.09	0.08
Pressure [bar]	2	2	2

Table 8: Stripper design parameters for different MDEA wt. fraction in the solvent mixture

Selexol capture process

The flowsheet is based on reference [21] and is illustrated in Figure 21. The operating process temperature range from 313 to 253 K (40 °C to -20 °C) covers most of the commercial applications [21]. The Australian operation constrains impose a cooling temperature (without using a refrigeration system) of 313 K (40°C). The condensate water is removed from the syngas before being sent in the absorber, which operates at 30 bar.

Although the H_2 solubility in DEPG is much lower than for CO_2 and H_2S, a significant fraction of the H_2 could be absorbed in the column by the solvent. Consequently, the vapor phase stream coming from the first flash (18 bar) drum contains such H_2. To minimize the efficiency lost by not recovering this H_2 content, the vapor is compressed and recycled by sending it back to the absorber. The CO_2 and H_2S are recovered together in two different pressure flash drums (2 and 0.3 bar). The CO_2 is then compressed to 100 bar by four compressor stages.

To close the loop between the outlet regenerated solvent and inlet lean solvent, CO_2, H_2S and water are added to the DEPG lean solvent. Small amount of fresh solvent is refilled to the regenerated solvent to close the mass balance.

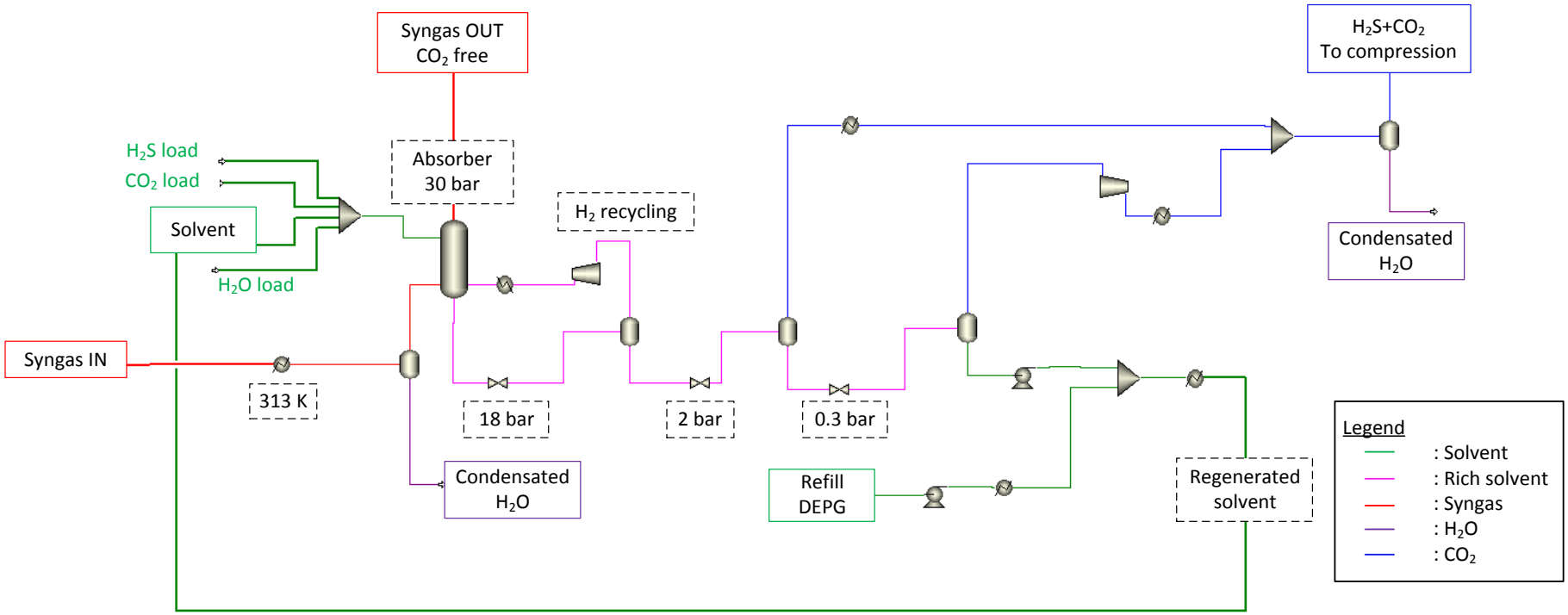

Figure 21: Selexol CO_2 capture model

Absorber

The model for the absorber is based on reference [30], which is in agreement with some previous work [31]. The process model for the absorber is based only on the equilibrium stage distillation, in contrast to the rate-based model, because only the equilibrium stage results are available in the literature. The model uses an average molecular weight of 280 g/mole, corresponding to n=5.3, to represent the DEPG solvent in Aspen Plus data bank. Table 9 presents the main characteristics for the DEPG absorber. The same approach as the MDEA case was applied in order to model the DEPG absorber (explained in Annex II).

DEPG absorber design parameters	
Type of calculation	Equilibrium
Type of column	Packing
Number of stages	16
Diameter [m]	7.9
Height of the absorber column [m]	1
Pressure [bar]	30

Table 9: DEPG absorber design parameters

The CO_2 (eq. 31) and H_2S (eq.32) desorption efficiency and the CO_2 mole lean loading (eq. 33) are defined below and presented in Table 10.

$$CO_2\ desorption\ efficiency = \frac{CO_2\ absorbed}{CO_2\ regenerated\ \ (to\ storage\ )} \quad \text{(eq. 31)}$$

$$H_2S\ desorption\ efficiency\ = \frac{H_2S\ absorbed}{H_2S\ regenerated\ \ (to\ storage\ )} \quad \text{(eq. 32)}$$

$$CO_2\ mole\ lean\ loading\ = \frac{CO_2(moleflow\ \ inlet\ )}{DEPG\ (moleflow\ \ inlet\ )} \quad \text{(eq. 33)}$$

Absorber result at 40°C	
Rate of capture [%]	90
Lean solvent mass-flow [kmol DEPG/kmol CO_2]	3.48
CO_2 desorption efficiency [%]	97.7
H_2S desorption efficiency [%]	67.3
CO_2 lean loading [-]	0.005
Lean solvent mass-flow [kmol DEPG/kmol CO_2]	3.48
Pressure [bar]	30

Table 10: DEPG regeneration simulation results

Hot potassium carbonate UNO capture process

Potassium carbonate K_2CO_3 is at a concentration of 30% wt. in an aqueous solution. The process operates in the same way as the MDEA and is illustrated in Figure 22. With the potassium carbonate solvent, the absorber can operate at higher temperature. Therefore, the water present in the syngas is not condensed before being sent to the absorber.

If the absorber is operating at high temperature, more water is released with the syngas. For this reason, the system has to be refilled with water in the system to guaranty the mass-flow balance. But at lower operating temperature, the water present in the syngas is absorbed with the solvent and some water has to be removed from the system after the stripper to maintain the mass-balance (close loop).

The same approach as for the MDEA case was applied for modeling of the UNO absorber and stripper (explained in Annex II).

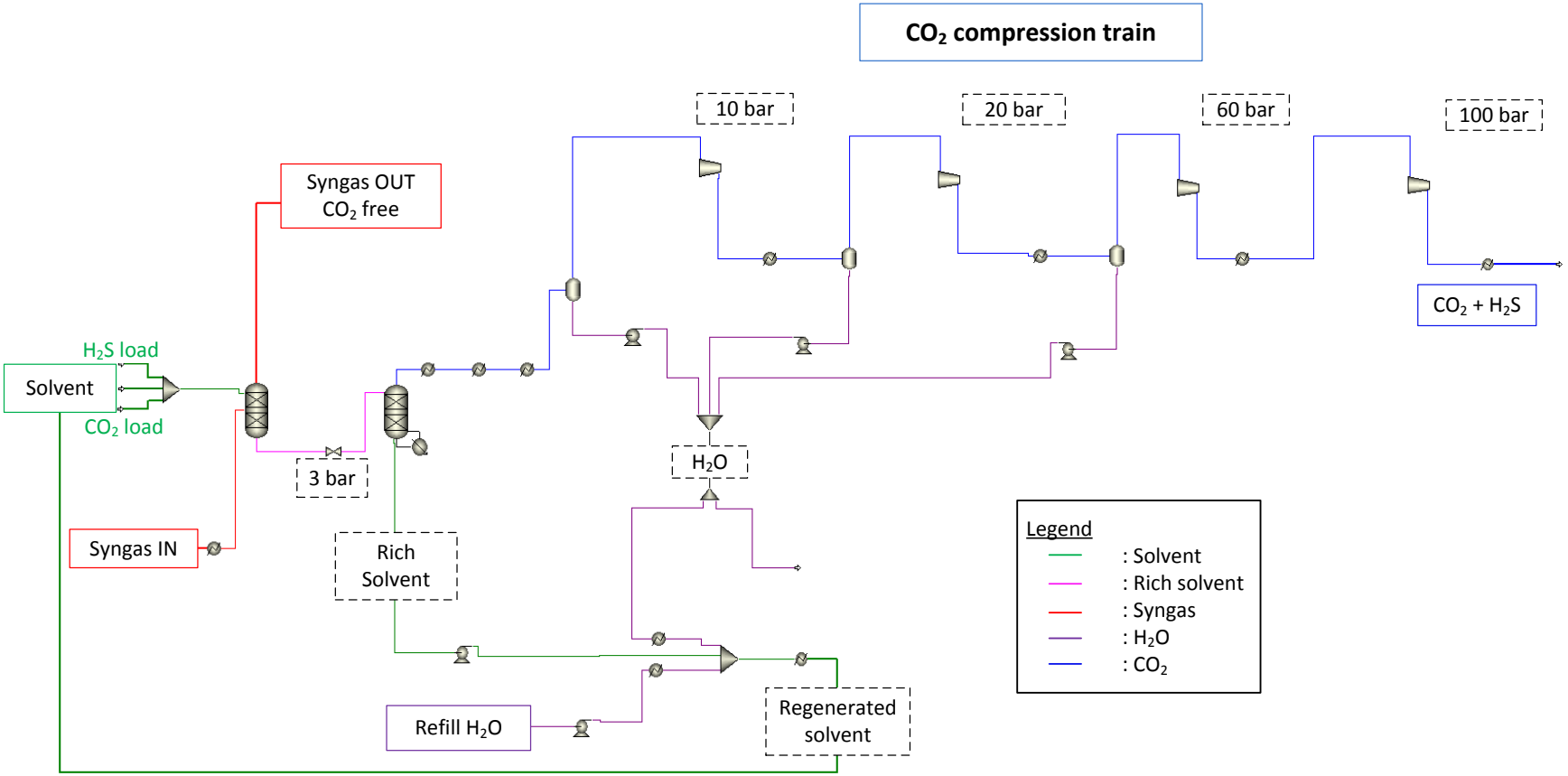

Figure 22: Hot potassium carbonate UNO CO_2 model

Absorber and stripper

The absorber and stripper model is based on Trent Harkin work from the CO_2CRC in Melbourne and on reference [32] for the VLE regressed data process. The mole ratio of solvent recovered in the stripper is imposed to be 0.2. The stripper mole ratio is defined in eq.34:

$$Stripper\ mole\ ratio = \frac{CO_2}{K_2CO_3} = HCO_3^-/K^+ = 0.2 \qquad \text{(eq. 34)}$$

The absorber operates from 393K to 493K at the pressure of the syngas, that is 30 bar. With the UNO process, the rich solvent doesn't have to be reheated before entering into the stripper. The rich solvent is flashed to 3 bar before being sent to the stripper. The CO_2 absorption is not modelled by an equilibrium approach but can only be achieved using a rate-based non-equilibrium model as it is done in this study. All the design parameters have been adapted with the same methodology than the MDEA and Selexol systems. Table 11 resumes the design parameters for the absorber and the stripper.

UNO parameters	*Absorber*	*Stripper*
Type of calculation	Rate-based	Rate-based
Type of column	Rate-based	Rate-based
Number of stages	10	10
Diameter [m]	5.45	7.91
Height of the column [m]	15	15
CO_2 lean loading [mole CO_2/mole K_2CO_3]	0.2	0.2
Pressure [bar]	30	3

Table 11: UNO absorber and stripper characteristics

4.2.7 *Combined cycle gas turbine*

The H_2-rich gas, which is CO_2 free, can be sent into the gas turbine. The gas turbine exhaust stream is sent to a heat recovery steam generator where superheated steam is produced. This steam is sent to a steam turbine to produce electricity.

Gas turbine

The H_2O content before the expender must not exceed 15 % mole fraction. For this reason the syngas is first cooled down to condense the right amount of water in order to respect this limit.

The syngas is preheated until 773 K (500°C). Then it is sent to the combustion chamber with compressed air. The air could be also preheated before entering the combustion chamber. Therefore more air is necessary to reach the combustion temperature, thus the mass-flow is bigger and more power could be produced in the expander. The combustion occurs at 1568 K (1295°C) and the flue gas is sent in an expander with 90% efficiency and then cooled down to 313 K (40°C). The combustion chamber does not operate at stoichiometry combustion. Indeed more air is sent into the combustion chamber, in order to maintain the combustion temperature at 1568 K.

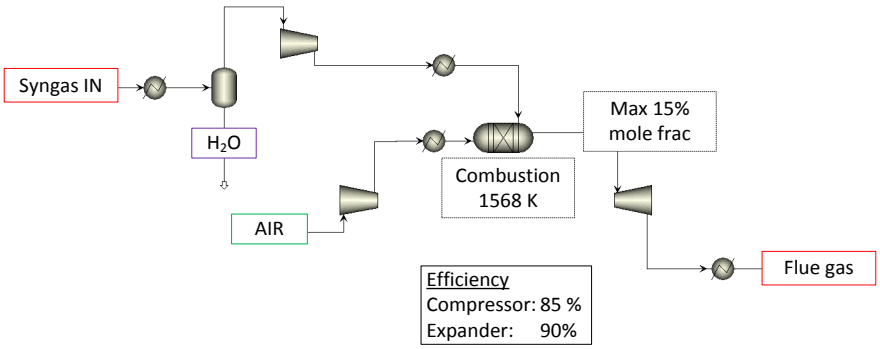

Figure 23: Gas turbine model

Steam combined cycle

The excess of heat is recovered into a Rankine cycle for power production. The modelisation of the cogeneration steam cycle is performed by introducing three pressure levels HP/MP/LP, which could be optimized to get a best efficiency.

The HP pressure stage production is imposed at 125 bar. Then the pressure for the MP, LP drawoff stage and the condensation stage are optimized for each case.

This part is not designed in ASPEN PLUS but rather in the energy integration.

4.3 Main modeling assumptions

The main modeling assumptions for the base cases are described in Table 12. The same IGCC configuration is taken for the three solvent simulations.

Design parameters	***Value***
Coal mass flow [MW]	1200
Gasification temperature [K]	2273
Gasification pressure [bar]	30
Type of quench cooling	Recycle quench
WGS: steam/water ratio [-]	2
WGS: 1st reactor temperature [K]	673
WGS: 2^{sd} reactor temperature [K]	527
GT: pre-heat syngas temperature [K]	773
GT: pre-heat air before combustion chamber [K]	No pre-heat
GT: combustion temperature [K]	1568
Process: cooling temperature [K]	313
Process: pump efficiency (isentropic) [-]	0.8
Process: compressor efficiency (isentropic) [-]	0.85
Process: Expander efficiency (isentropic) [-]	0.9

Table 12: Characteristic parameters for base cases simulations

Remarks: Some simulations with the water quench cooling unit were performed, but the efficiency was lower with each solvent. These results were predictable, because some heat is lost in the heating of the quench water. For all the next simulations the recycle cooling quench will be used.

Chapter 5

Energy integration

5.1 Energy integration concept

The energy integration, also known as Pinch analysis method, provides information about the different heat demands in the system. It minimizes the energy consumption of the process by calculating thermodynamically feasible energy targets and optimizing heat recovery systems, energy supply methods and operating conditions. This method allows the modeling of integrated heat exchange system without imposing a heat exchange network structure. The hot and the cold streams of the process are identified from the energy flow model.

The process integration method is typically applied in two major steps [28]. The first step calculates the minimum energy requirement (MER) by identifying the possible energy recovery from the hot and the cold streams. The second step is the implementation of the heat exchange network to reach the targeted energy recovery by satisfying the utility requirement.

The definition of a list of cold and hot streams allows to draw as function of the temperature the 'hot composite curve', which represents the heat available in the process, and the 'cold composite curve', which represents the heat required in the process. The maximum heat recovery can be computed by considering that the heat exchange is technically feasible if the temperature difference between the hot and the cold composite is superior to a pre-defined ΔT_{min} (minimum approach temperature). The physical properties of the stream determine the different $\Delta T_{min}/2$ as illustrated in Table 13 [28]. The pinch point is characterized by the minimal temperature difference between the hot and the cold composite curve.

The Grand Composite Curve (GCC) represents the difference between the enthalpy of the hot and the cold curve for each temperature; the pinch point appears where the curve touches the temperature axis. "Globally the process needs energy above the pinch point (heat sink) and releases energy (heat source) below it" [33]. More details are explained in reference [28].

State	*Phase change*	*Liquid*	*Gas*	*Heat exchanger*
$\Delta T_{min}/2$	2	4	8	20

Table 13: Different assumptions for the ΔT_{min}

There are three heuristic rules that must be respected:

- No cold utility used above the pinch point
- No hot utility used below the pinch point
- No exchanger can transfer heat across the pinch point

The list of all the hot and the cold streams, defined from the Aspen Plus [4] flowsheet model calculation, is introduced in the energy integration performed by the software AMPL [5] and the pinch analysis is computed based on this heat stream data.

The steam network and the mechanical power, which define the electricity export and import, respectively, in the system, are resulted by the overall energy model of the process. The problem resolved by Ampl is a minimization of the input mechanical power. Figure 24 illustrates the MER for the UNO process operating at 413 K (140 °C). Only a cold utility is required in this case. Figure 25 presents the integrated composite curve including the cold utility and the steam network. The efficiency improvement, achieved by adding the steam network system, can be observed by the reduction of the area between the hot and the cold curve in Figure 25.

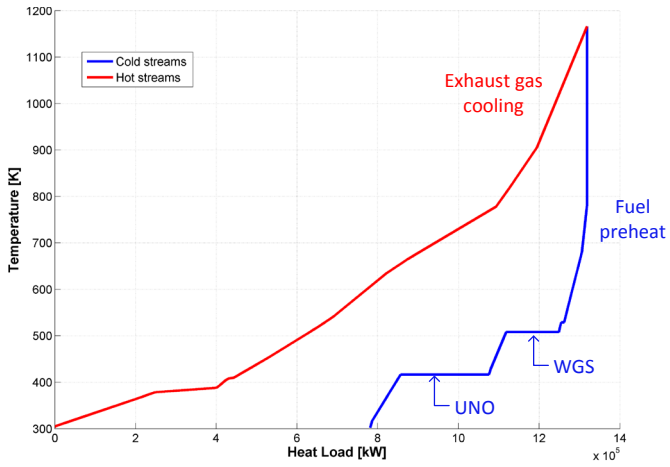

Figure 24: MER of the IGCC process with the UNO CO_2 capture operating at 413 K

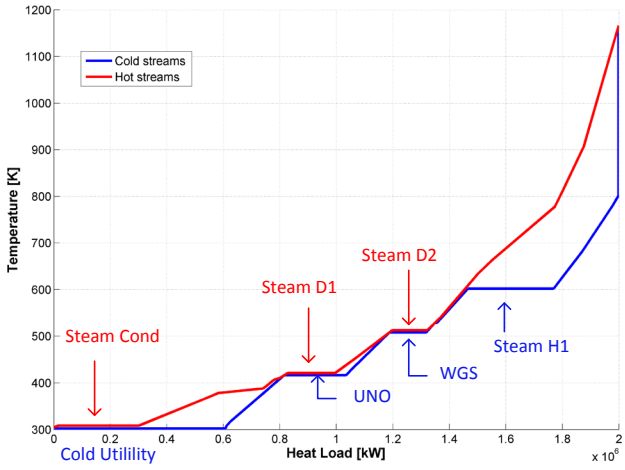

Figure 25: Integrated composite curve of the IGCC with the UNO CO_2 capture operating at 413 K

5.2 Performance indicators

Performance indicators are measurable quantities used to quantify the "quality" of a system. The overall process performance is defined as the global energy efficiency, given by the eq. 35:

$$\varepsilon = \frac{Net\ power\ production}{Energy\ \ coal}$$

$$= \frac{Power\ \ produced\ \ (turbine\ ) - Power\ \ consummed\ \ (compressor\ ,pump\ )}{fuel\ \ entering\ \ \ heating\ \ value\ * \dot{m}_{coal\ \ inlet}}$$

$$= \frac{\dot{E}^{-}_{GT} + \dot{E}^{-}_{steam} - (\dot{E}^{+}_{O_2} + \dot{E}^{+}_{gasification} + \dot{E}^{+}_{quench} + \dot{E}^{+}_{WGSpump} + \dot{E}^{+}_{CO_2 capture})}{\dot{m}_{coal} * \Delta h^{o}_{coal}} \qquad \text{(eq. 35)}$$

In addition, the chemical conversion is introduced and given by the eq. 36:

$$\varepsilon_{chemical} = \frac{Energy\ \ syngas\ \ (after\ \ gasifier\ )}{Energy\ \ coal} = \frac{\dot{m}_{syngas\ \ \ gasifier\ } * \Delta h^{o}_{syngas}}{\dot{m}_{coal\ \ inlet\ } * \Delta h^{o}_{coal}} \qquad \text{(eq. 36)}$$

Chapter 6

Performance integration

The simulated cases without capture and with the three different CO_2 capture technologies (MDEA, Selexol and UNO) are referenced in the next Table 14 to Table 17. Each case will be explained in details separately in different sub-sections and referred to these tables.

In this section, the Moo optimization is performed only on the capture process to compare each solvent with the same IGCC base (gasification, cooling, WGS units). Overall Moo optimization on the all IGCC process is performed in section 7 for the best solvent case.

For the cases with CCS, design specification operates on the mass-flow of each solvent to reach 90% of CO_2 capture.

Without CO_2 capture	***Description***
NoCC-Case 1	With WGS- no condensation
NoCC-Case 2	With WGS – Full condensation (cool down syngas to 40°C)
NoCC-Case 3	With WGS – Partial condensation
NoCC-Case 4	No WGS – No condensation

Table 14: Description of the studied IGCC cases without CO_2 capture

With CO_2 Capture: MDEA process	***Description***
MDEA- Case 1.1 (33%)	33 wt. % MDEA Syngas temperature: 313 K Solvent temperature: 317 K
MDEA- Case 1.2 (33%)	33 wt. % MDEA Syngas temperature: 338 K Solvent temperature: 338 K
MDEA- Case 2.1 (40%)	40 wt. % MDEA Syngas temperature: 313 K Solvent temperature: 317 K
MDEA- Case 3.1 (50%)	50 wt. % MDEA Syngas temperature: 313 K Solvent temperature: 317 K

Table 15: Description of the studied IGCC cases with the MDEA CO_2 capture

With CO_2 Capture: SELEXOL process	*Description*
Selexol-Case 1.1	Solvent temperature IN: 313 [K] Syngas temperature IN: 313 [K]
Selexol-Case 1.2	Solvent temperature IN: 324 [K] Syngas temperature IN: 324 [K]
Selexol-Case 2	Solvent temperature IN: 313 [K] Syngas temperature IN: 313 [K] Optimization of the steam network

Table 16: Description of the studied IGCC cases with the SELEXOL CO_2 capture

With CO_2 Capture: UNO process	*Description*
UNO-Case 1.1	Solvent temperature IN: 413 [K] Syngas temperature IN: 413 [K]
UNO-Case1. 2	Solvent temperature IN: 433 [K] Syngas temperature IN: 433 [K]
UNO-Case 1.3	Solvent temperature IN: 493 [K] Syngas temperature IN: 493 [K]
UNO-Case 1.4	Solvent temperature IN: 393 [K] Syngas temperature IN: 393 [K]
UNO-Case 1.5	CO_2 recompression variant (Best case at 413 K)
UNO-Opticase 2.1	Optimized case 70% capture rate (max efficiency)
UNO-Opticase 2.2	Optimized case 98% capture rate (max capture)
UNO-Opticase 2.3	Optimized case 90% CO_2 capture

Table 17: Description of the studied IGCC cases with the UNO CO_2 capture

6.1 IGCC without CO_2 capture

Different configurations are compared for the case without capture (mentioned in Table 14) as illustrated in Figure 26. The water content before the expender must not exceed 15% mole. For this reason, the flue gas has to be cooled down to condense the adequate amount of water. To measure the influence of this parameter, different cases are simulated below. In the three first cases, the syngas from the gasifier is sent to the WGS unit before being burnt in the gas turbine. In the NoCC-case 1, no water is condensed; in the ''NoCC-case 2'', all the water is condensed by cooling down the syngas until 313 K (40°C) before the combustion chamber; in the ''NoCC-case 3''case, the syngas is cooled down until the maximum water content before entering the expander is reached. In the ''NoCC-case 4'', the syngas is directly sent to the gas turbine without going through the WGS. The water content is low enough not to exceed the maximum water content.

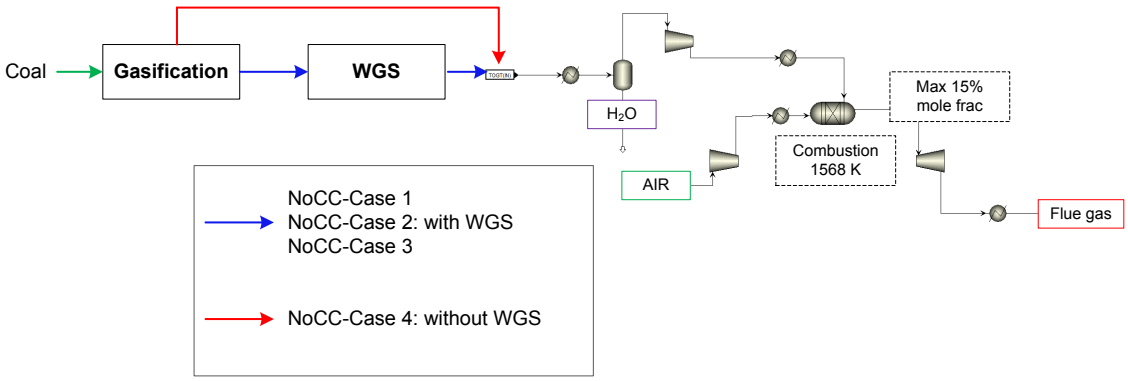

Figure 26: Description of the studied IGCC cases without CO_2 capture

Results

Table 18 presents the simulation results for the four cases without capture. For each case, the steam network has been optimized. The first case (NoCC-case 1) yields the best efficiency but the water content condition is not respected. Therefore, this case is not realistic. The best feasible efficiency of 45% is reached for the case with partial condensation (NoCC-Case 3) and for the case without using a WGS unit (NoCC-case 4), which gets 44.6 % efficiency.

Cases	*NoCC-Case 1*	*NoCC-Case 2*	*NoCC-Case 3*	*NoCC-Case 4*	*Reference without CC*[1]
	WGS no condensation	WGS Full condensation	WGS Partial condensation	No WGS No condensation	-
Efficiency [%]	47.1	42.8	45	44.6	43.1 - 47
Water content (Before expander [mole%]	19.1 Max 15 % mol ⚠	0.27 ✔	14.9 ✔	4.6 ✔	-

Table 18: Efficiency of the studied IGCC cases without CO_2 capture

Figure 27 compares the performance for each case. The green column represents the net electricity produced by the power-plant and the blue the power consumed in the process. The sum of the green and blue columns is the total power produced by the gas turbine and the steam network (cogeneration Rankine cycle). The net electricity generated by the steam network and the gas turbine are illustrated by the red and purple column in negative side, respectively.

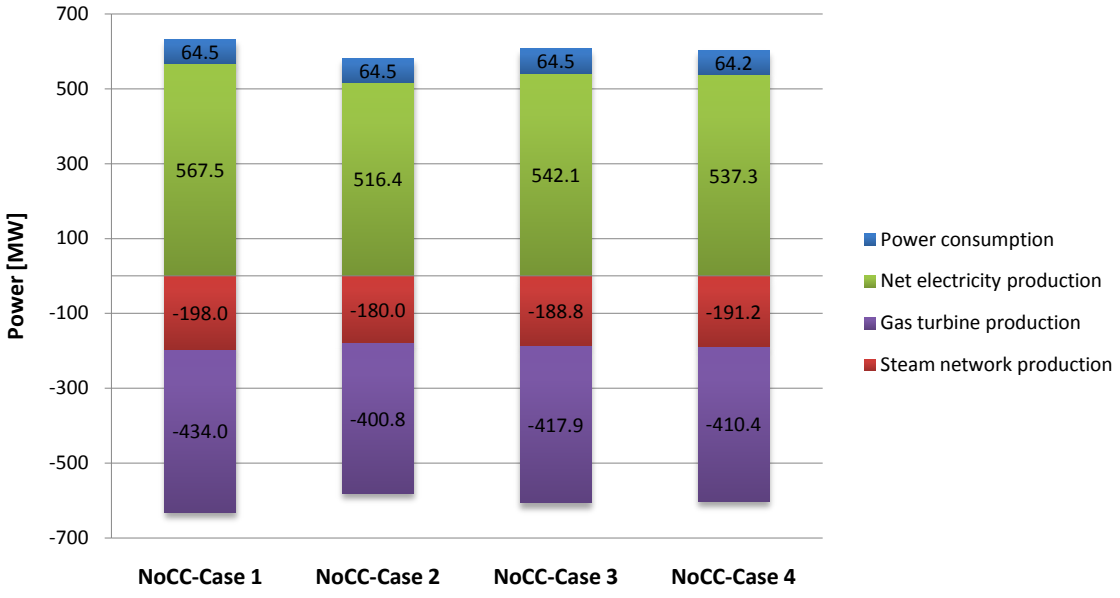

Figure 27: Comparison power produced and consumed of the studied IGCC cases without CO_2 capture

[1] Reference: [34], [41], [39], [10]

Figure 28 presents the integrated composite curves for the two best cases (45% NoCC-case 3 and 44.6% NoCC-case 4). The blue curve represents the heat stream of the process and the red curve the steam network integration.

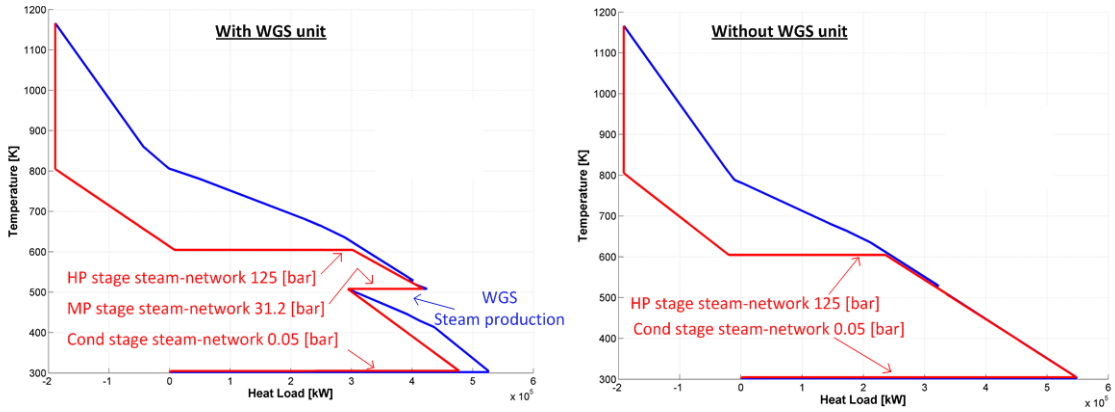

Figure 28: At left, the integrated composite curve with the steam network integration for IGCC without CO_2 capture (NoCC-Case 1.3 WGS-partial condensation). At right, the integrated composite curve with the steam network integration for IGCC without CO_2 capture (NoCC-Case 1.4 no WGS-no condensation)

6.2 IGCC with MDEA CO_2 capture

Four different cases are compared for the MDEA CO_2 capture unit simulation. For the MDEA-case 1.1, 33% wt. MDEA fraction is mixed with water. The MDEA-Case 2.1, the solvent mixture contains 40% wt. MDEA and the case MDEA-Case 3.1 50% wt. MDEA. The solvent is sent to the absorber at 317 K (43°C) and the syngas coming from the WGS unit is cooled down to 313 K (40°C). The condensate water is separated before sending the syngas to the absorber. The case MDEA-Case 1.2 is performed at higher temperature with the solvent and syngas both entering into the absorber at 338 K (65°C). For each case, the solvent mass-flow is adjusted to reach 90% of CO_2 capture. Table 19 summarizes the results for all the MDEA cases.

Cases	***MDEA-Case 1.1***	***MDEA-Case 1.2***	***MDEA-Case 2.1***	***MDEA-Case 3.1***	***Reference with MDEA[2]***
	Solvent: 317 [K] Syngas: 313 [K] 33 % wt. MDEA	Solvent: 338 [K] Syngas: 338 [K] 33 % wt. MDEA	Solvent: 317 [K] Syngas: 313 [K] 40 % wt. MDEA	Solvent: 317 [K] Syngas: 313 [K] 50 % wt. MDEA	Solvent: 317 [K] Syngas: 313 [K] -
Efficiency [%]	36.22	35.89	36.31	36.39	35-37
Reboiler heat duty [MW]	174.7	218.4	161.8	145.1	-
Reboiler heat duty [GJ/tCO_2]	1.84	2.31	1.71	1.53	

Table 19: IGCC with the MDEA CO_2 capture case simulations

Cases	***MDEA-Case 3.1***	***NoCC-Case 3***
	Solvent: 317 [K] Syngas: 313 [K] 50 % wt. MDEA	Without capture -
Efficiency [%]	36.39	45

Table 20: Comparison of IGCC with the MDEA CO_2 capture and with the case without CC

[2]Reference: [38] [40]

Figure 29 compares the performances with the case without capture (NoCC-Case 3). The green column represents the net electricity produced by the power-plant, the blue the power consumed in the process. The sum of the green and blue columns is the total power produced by the gas turbine and the steam network (cogeneration Rankine cycle). The net electricity generated by the steam network and the gas turbine are illustrated by the red and purple column in negative side, respectively.

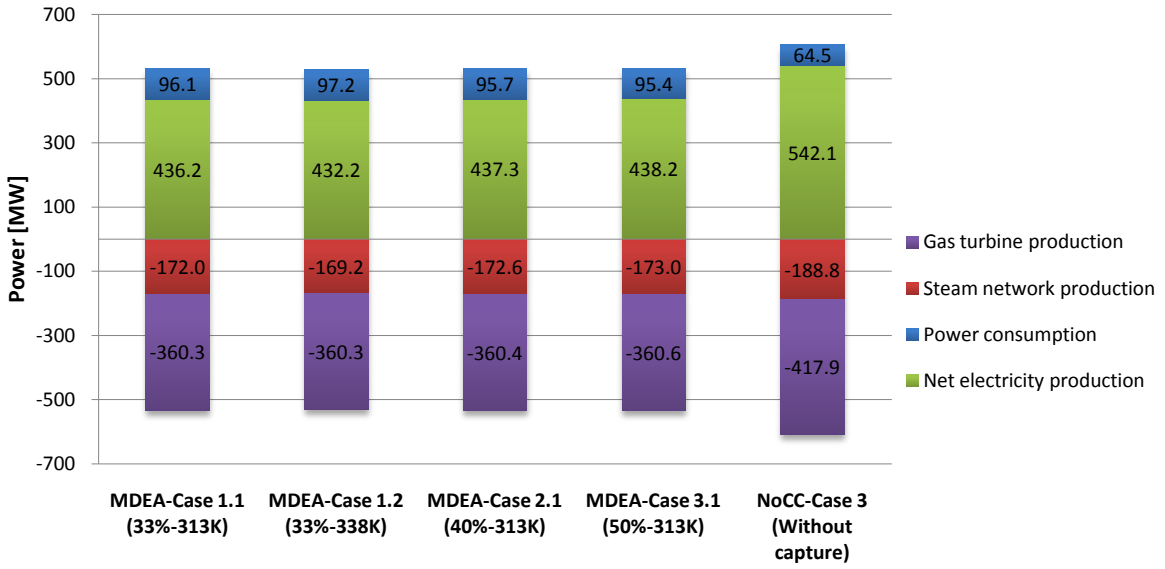

Figure 29: Comparison power produced and consumed for the different IGCC cases with and without MDEA CO_2 capture

The streams description is detailed in Annex IV.

Discussion

The case MDEA-Case 3.1 yields the highest efficiency with 36.39%. The efficiency is a little better compared to the case with 33% MDEA (MDEA-Case 1.1) and 40% MDEA case (MDEA-Case 2.1) because less solvent is required to capture the same amount of CO_2. Therefore the reboiler heat duty to regenerate the solvent and the pumping power required are lower.

The integrated composite curve and the grand composite curve with the steam network integration (in red) are illustrated in Figure 30 and Figure 31 compared to the one without CC in Figure 28.

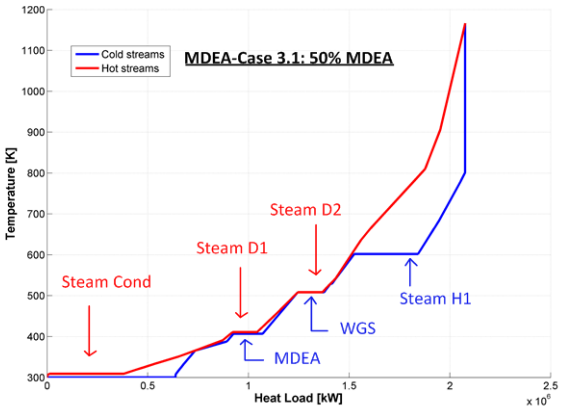

Figure 30: Composite curve for the MDEA-Case 3.1 with a 50% wt. MDEA solvent mixture

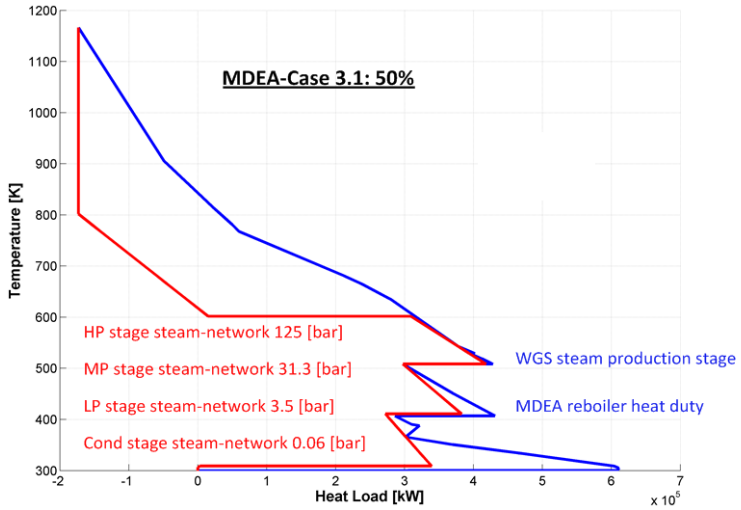

Figure 31: Integrated composite curve with the steam network integration in red for the IGCC MDEA-Case 3.1 with a 50% MDEA solvent mixture

Sensitivity analysis on the solvent temperature

According to the reference [17], the absorber can operate at temperature from 298 K to 343 K (25 to 70°C). The outdoor temperature constrains in Australia allow only to cool down the stream to 313 K and the model configuration of the absorber converges only until 338 K.

The sensitivity analysis is performed by changing the temperature of both the solvent and the syngas entering the absorber between 313 and 338 K (40 - 68°C). Figure 32 shows that the reboiler heat duty increases with the increasing temperature of the absorber. A hotter column increases the reaction rate but decreases the solubility of the CO_2 in the solvent. Therefore more solvent is required and the reboiler heat duty increases [19].

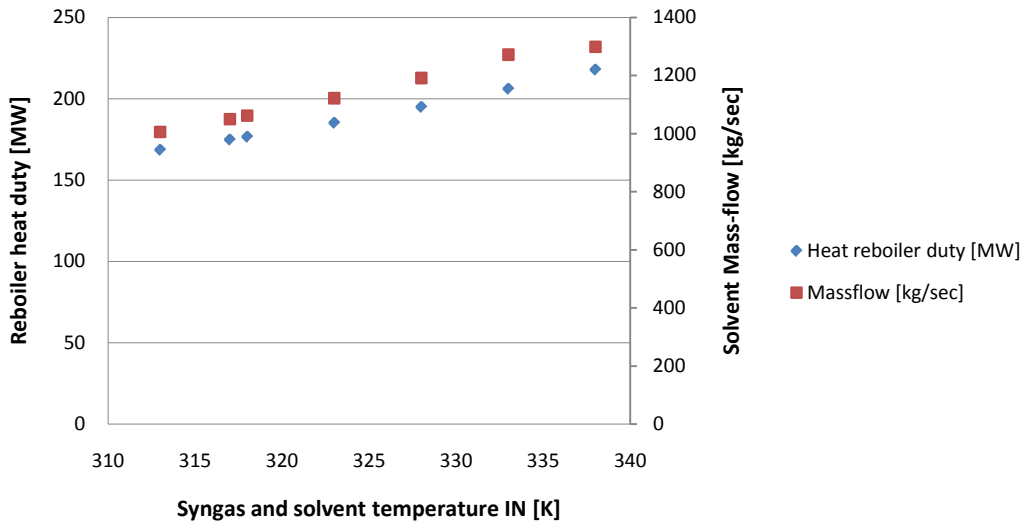

Figure 32: Sensitivity analysis on the absorber temperature for the IGCC case with 33% wt. MDEA CO_2 capture

The same results could be observed for the two other cases with 40% -50% wt. MDEA in the lean solvent.

The case MDEA-Case 1.2 operating at higher temperature for the absorber shows that more solvent is required to capture the same amount of CO_2. Therefore the reboiler heat duty and the power consumption in the MDEA CO_2 unit are higher compared to the base case MDEA-Case 1.1, thus the efficiency is lower (Table 19).

6.3 IGCC with Selexol CO_2 capture

Different cases are compared for the Selexol CO_2 capture unit. In the Selexol-Case 1.1, the solvent is sent to the absorber at 313 K (40°C) and the syngas coming from the WGS unit is cooled down to 313 K (40°C). The condensate water is separated before sending the syngas to the absorber. The Selexol-case 1.2 is performed at higher temperature with the solvent and syngas both entering into the absorber at 324 K (51°C). In the Selexol-Case 2, operating at 313 K (40°C), the steam network is improved by adding a second steam production stage at 1.85 bar (see Figure 34), which increases the efficiency with a bigger cogeneration steam power production. The stage pressure of 1.85 bar results from the Moo optimization (see sensitivity analysis in Figure 35).

For each case, the solvent mass-flow is adjusted to reach 90% of CO_2 capture. Table 21 summarizes the Selexol case results.

Cases	***Selexol-Case 1.1***	***Selexol-Case 1.2***	***Selexol-Case 2***	***NoCC-Case 3***	***References with selexol***[3]
	Solvent: 313 [K] Syngas: 313 [K]	Solvent: 324 [K] Syngas: 324 [K]	Solvent: 313[K] Syngas: 313 [K]	-	Solvent: 313 [K] Syngas: 313 [K]
	-	-	Opti-steam network	-	-
Efficiency [%]	36.15	35.83	36.42	45	34.5-37
Solvent mass-flow *[kg DEPG/kg CO_2]*	27.03	32.23	27.03	-	22-28.95[4]

Table 21: IGCC with the Selexol CO_2 capture case simulations

[3] Reference for efficiency: [27], [2], [14]
[4] Reference for solvent mass-flow: [27]

The performances of different Selexol cases are discussed in Figure 33. The green column represents the net electricity produced by the power-plant, the blue the power consumed in the entire process. The sum of the green and blue columns represents the total power produced by the gas turbine and the steam network (cogeneration Rankine cycle). The net electricity generated by the steam network and by the gas turbine are illustrated by the red and purple column in negative side, respectively.

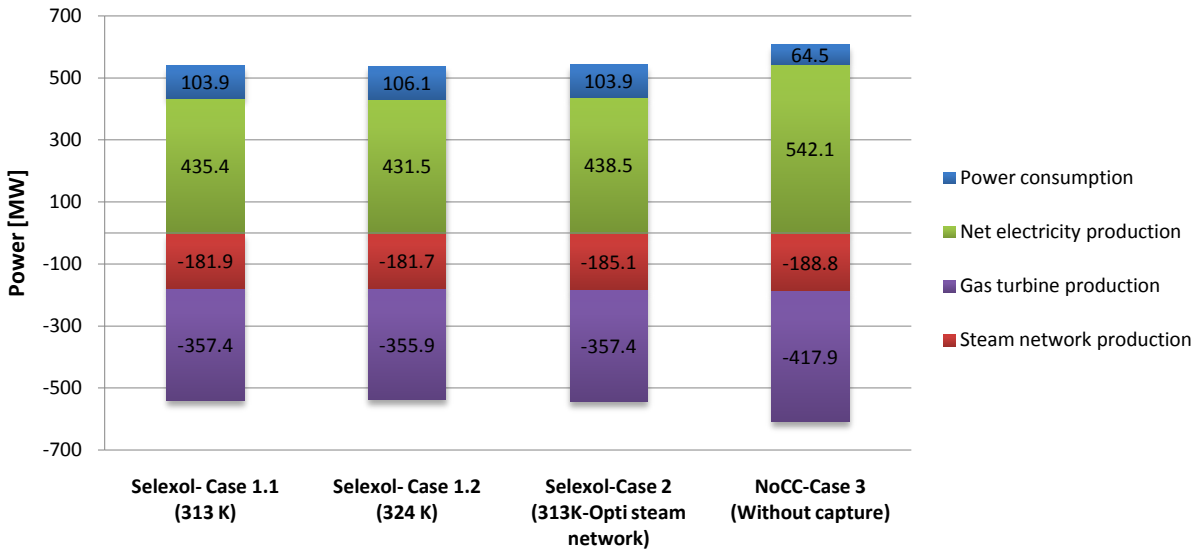

Figure 33: Overall performance comparison of IGCC with and without Selexol CO_2 capture

The stream description is detailed in Annex V.

Discussion

The Selexol-Case 2.1 yields the highest efficiency with 36.42 %. The integration of a low pressure steam production stage increases the overall efficiency compared to the case with only one stage steam production (Selexol-Case1.1: 36.15%). Indeed the steam network produces 3.1 MW more power.

When the absorber operates at higher temperature (Selexol-Case 1.2), the same conclusion could be drawn as in the MDEA case (MDEA-Case 1.2). A hotter column decreases the solubility of the CO_2 into the solvent. Therefore the efficiency drops off to 35.83% with only 11 degrees higher absorber temperature, which is 324 K (51°C).

The grand composite curves the steam network optimization (in red) is illustrated below in Figure 34 compared to the one without CC in Figure 28.

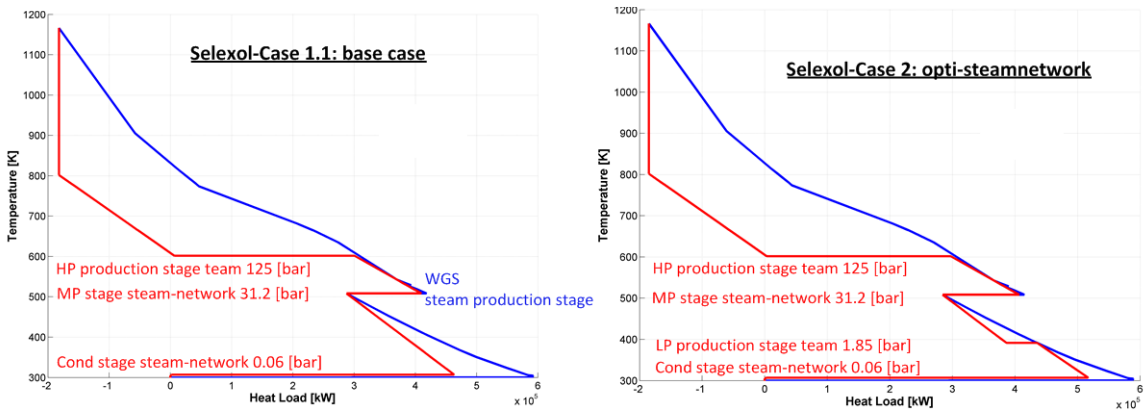

Figure 34: Integrated composite curve for the IGCC - Selexol-Case 1.1 and the Selexol-Case 2 with the optimization of the steam network

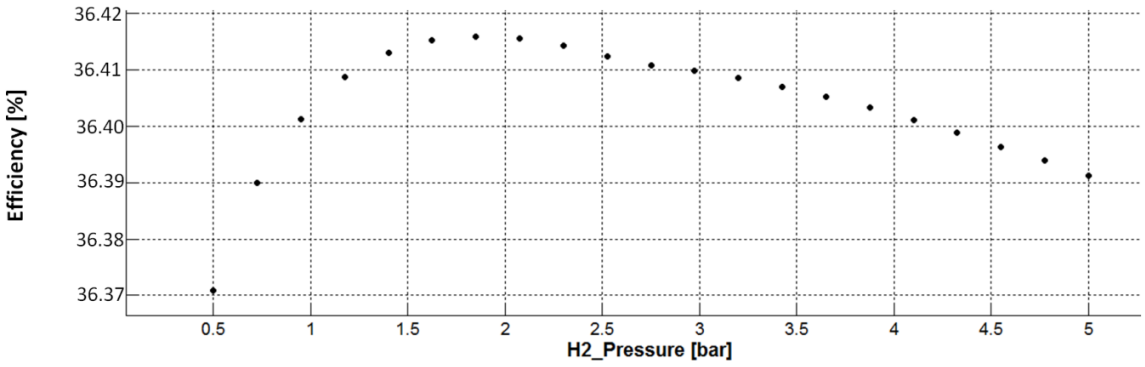

Figure 35: Sensitivity analysis on the second steam production stage pressure for the IGCC with the Selexol CO_2 capture

6.4 IGCC with UNO CO_2 capture

Only the most promising options of the multitude of studied options are presented in this section. The different variants simulated are attached in Annex III.

6.4.1 Base cases simulations with UNO

First of all, sensitivity analyses were performed to determine an operating temperature range for the solvent and the syngas entering into the absorber. Figure 36 illustrates the results for the variation of the syngas and solvent temperature from 363 to 493 K (90-220°C). The reboiler heat duty decreases with the increasing temperature, but after a certain point at 460 K (187°C), some water has to be refilled in the system to insure the mass-balance of the solvent (close loop). Less water is absorbed with the solvent in the absorber as illustrated by the green and violet curves in Figure 36.

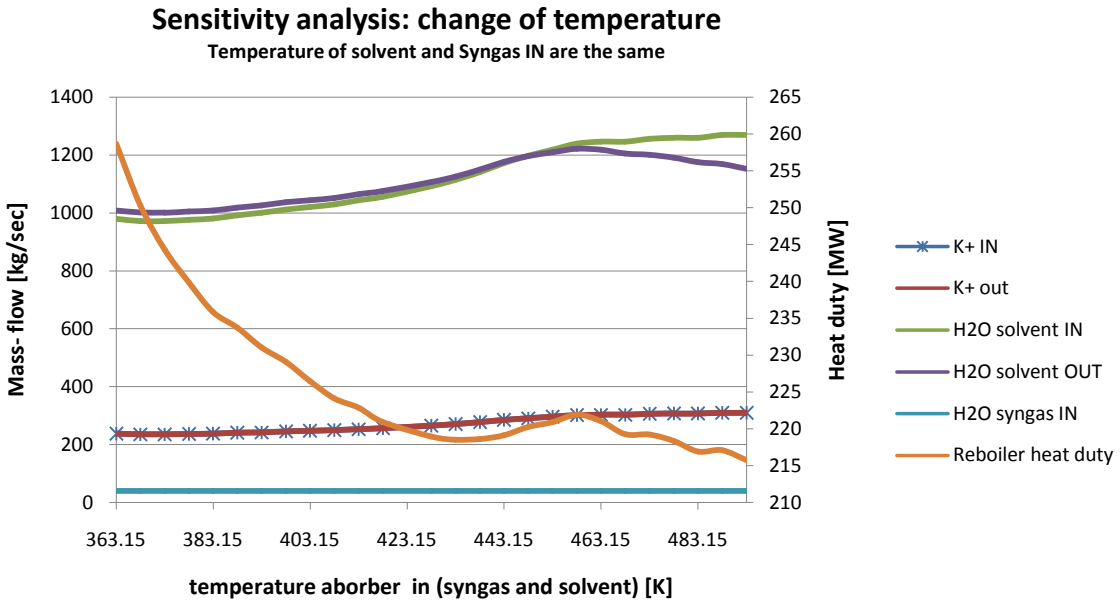

Figure 36: Four IGCC UNO cases chosen for the first simulation. The sensitivity analysis describes the reboiler heat duty, the water content entering in the absorber (lean solvent IN) and the water content leaving the stripper(lean solvent OUT). To match the mass-flow balance between the inlet and the outlet stream (solvent), some water has to be refill in the lean solvent at high temperature (up to 450 K).

Four different base cases have been chosen to be compared in a first study. These cases are summarized in Table 22. The base case is the UNO-Case 1.1 at 413 K. The second case UNO-Case 1.2 is performed at higher temperature (433 K), for which the reboiler heat duty is minimal without refilling water in the system. The third case UNO-Case 1.3 (493 K) has the lowest reboiler heat duty but some water has to be injected in the system to guaranty the mass-flow balance

between the outlet and the inlet. The last case UNO-Case 1.4 is performed at low temperature (393 K) to illustrate the difference.

Cases	***UNO-Case 1.1***	***UNO-Case 1.2***	***UNO-Case 1.3***	***UNO-Case 1.4***	***NoCC-Case 3***
	Solvent: 413 [K] Syngas: 413 [K]	Solvent: 433 [K] Syngas: 433 [K]	Solvent: 493 [K] Syngas: 493 [K]	Solvent: 393 [K] Syngas: 393 [K]	-
Efficiency [%]	36.86	36.41	34.28	36.45	45
Reboiler heat duty [MW]	218.1	215.2	207.9	227.1	-
Reboiler heat duty [GJ/t CO_2]	2.3	2.26	2.19	2.39	-

Table 22: IGCC with UNO CO_2 capture base case simulations

Results

Figure 37 compares the power balances for each case in the power-plant. The green column represents the net electricity produced by the power-plant, the blue the power consumed in the power-plant including CO_2 capture and compression. The sum of the green and blue columns is the total power produced by the gas turbine and the steam network (cogeneration Rankine cycle). The net electricity generated by the steam network and gas turbine are illustrated by the red and purple column in negative side, respectively.

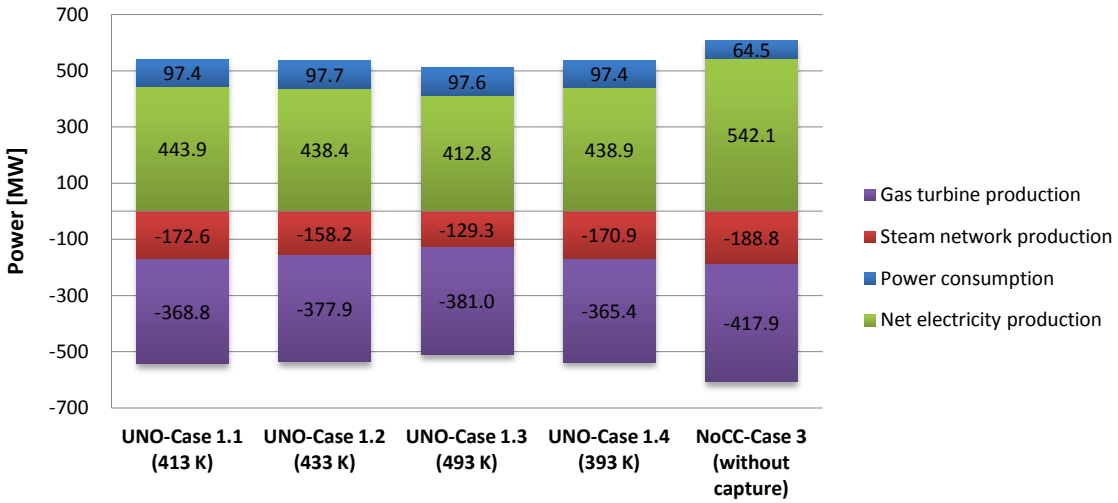

Figure 37: Comparison between the powers produced and consumed in the process between each IGCC with UNO CO_2 base case (UNO-Case 1.1 (413K), UNO-Case 1.2 (433K), UNO-Case 1.3 (493K), UNO-Case 1.4 (493 K), NoCC-Case 3 (without capture). The steam network power production is detailed by the red column.

The stream description is detailed in Annex VI.

Discussion

The ''UNO-case 1.1''occurring at 413 K for both solvent and syngas entering into the absorber has an overall efficiency of 36.86% and is the best of the four base cases simulated. Figure 38 illustrates the integrated composite curve with the steam network integration for IGCC with the UNO CO_2 capture compared to the one without CC in Figure 28.

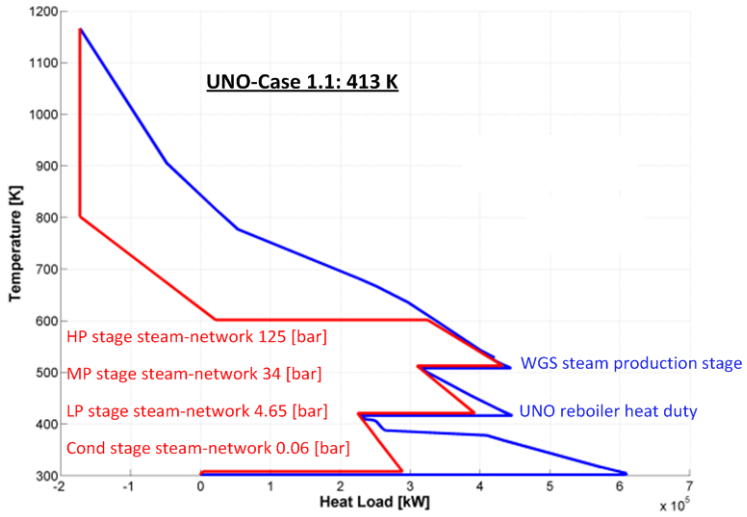

Figure 38: Integrated composite curve with steam network integration (red curve) for the IGCC with UNO CO_2 capture (UNO-Case 1.1 413K).

The results not corresponding to what had been expected for the cases at high temperature (UNO-Case 1.2 and UNO-Case 1.3). It was predicted that the efficiency would be higher when the absorber was operating at high temperature because the reboiler heat duty is lower. To understand the results, the integrated composite curve for the UNO-Case1.3 (493 K) is compared with the UNO-Case 1.1 (413 K) in Figure 39.

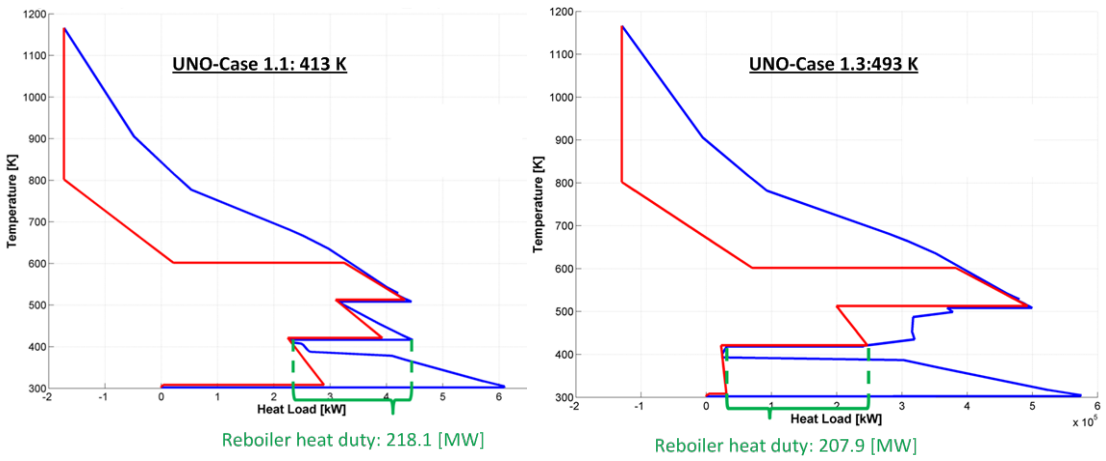

Figure 39: Comparison between the integrated composite curves for two operation temperature for the IGCC with UNO CO_2 capture cases. The two blue circles illustrate the solvent reheat which penalizes the hot temperature case.

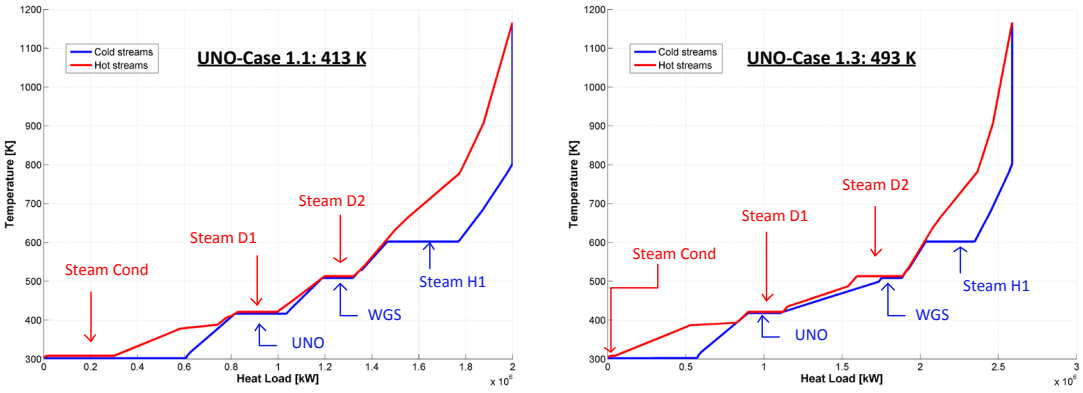

Figure 40: Composite curve for the IGCC with UNO CO_2 capture cases UNO-Case1.1 and UNO-Case1.3

As shown on Figure 39, the reboiler heat duty is lower at high temperature (UNO-Case 1.3) but when the stripper is operating at high temperature, more water is released in the vapor phase with the CO_2 gas stream. This water has to be condensed by cooling down the CO_2 gas stream until 313 K. After separation from the CO_2, this condensed water has to be heated up before mixing with the outlet lean solvent at high temperature (red line in Figure 41). Furthermore some refill water has to be injected to match the mass-flow balance between the outlet and inlet lean solvent stream. This refill water also has to be heated up before getting mixed with the outlet lean solvent (blue line in Figure 41). These heat demands are bigger than for the UNO-case 1.1 at 413 K and counter-balance the advantage of the lower reboiler heat duty. For this reason, the power generated by the steam network is lower (Figure 37) and consequently the efficiency is lower at elevated temperature.

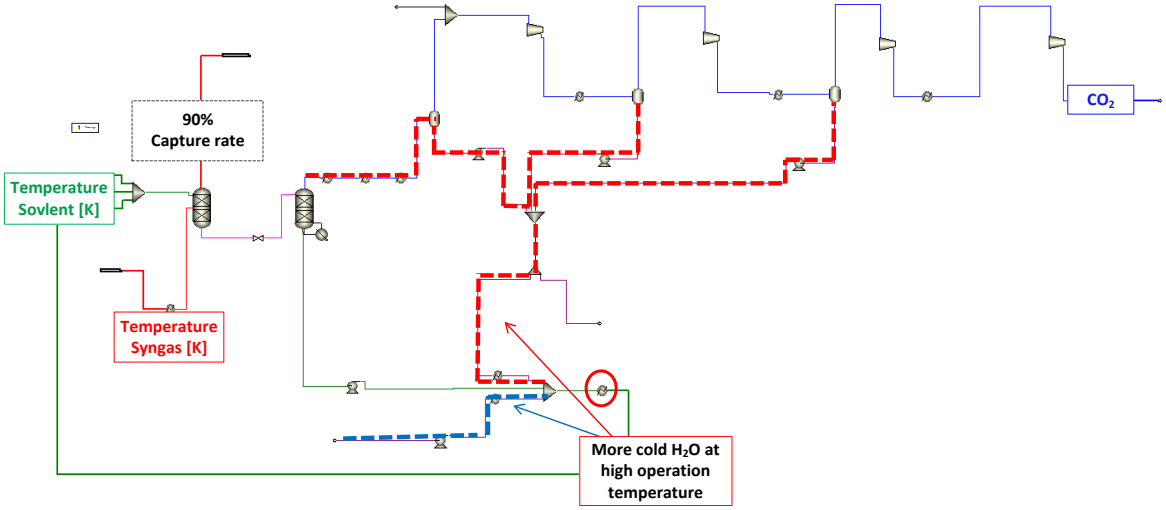

Figure 41: Explanation of the IGCC with UNO CO_2 capture case UNO-Case 3.1 (493 K)**.** In blue the refill water which has to be heated up in case of refill water need. In red, water coming from the condensation and has also be heated up to match the temperature of the close solvent loop.

6.4.2 CO_2 recompression variant

Based on the four previous cases, the goal of this variant is to increase the efficiency especially at high operating temperature for the UNO system by improving the integration of the stripper heat demand and the steam network integration. As illustrated on Figure 42, this system is operating like a heat pump by introducing a compressor followed by a series of heat exchangers on the CO_2 gas stream, which is leaving the stripper. The heat available in these heat exchangers is used to satisfy the reboiler heat duty demand. By decreasing this stripper duty, the steam network integration could be improved and produces more power.

One advantage compared to adding a real heat pump is that the CO_2 itself is already partially compressed to 100 bar for the storage.

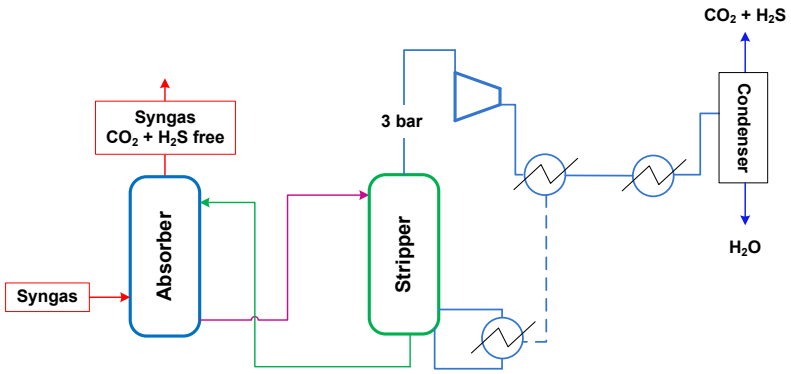

Figure 42: IGCC with UNO CO_2 capture recompression variant

Figure 43 presents the CO_2 recompression variant: UNO-Case 1.5. The outlet temperature of the heat exchanger UNOHXC1 is imposed to be 8 degree higher than the reboiler temperature. Then the option to connect directly or not the heat exchanger ''UNOHXC1'' to the reboiler could be chosen and is a variable decision. Both types of heat integration system (directly connect or not to the stripper) will be compared in a sensitivity analysis.

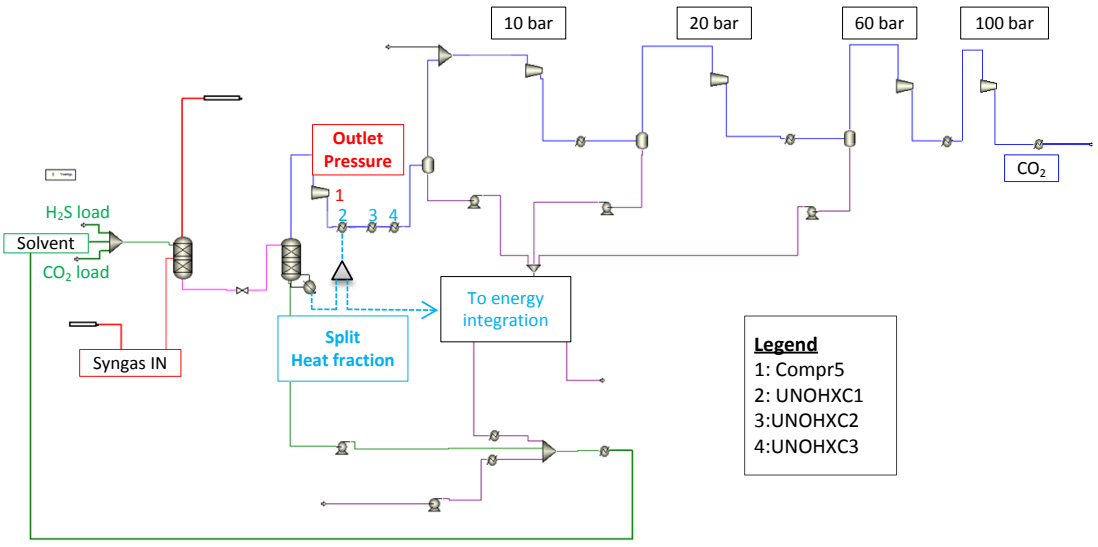

Figure 43: UNO CO_2 recompression variant model

Two parameters are important in this case. The first one is the outlet pressure of the compressor "Compr 5" and the second one is how much heat is directly sent to the reboiler (red frames "Split Heat'' in Figure 43). A first sensitivity analysis was computed at 493 K (syngas and solvent inlet temperature) by varying the pressure of the compressor ''compr 5'' (heat split fraction equal to 0) (see Figure 44) and then a second sensitivity analysis is performed by varying the split heat fraction (how much heat is send directly to the reboiler) (see Figure 45).

Sensitivity analysis results

Figure 44 and Figure 45 below present the results for the two different sensitivity analyses on the CO_2 recompression pressure and on the heat split fraction sent to the reboiler. The best efficiency is obtained by compressing the stream (with the compressor ''compr 5'') to 9 bar at 493 K. Moreover, sending the heat directly from the heat exchanger ''UNOHXC1" to the reboiler is less efficient than performing the energy integration by solving the heat cascade (this has been observed at each pressure).

Remark: Heat split fraction equal to 1 means that all the heat is sent directly to the reboiler; heat split equal to 0 means that all the heat integration is leaving entirely to OSMOSE.

This can be explained by regarding the integrated composite curve of Figure 46. One stage of the steam network is used to heat partially the reboiler, leading to an improvement of the heat integration coming from the heat exchanger UNOHXC1 (see green circle in Figure 46).

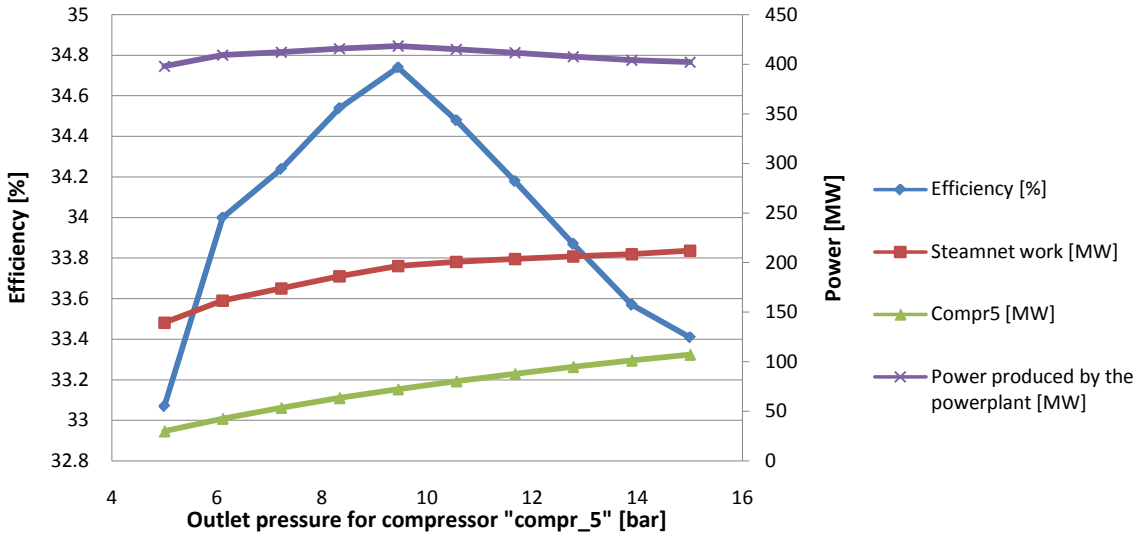

Figure 44: Sensitivity analysis on the recompression pressure (''compr 5'' outlet pressure) for the IGCC with UNO CO_2 recompression variant at 493 K (solvent).

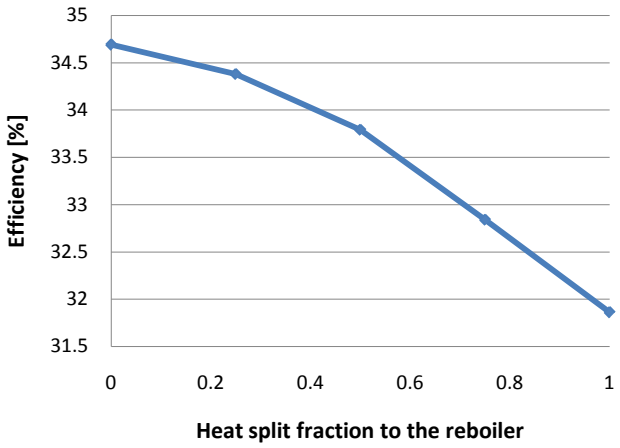

Figure 45: Sensitivity analysis on heat split fraction for a solvent temperature of 493 K for the IGCC with UNO CO_2 recompression variant. When the heat split fraction is equal to 1, all the heat is sent directly to the reboiler.

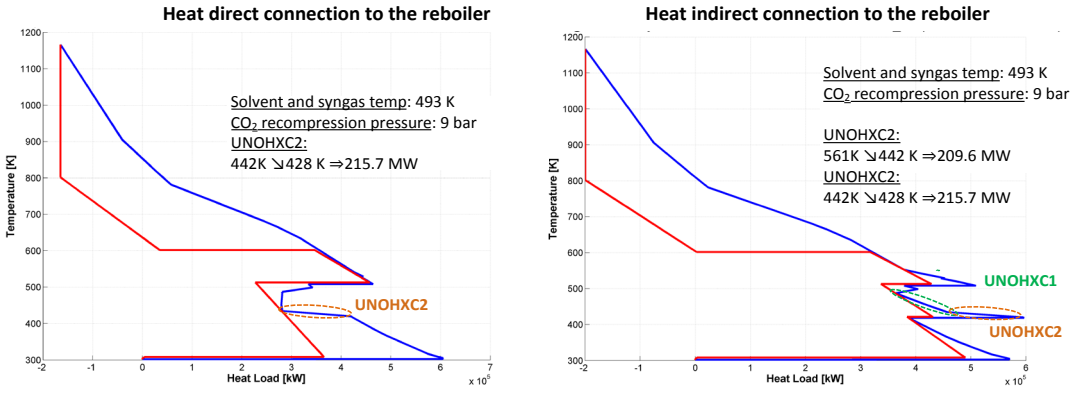

Figure 46: Integrated composite curve for the IGCC with UNO CO_2 recompression variant. At left: the integrated composite curve with the direct connection between the UNOHXC1 to the reboiler. As you can the stage of the reboiler is completely removed. At right: the integrated composite curve without direct connection between UNOHXC1 and the reboiler.

To explain the poor efficiency in the case where the CO_2 stream leaving the stripper is compressed to 5 bar using the compressor ''Compr 5'' (in Figure 44), the heat available at higher temperature than the reboiler temperature is very low (Figure 47). Some heat from the steam network has then to be used to satisfy the reboiler duty. Therefore the steam network produces less power (see Figure 44). As we can see with the low compression case (5 bar), the temperature of the heat coming from the ''UNOHXC2 is under the reboiler temperature and cannot be used to satisfy the heat demand of the reboiler (see Figure 47).

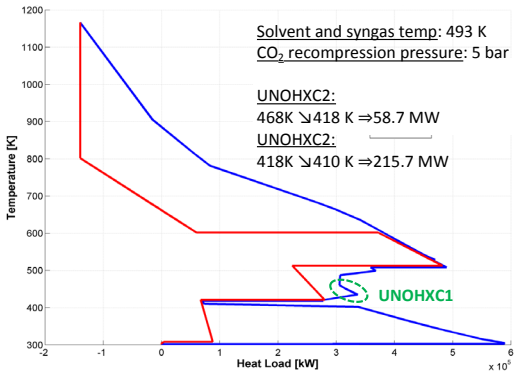

Figure 47: Integrated composite curve for the IGCC with UNO CO_2 recompression variant: re-compression at 5 bar with "compr_5".

Results comparison

Figure 48 compares the cases with and without the use of CO_2 recompression system. For each temperature, the CO_2 recompression pressure is optimized to have the best efficiency. The efficiency is improved when the UNO process is operating at high temperature (> 443 K); but even this temperature, the process is less efficient than the best case without the recompression system (UNO-Case 1.1).

Although the steam network power is improved at each temperature, the compression energy demand is too high to improve significantly the efficiency of the overall process.

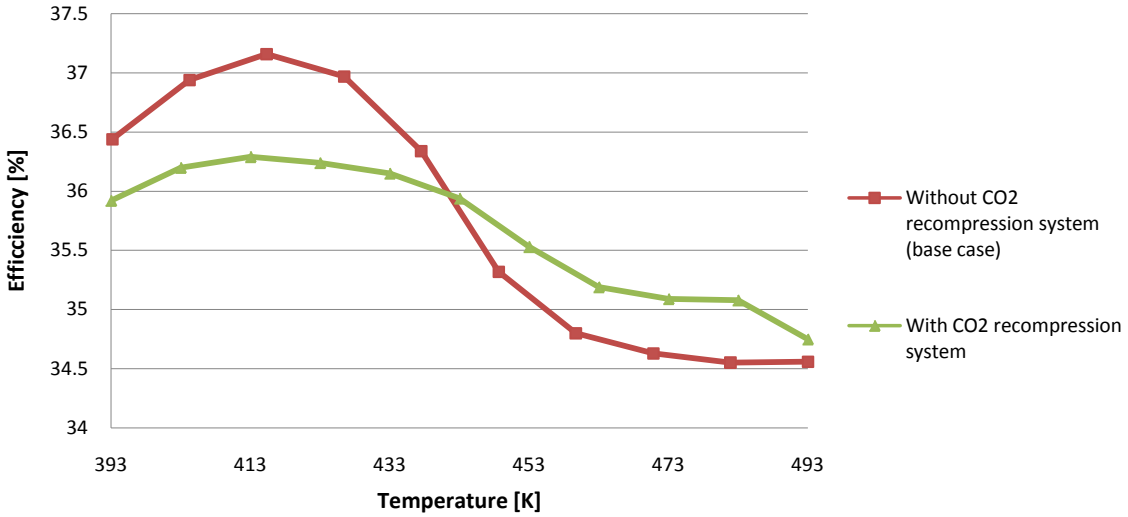

Solvent and syngas IN temperature [K]	*393*	*403*	*413*	*423*	*433*	*443*	*453*	*463*	*473*	*483*	*493*
Optimal recompression pressure [bar]	13.5	13	11	10.5	6.5	5.5	5.5	9.5	9.5	9.5	9.5

Figure 48: Sensitivity analysis comparison with and without the recompression system for the IGCC with UNO CO_2 recompression variant. For each temperature the optimal pressure is presented in the table below the graph.

Figure 49 and Figure 50 illustrate the comparison between the net electricity produced and the consumption in the process, and the power-plant overall efficiency.

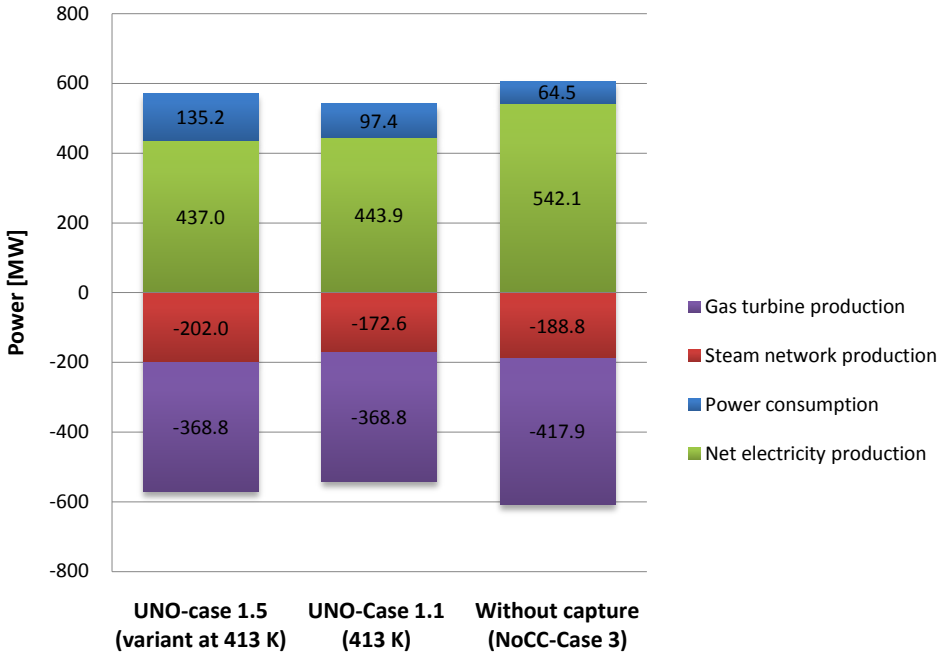

Figure 49: Comparison between the powers produced and consumed in the process between the IGCC with the CO_2 recompression variant UNO-Case 1.5, the base case IGCC with UNO CO_2 capture UNO-Case 1.1 (413 K) and the IGCC without capture NoCC-Case 3.

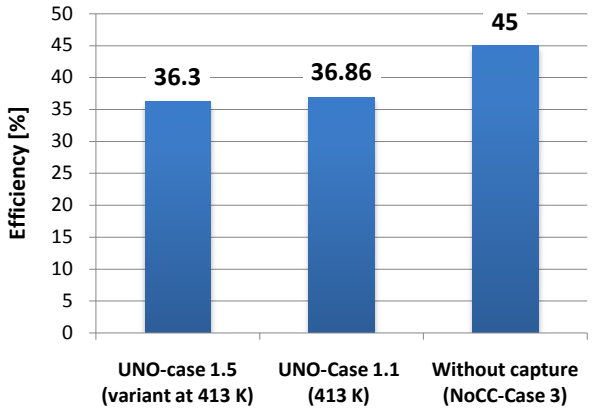

Figure 50: Overall efficiency comparison between between the IGCC with the CO_2 recompression variant UNO-Case 1.5, the base case IGCC with UNO CO_2 capture UNO-Case 1.1 (413 K) and the IGCC without capture NoCC-Case 3.

Remark: It would be interesting in a more detailed work to introduce an external heat pump around 400 K to exchange between the reboiler heat stage and compare the efficiency with this CO_2 recompression variant.

6.4.3 UNO process optimization

A first Moo optimization was performed on the different parameters of the UNO process. All these parameters are listed below. The CO_2 capture rate variation is performed by a design specification, which adjusts the mass-flow of solvent to reach the imposed capture rate.

Decision variables: absorber	***Value range***
Temperature of the syngas IN [K]	393-493
Temperature of the solvent IN [K]	393-493
CO_2 capture rate [%]	70-98
Decision variables: Steam network	
Condensation pressure [bar]	0.05-0.8
MP pressure stage [bar]	31-50
LP pressure stage [bar]	3-8
Decision variable: Gas turbine	
Air pre-heat in GT	No

Table 23: Decision variables for the UNO process optimization

Two objectives were performed:

- Maximize the overall efficiency (eq. 35)
- Maximize the CO_2 capture rate

And the Moo characteristics:

- Max evaluations : 3000
- Initial population: 300

Remark: The pressure of the stripper wasn't taken as a decision variable because the convergence was difficult to obtain without any design change of the column. This parameter could be interesting to be included in a future work.

Moo optimization results

The pareto curve from the Moo optimization is presented in Figure 51. This optimization is performed in the UNO solvent by taking as starting point the UNO-Case 1.1 (red point in Figure 51).

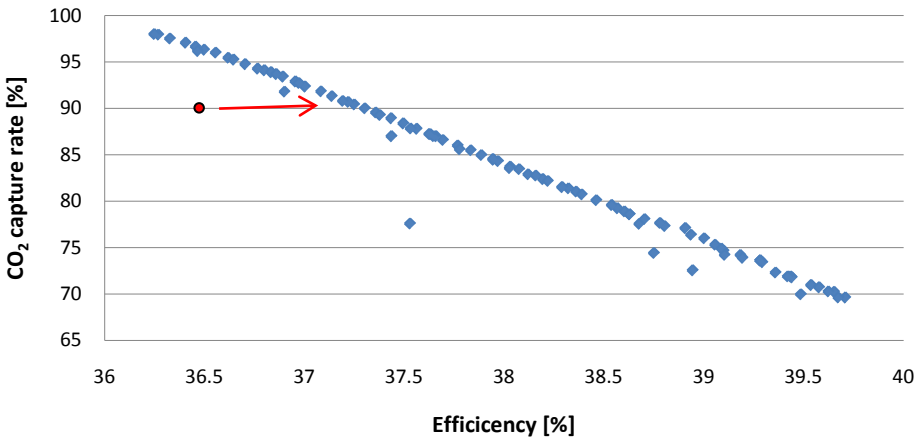

Figure 51: Pareto curve for the IGCC with the UNO CO_2 capture process. The red point presents the starting point with the UNO-Case 1.1 (IGCC with UNO CO_2 capture).

Compared to the starting point UNO-Case 1.1 in red on Figure 51, the efficiency is improved. The efficiency decreases when increasing the CO_2 capture rate because the reboiler heat duty and the required power in the UNO process are increase. Moreover, the mass-flow of the syngas sending into the gas turbine is lower because more CO_2 is absorbed, which produces less power in the expander. The results for the two objectives are listed below:

Objective 1: max efficiency	39.7% efficiency with 69.6% CO_2 captured
Objective 2: max capture rate	36.24% efficiency with 97.9%CO_2 captured

The parameters for the best case with a CO_2 capture rate of 90% are:

- Efficiency (with 90 % capture): 37.33 %
- Solvent temperature: 425.14 K
- Syngas temperature: 395.59 K

This optimization shows us that the efficiency is better if the solvent is a little hotter than the syngas because less water is absorbed with the solvent. Therefore the mass-flow of the syngas sending into the gas turbine is higher and the power production increases. Figure 52 illustrates the detail of the consumption and power produced for four optimized simulations, without capture and with 70 %, 90 % and 98 % CO_2 capture.

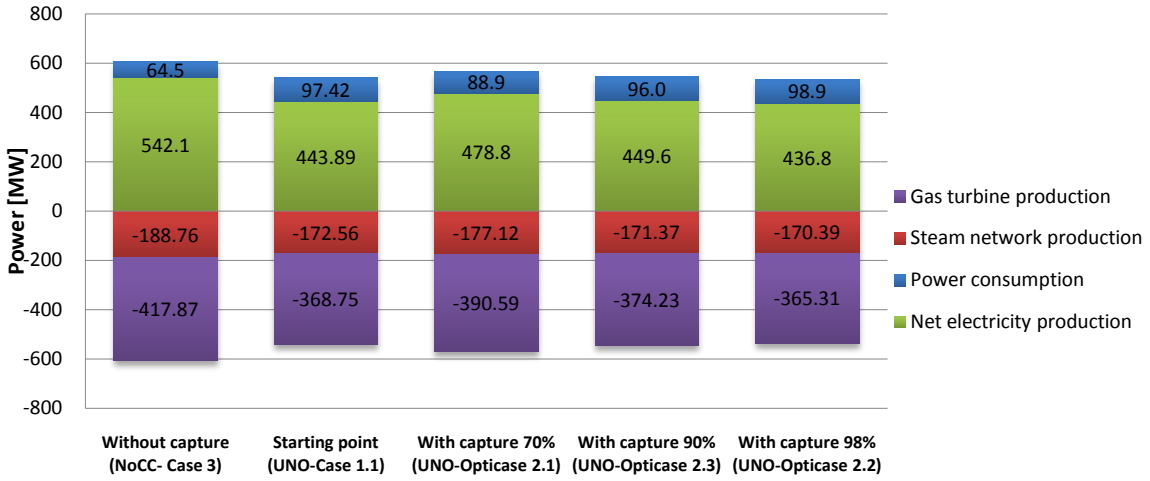

Figure 52: The consumption and power produced for optimized IGCC simulations with and without capture, the starting case: the IGCC with UNO CO_2 UNO-Case 1.1 (90% capture) and with 70%, 90 % and 98 % capture

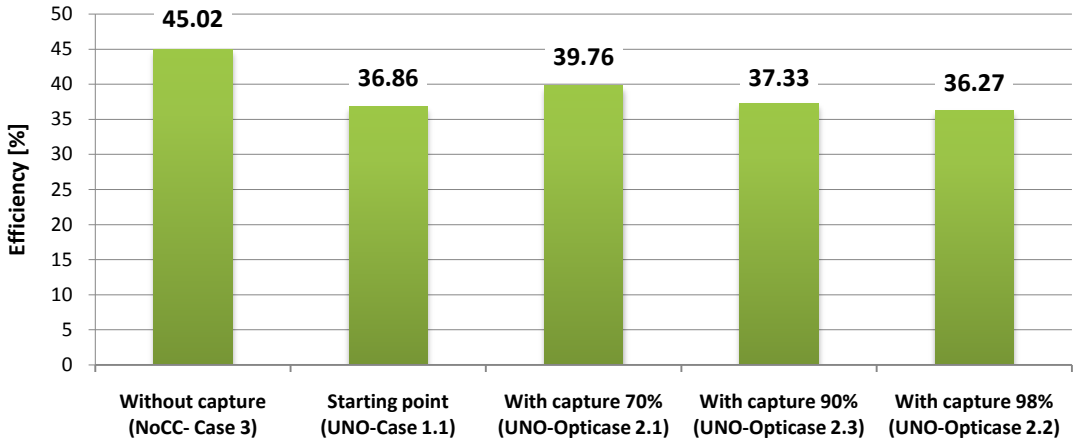

Figure 53: Overall efficiency for optimized IGCC simulations without capture, the starting case IGCC with UNO CO_2 UNO-Case 1.1 (90% capture) and with 70%, 90 % and 98 % capture

One Moo optimization was also performed by varying the temperature of the solvent and the syngas together, but with this configuration the efficiency was lower. That confirms the positive results obtained with the first optimization.

Chapter 7

Process Performance Comparison

In this section, the important parameters are compared for each best case simulated without and with CCS. To remind the main characteristics, each case is briefly re-explained before being analyzed and presented in Table 25.

The best cases without CCS are 1) the NoCC-Case 3 (45% efficiency), in which the syngas passes through the WGS unit and is further cooled down until the maximum water content (before the expander) is reached (15% mol) and 2) the NoCC-Case 4 (44.62 % efficiency) in which the syngas is directly sent into the gas turbine without passing through the WGS.

The best cases for the CCS are 1) MDEA-Case 3.1 (36.39% efficiency), where a solvent mixture of 50% wt. MDEA and an absorber operation temperature of 313 K (40°C) are used 2) the Selexol-Case 2 (36.42 % efficiency) in which the absorber is operating at 313 K 3) the UNO-opti-Case 2.3 (37.33 efficiency) in which the solvent is sent at 425.1 K and the syngas at 395.5 K to the absorber. These three CCS cases have a capture rate imposed at 90%.

Discussion

Due to a lack of time, the economic evaluation could unfortunately not be performed. The comparison is only based on the thermo-energetic analysis. For this reason, the best case is probably not the most economically viable. To determine the most sustainable process, a thermo-economic Moo optimization has to be performed.

The best efficiency for the CCS is found for the UNO-Case 2.3 and is of 37.33% for a 90% CO_2 capture rate. This case is 0.91% more efficient than the Selexol CCS and 0.94% more than the MDEA CCS, which represents 11.4 MW more.

Although the UNO process requires a higher reboiler heat duty, which corresponds to a lower potential of steam power production by the Rankine cycle compared to the MDEA process, the syngas send to the gas turbine has a higher mass-flow. Indeed by operating a higher temperature in the absorber, the water present in the syngas does not get condensed before the absorber. Moreover, by adjusting the inlet temperature of the syngas and the hot potassium solvent, the water is not absorbed by the solvent either. Therefore with a higher syngas mass-flow, more power can be produced in the gas turbine.

Despite the fact that the Selexol CCS does not required a stripper, the efficiency is only a bit higher than the one of the MDEA case. Indeed the steam network produces more power with the Selexol unit, but the higher solvent volume flow-rate and the flash until vacuum cause a big

penalty in term of energy consumption. Additionally, the syngas has to be cooled down to 313 K as well, which limits the syngas mass-flow by condensing the water. Moreover, the small amount of water, which is not condensed, is absorbed in the solvent.

Comparison with references

Results can be compared with the literature, more especially with the IEA and NETL report [34][5]. Table 24 compares different parameters with the literature data. The most popular CCS used in these reports is generally the Selexol.

Cases	***No CCS- WGS***	***MDEA CCS***	***Selexol CCS***	***UNO CSS***	***Reference: NETL-IEA report***	
Coal inlet: 1200 [MW]	NoCC-Case 3	MDEA-Case3.1	Selexol-Case 2	UNO-Case2.3	**Without capture**	**With capture**
Efficiency [%]	45.02	36.39	36.42	37.33	43.1-47.4	34.5-40.1
CO_2 capture comparison						
CO_2 emission rate after gas turbine [kg/MWh]	713.7	101.9	99.9	98.6	682-763	-
CO_2 emission rate after CO_2 capture unit [kg CO_2/MWh]	-	86.25	86.76	82.57	-	70-142

Table 24: Comparison with literature data for IGCC plants with and without CO_2 capture

Remark: in Table 24, two CO_2 emission rates are compared with literature. The first one is the emission rate measured in the flue gas at this exit of the gas turbine and the second one is measured in the stream leaving the CO_2 absorber and sending into the gas turbine. There is a small difference because some CO_2 are produced in the combustion chamber of the gas turbine.

[5]The IPCC report regroups the IEA an NETL results.

Cases	***No CCS- WGS***	***No CCS- NoWGS***	***MDEA CCS***	***Selexol CCS***	***UNO CSS***
	NoCC-Case 3	***NoCC-Case 4***	***MDEA-Case3.1***	***Selexol-Case 2***	***UNO-Case2.3***
	without capture	without capture	Solvent:317[K] Syngas: 313 [K]	Solvent: 313[K] Syngas: 313 [K]	Solvent: 425.1 [K] Syngas: 395.5 [K]
CO_2 capture rate[%]	-	-	90	90	90
Efficiency [%]	45.02	44.62	36.39	36.42	37.33
Net electricity production [MW]	542.15	537.33	438.17	438.54	449.56
Steam network production [MW]	188.76	191.16	172.95	185.08	171.37
Gas turbine production [MW]	417.87	410.35	360.59	357.35	374.23
Power consumption [MW]	64.48	64.18	95.37	103.89	96.04
CO_2 capture comparison					
CO_2 emission rate [kg/MWh]	713.7	720.6	101.9	99.9	98.6
CO_2 emission rate after capture [kg CO_2/MWh]	-	-	86.25	86.76	82.57
CO_2 avoided [kg CO_2/MWh]	-	-	618.6	620.6	622.1
Reboiler heat reboiler [GJ/tCO_2]	-	-	1.53	-	2.27
Installation characteristics					
Solvent vol-flow[m^3/sec]	-	-	0.85	2.48	1.34
Absorber diameter [m]	-	-	7.25	7.9	5.45
Absorber stages [-]	-	-	14	16	10
Stripper diameter [m]	-	-	7.3	-	7.91
Stripper stages	-	-	10	-	10

Table 25: Cases comparison for IGCC plants with and without CO_2 capture

Figure 54 shows the comparison of electricity production for each case; Figure 55 and Figure 56 illustrate the consumption power of the different processes. As mentioned before, the UNO process has the lowest steam power production, with 171 MW compared to 185 MW for the Selexol, but the biggest power produced by the gas turbine with 374.1 MW (compared to 357.35 MW in the Selexol).

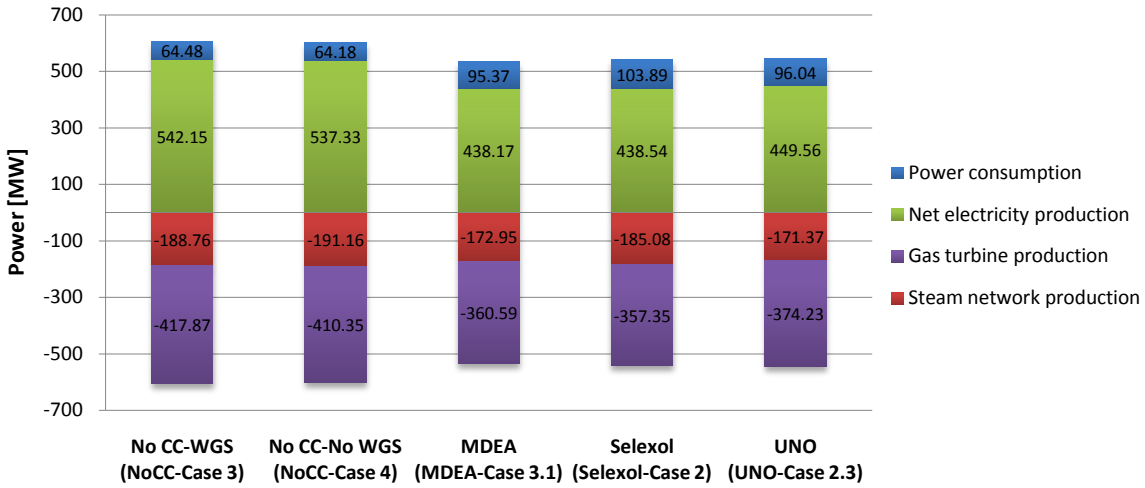

Figure 54: Comparison of the power produced and power consumed in the IGCC power-plant without and with different CO_2 capture technologies

As illustrated in Figure 55, the main power consumptions come from the O_2 production, the compression needed (O_2 and steam) in the gasification unit and for the CO_2 compression (100 bar) in the CO_2 capture unit.

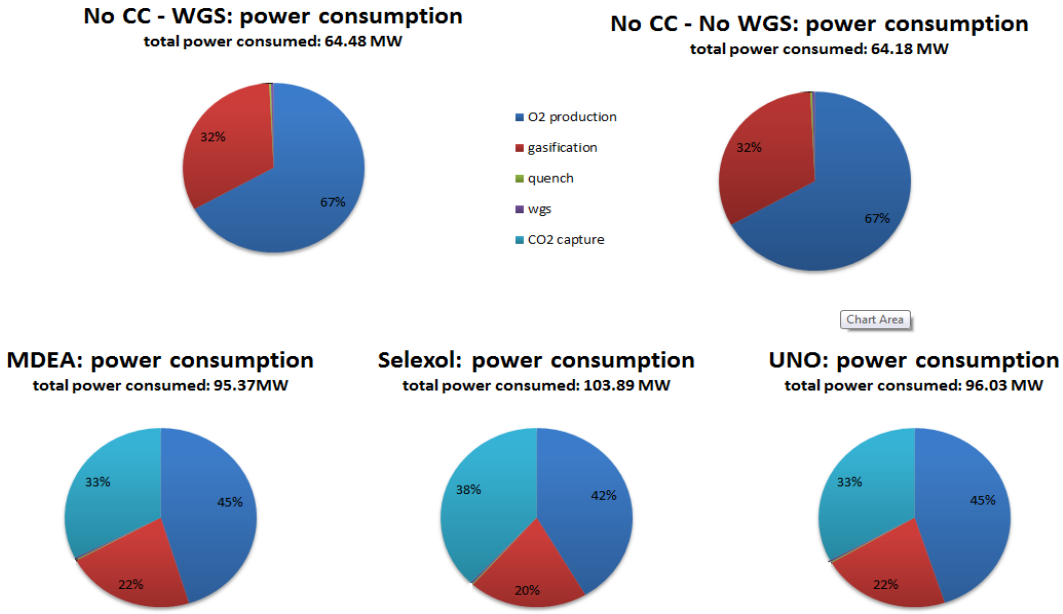

Figure 55: Comparison of power consumed in each simulated IGCC case without and with different CO_2 capture technologies

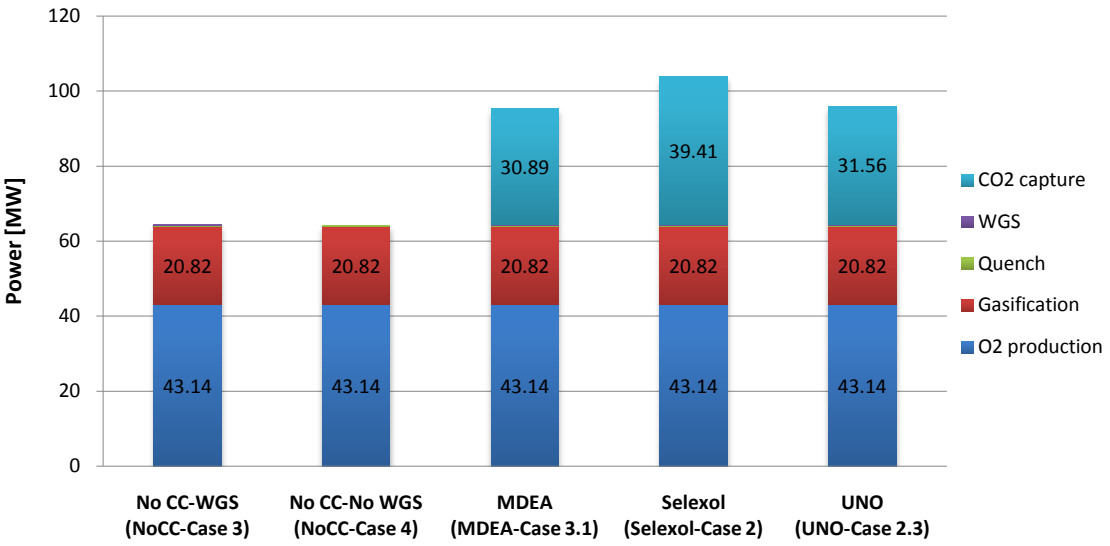

Figure 56: Detail of power consumption in the studied IGCC power-plants without and with different CO_2 capture technologies

Figure 57 illustrates the CO_2 avoided with the capture. It demonstrates that CO_2 can be captured but with an energy penalty. Furthermore more CO_2 is produced. The $CO_{2\ avoided}$ is calculated in the next equation.

$$CO_{2\ avoid\ ed} = CO_{2\ produced\ \ wit\,hout\ \ CO_2 capture} - CO_{2\ produced\ \ wit\,h\ CO_2 capture} \quad \text{(eq. 37)}$$

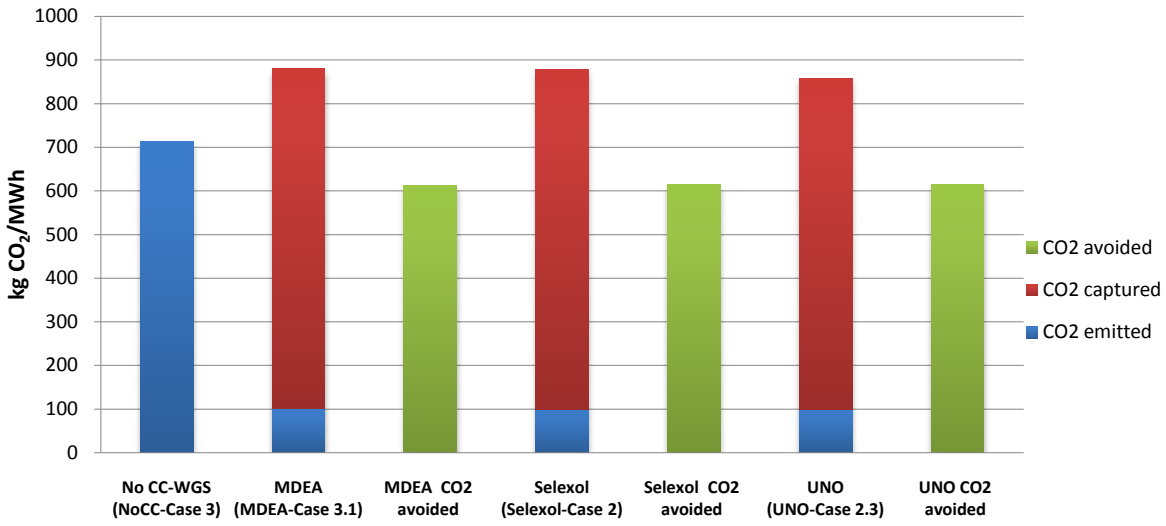

Figure 57: Illustration of the quantity of CO_2 avoided for the for IGCC power-plants without and with different CO_2 capture technologies

Chapter 8

Overall Moo optimization

The comparison case has shown the best CO_2 capture technology to be achieved by the IGCC with the UNO CO_2 capture system, in term of efficiency. Moreover, this system allows more liberty with the decision variables to operate a Moo optimization compared to both the MDEA and Selexol systems. Sub-section 8.1 defines the different decision variables. Sensitivity analyses are then performed to illustrate the improvement potential of each decision variable on the efficiency in sub-section 8.2. A Moo optimization on the overall IGCC with the UNO CO_2 capture system is finally presented in sub- section 8.3 in order to determine the highest efficient configuration.

8.1 Decision variables

In the approach taken here, the decision variables are mainly intensive variables that characterize thermodynamic performances to be reached by the process operation. Table 26 resumes the decision variables for each unit. In the gasification unit, the pressure and the temperature of the gasifier are taken as constant. Indeed the temperature of 2273 K (2000°C) and the pressure of 30 bar constitute the characteristics of the Shell gasifier. But the temperature of both the steam and the O_2 injected in the gasifier and the steam-to-coal mole ratio are decision variables. In the WGS unit, the Steam-to-CO mole ratio and the temperature of the two shift reactors can be varied. As the first Moo optimization in the UNO simulation case (UNO-optiCase 2.3), the solvent and syngas temperatures and the CO_2 capture rate are part of the CO_2 unit decision variables. In the Rankine steam network unit, the LP, MP and the condensate stage pressure can be adjusted to produce as much power as possible. Finally the gas turbine power production could be raised by varying the air and fuel pre-heat.

Decision Variables: Gasification	*Value range*
Steam preheat [K]	527-990
O_2 preheat [K]	350-990
Steam-coal mole ratio [-]	0.05-0.15
Decision variables: WGS	
Steam-carbon mole ratio [-]	2-3
WGS Reactor 1 temperature [K]	623-823
WGS Reactor 2 temperature [K]	423-623
Decision variables: absorber	
Temperature of the syngas IN [K]	393-493
Temperature of the solvent IN [K]	393-493
CO_2 capture rate [%]	70-98
Decision variables: Steam network	
Condensation pressure [bar]	0.05-0.8
MP pressure stage [bar]	31-50
LP pressure stage [bar]	3-8
Decision variable: Gas turbine	
Fuel pre-heat [K]	423-990
Air pre-heat [K]	423-990

Table 26: Decision variables for IGCC power-plant with UNO CO_2 capture

8.2 Sensitivity analysis

Figure 58 illustrates the sensitivity analysis performed on each decision variable. The UNO-OptiCase 2.3 is taken as basis. The red part on Figure 58 illustrates the improvement potential on the efficiency by varying separately each decision variable. The CO_2 capture rate [70-98 %], the absorber temperature (by varying the solvent and syngas temperature) in the CO_2 capture unit and the air pre-heat in the gas turbine unit have the highest influence on the efficiency improvement. The overall Moo optimization will show the best configuration to reach the highest efficiency. Again the economic evaluation isn't taken into account; the best configuration will certainly be economically not viable.

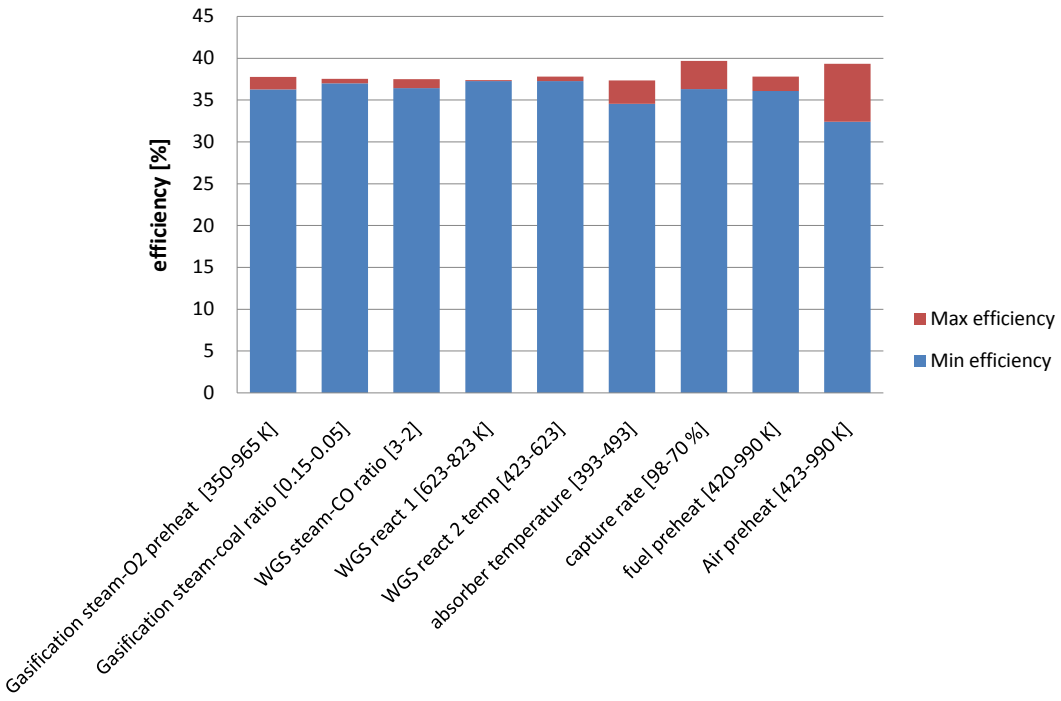

Figure 58: Sensitivity analysis on the efficiency for IGCC power-plant with UNO CO_2 capture

The highest improvement potential with the air preheat could be understood with Figure 59. Indeed by recovering the high temperature available, the air sent into the gas turbine could be pre-heated. Therefore a higher mass-flow is required to maintain the temperature of the combustion chamber at 1568 K. More flue gas is passing through the expander, which produces more electricity.

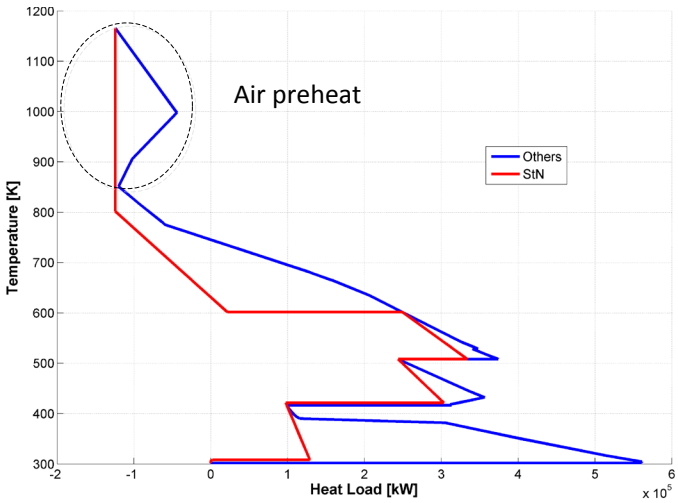

Figure 59: Illustration of the air preheat in the gas turbine unit for IGCC power-plant with UNO CO_2 capture

8.3 Overall Moo optimization results

Two objectives are performed:

- Maximize the overall efficiency (eq. 35)
- Maximize the CO_2 capture rate

The Moo characteristics are:

- Max evaluations : 8000
- Initial population: 600

Moo optimization results

The pareto curve from the Moo optimization is presented in Figure 60. This optimization is performed on the overall IGCC power-plant with the UNO CO_2 capture system, by taking as starting point the UNO-OptiCase 2.3.

Compared to the starting point UNO-OptiCase 2.3 with 90% CO_2 capture represented by the red arrow on Figure 60, the efficiency of the IGCC power-plant with 90% capture rate is improved from 37.33% to 39.31%. The results for the two objectives are listed below:

Objective 1: maximum efficiency	42.66% efficiency with 70.01% CO_2 captured
Objective 2: maximum capture rate	38.31% efficiency with 97.88% CO_2 captured

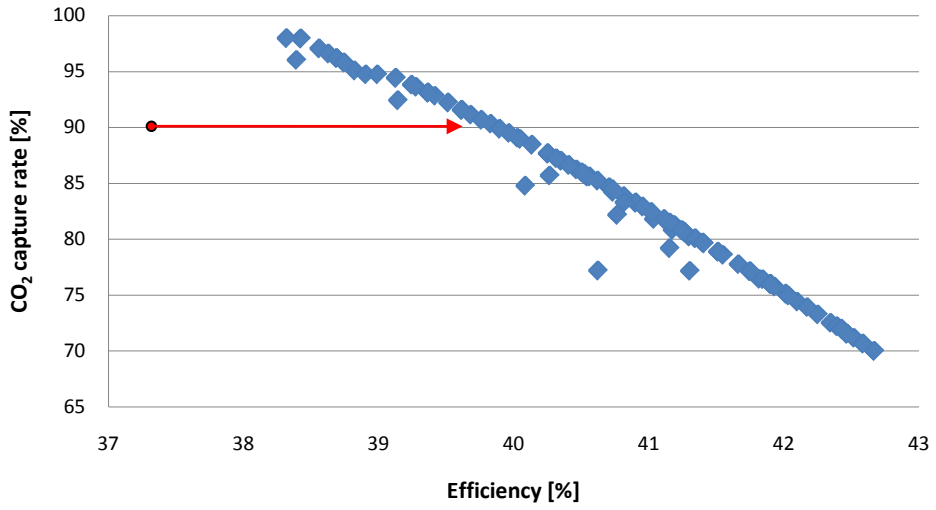

Figure 60: Pareto curve for the overall optimization of the IGCC with UNO CO_2 capture process. The red point presents the starting point with the UNO-OptiCase 2.3.

Optimized case with 90% CO_2 capture: Moo-Case 1 (90%)

The decision variables results for the IGCC with UNO CO_2 capture for 90% capture are presented in Table 27. The power produced and consumed in the IGCC process for the Moo-Case 1 and the starting point UNO-OptiCase 2.3 are illustrated in Figure 61.

Different conclusions can be drawn: the air pre-heat before the combustion chamber in the gas turbine is the key point of the efficiency improvement. Despite the fact that the heating of the air decreases the power produced by the cogeneration Rankine steam network, more electricity is generated in the gas turbine. By heating the air at high temperature, a higher air mass-flow is required to maintain the temperature of 1568 K in the combustion chamber (gas turbine), thus a higher flue gas mass-flow passes through the expander, which produces more electricity.

The syngas composition sent to the gas turbine is optimized by varying the S-C ratio in the WGS unit, the WGS reactor temperatures (both reactors), and the absorber temperature in the UNO CO_2 capture unit. Indeed the water management (amount of water) in the syngas, by varying the inlet absorber temperatures (solvent and syngas), has an important influence on the efficiency.

Remarks

The CO_2 capture rate influences of course the efficiency. Indeed by capturing less CO_2, the syngas sent to the gas turbine has a higher mass-flow, which produces more power in the gas turbine. It reduces also the required electricity power in the CO_2 process (lower solvent mass-flow) and the reboiler heat duty, which increases the steam network power production by the cogeneration Rankine cycle.

The efficiency of the IGCC without and with the MDEA and Selexol CO_2 capture could also be increased by increasing the air pre-heat temperature. But this solution is probably not sustainable from an economic point of view for each case (size of the heat exchanger). For this reason, an economic evaluation should be performed to evaluate the best thermo-economic solution.

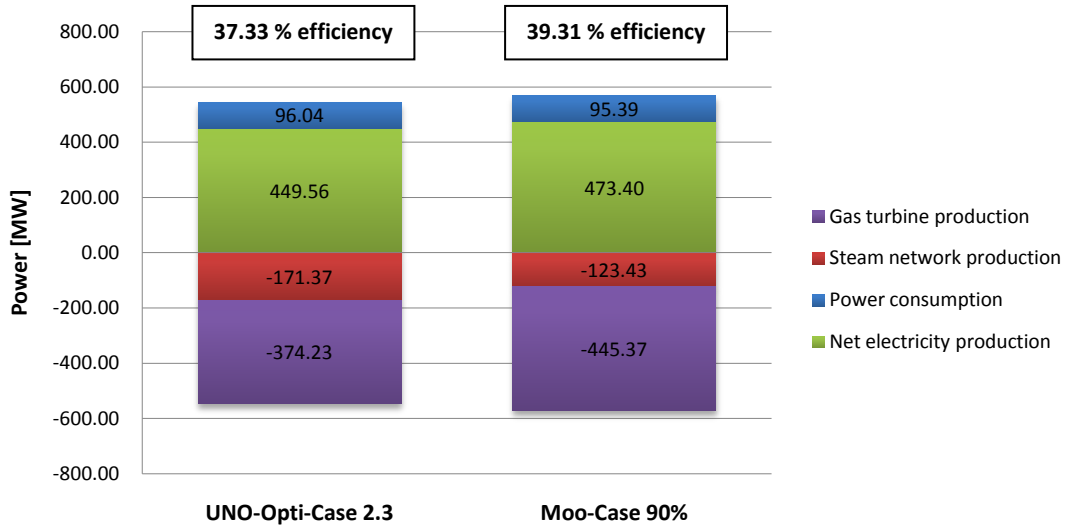

Figure 61: Comparison of the power produced and power consumed in the IGCC power-plant with the UNO CO2 capture for the starting point UNO-OptiCase 2.3 and the Moo-Case 90%

Decision Variables: Gasification	*Moo results Moo-Case 1 90% (90% capture)*	*Starting point UNO-Opticase 2.3 (90% capture)*
Steam preheat [K]	738.9	673
O_2 preheat [K]	687.9	673
Decision variables: WGS		
Steam-Carbon mole ratio [-]	2.3	2
WGS Reactor 1 temperature [K]	726.9	673
WGS Reactor 2 temperature [K]	602.1	527
Decision variables: absorber		
Temperature of the syngas IN [K]	393.1	395.5
Temperature of the solvent IN [K]	455.7	425.1
CO_2 capture rate [%]	90.27	90
Decision variables: Steam network		
Condensation pressure [bar]	0.059	0.053
MP pressure stage [bar]	4.94	4.69
LP pressure stage [bar]	31.27	31.35
Decision variable: Gas turbine		
Fuel pre-heat [K]	648.15	773
Air pre-heat [K]	989.9	-

Table 27: Optimized variable decision results for the IGCC with UNO CO_2 capture for 90% CO_2 capture

Chapter 9

Conclusion

The global electricity demand and the greenhouse gas emissions are constantly increasing. Even if renewable energies are more and more promoted, fossil fuels such as coal still supply a big part of the electricity demand. Pre-combustion CO_2 capture technologies are developed to minimize the impact and reduce the atmospheric greenhouse gas emissions.

This work studies IGCC coal power-plants with three different pre-combustion CO_2 capture technologies such as the chemical absorption with amine MDEA and hot carbonate potassium UNO Mk1 and the physical absorption with Selexol solvent. The goal of the study is to assess the penalty of the pre-combustion CO_2 capture system by comparing the energy efficiency of an IGCC power-plant operating without and with different capture unit. The CO_2 capture unit introduces a penalty in term of energy with the heat required to separate the CO_2 from the solvent and to compress it for the storage.

In this study, an energy integration, also known as Pinch analysis method, is performed. The IGCC power-plant has been modeled with the commercial software Aspen Plus [4]. Based on the results from the mass and energy balances, the energy integration has been performed by solving the heat cascade and optimizing the combined heat and power generation with AMPL [5]; the performance indicators have then been calculated.

Different cases are simulated without CO_2 capture. The best efficiency of 45% is reached by passing through the WGS unit and by cooling down the syngas before the gas turbine until the maximum water content before the expander is reached (15% mole fraction before the expander).

Three different units are compared to capture the CO_2 and the H_2S together. The highest efficiency reached by an IGCC with MDEA CO_2 capture, is 36.39% with 50 wt% MDEA in the solvent and with an absorption temperature of 313 K (313 K for the syngas; 317 K for the solvent). By operating the absorption column at higher temperature, the efficiency is not improved because the CO_2 solubility decreases with increasing temperature. Therefore more solvent is required, the reboiler heat duty increases and the steam network power production by the cogeneration Rankine cycle decreases. The heat required to strip the CO_2 from the MDEA rich solvent is 1.53 GJ/t CO_2.

The best efficiency reached by the IGCC with the Selexol unit is 36.42% and is obtained with an absorber temperature of 313 K. Although the IGCC with the Selexol unit produces more power in the steam network than the IGCC with the MDEA unit, more power is consumed in the process due to the higher solvent volume-flow rate, the flashing desorption until vacuum, and the

absorption of the entire water in the solvent, which counter-balance the reboiler heat duty penalty of the MDEA CO_2 capture cases.

The IGCC with UNO CO_2 capture process operates at higher absorber temperature than the MDEA and Selexol cases and do not require to cool down the syngas and condense the water before the absorber. Despite the fact that the reboiler heat duty is higher compared to the MDEA cases, the mass-flow of the free CO_2 syngas leaving the absorber is higher because the water is not condensed and separated before the absorber. Therefore the IGCC with the UNO CO_2 capture unit yields the highest efficiency with 37.33% by optimizing the inlet temperature of the syngas (395 K) and the solvent (425 K). The efficiency could probably be improved by adding a heat pump to satisfy the reboiler heat stage. The heat required to strip the CO_2 from the UNO rich solvent is 2.3 GJ/t CO_2.

An overall Moo optimization was performed on the IGCC with UNO CO_2 capture by varying different decision variables in the gasification, the WGS, the CO_2 capture, the gas turbine and the steam network units. In this system, the efficiency is increased from 37.33% to 39.31% compared to the starting point. The key point of the efficiency improvement is the air pre-heat before the combustion chamber in the gas turbine. The power produced in the gas turbine is highly increased by recovering the high temperature heat available in the process.

The highest efficiency is probably not the best from an economic point of view. Therefore this study leads to solid foundations in term of energy and opens the door to an economic evaluation. Moreover, another interesting study would be to model the air unit separation in order to send pure oxygen in the gasifier and to have the possibility to send the nitrogen in the gas turbine. The reboiler heat penalty should probably decrease by adding a heat pump between the reboiler heat stages, therefore increasing the overall efficiency.

The pre-combustion capture decreases the efficiency between 7.6% and 8.6%. But IGCC with the pre-combustion CO_2 capture system is promising and constitutes a necessary option to render the electricity production from coal more environmentally sustainable.

Acknowledgments

I would like to thank Prof. Andrew Hoadley and Dr. MER François Maréchal for giving me the opportunity to perform my master project at Monash University in Australia. I am thankful to the CO2CRC and to Trent Harkin for the help during the project. A very special thank to Laurence Tock, who supervised me and answered the multitude of questions I have asked to her.

Special thanks go to my family, my sister Caroline Urech and my girlfriend Charlotte Varenne for their constant support during the project and my studies at EPFL.

Bibliography

[1] IEA. www.iea.org/Textbase/nppdf/free/2009/key_stats_2009.pdf.

[2] B. Metz, O. Davidson, H. d. Coninck, M. Loos, and L. Meyer), "IPCC special report: Carbon Dioxide capture and storange," 2005.

[3] M. Gassner and F. Maréchal, "Methodology for the optimal thermo-economic, multi-objectives design of thermochemical fuel production from biomass," *Computers and Chemical Engineering*, vol. 33, pp. 769-781, 2008.

[4] Aspen, "www.aspentech.com/products/aspen-plus.aspx".

[5] AMPL, "www.ampl.com".

[6] LENI. leni.epfl.ch.

[7] DOE/NELT, "Cost and Performance Baseline for Fossil Energy: volume 1: Bitumous Coal and Natural Gas to Electricity," 1281, 2007.

[8] M. C.Bohm, H. Herzog, J. E.Parsons, and R. Sekar, "Capture-ready coal plants- Option, technologies and economics," vol. 1, no. 1, 2007.

[9] L. J.shadle and D. A.berry, "Coal gasification," 2002.

[10] H. Hiller and R. Reimert, "Gas production," 2007.

[11] (2012) majarimagazine.com/2008/06/igcc-major-igcc-sections-2/.

[12] A. Bonsu, "Impact of CO2 Capture On Transport Gasifier IGCC Power Plant".

[13] Haldor Topsoe, "Sulphur resistant/sour water-gas shift catalyst".

[14] IEA, "Potential for Improvement in Gasification Combined Cycle Power Generation with CO2 capture," 2003.

[15] O. I. Wolfgang Rueltinger, "Water Gas Shift Reaction (WGSR)".

[16] D. A. Qader and M. B. Hooper, "Pre-Combustion Carbon Dioxide Capture Technologies for Brown Coal Power Generation," 2011.

[17] M. Bolhar-Nordenkampf, A. Friedl, U. Koss, and T. Tork, "Modelling selective H2S absorption and desorption in an aqueous MDEA-solution using a rate-based non-equilibrium approach," *ELSEVIER*, vol. 43, pp. 70-715, 2004.

[18] C. Cormos, "Evaluation of energy integration aspects for IGCC-based hydrogen and electricity co-production with carbon capture and storag," vol. 35, no. 14, 2010.

[19] M. S. Zare Aliabad H., "Removal of CO2 and H2S using Aqueous Alkanolamine Solusions," *World Academy of Science, Engineering and Technology*, 2009.

[20] C. Chen, "A Technical and Economic Assessment of CO2 Capture Technology for IGCC Power Plants," 2005.

[21] R. L. S. R. W Bucklin, "Comparison of Physical Solvents Used for Gas Precessing," 1984.

[22] E. Keskes, C. S. adjiman, A. Galindo, and G. Jackson, "A physical absorption process for the capture of CO2 from CO2-rich natural gas streams".

[23] B. Burr and L. Lyddon, "A comparaison of physical solvents for acid gas removal," *Bryan Research and Engineering*, 2008.

[24] A. Kohl and R. Nielsen, "Gas Purfication".

[25] A. Kohl and R. Nielsen, "Gas Purfication: Alkaline Salt Solutions for Acid Gas Removal, Chapter 5".

[26] M. Gassner, "Energy Integration and thermo-econmoic Evalutation of a Process converting Wood to Methane," 2007.

[27] T. j.Flacke, A. Hoadley, D. J.Brennan, and S. E.Sinclair, "The sustainability of clean coal technology: IGCC with/without CCS," vol. 89, no. 41-52, 2011.

[28] F.Marechal, F.Palazzi, J.Godat, and D.Favrat, "Thermo-Economic Modelling and Optimisation of Fuel Cell system," *Fuell Cell*, 2004.

[29] Aspentech, "Rate-Base Model of the CO2 Capture Process by MDEA using Aspen Plus," 2006.

[30] AspenTech, "Aspen Plus Model of the CO2 Capture Process by DEPG".

[31] R. Doctor, J. Molburg, P. Thimmapuram, G. Berry, and C. Livengood, "Gasification Combined Cycle: Carbon Dioxide Recovery, Transport, and Disposal," *Energy System Divison, Argonne National Laboratory*, 1994.

[32] K. Endo, Q. Nguyen, and S. Kentish, "The effect of boric acid on the vapour liquid equilibrium of aqueous potassium carbonate," 2011.

[33] T. Laurence, "Thermo-Economic Evaluation of the Production of Liquid Fuels from Biomass," 2009.

[34] IPCC, "IPCC Special Report on Carbon Dioxide Capture and Storage. Prepared by Working

Group III of the Intergovernmental Panel on Climate Change," 2005.

[35] G. Göttlicher, "The Energetics of Carbon Dioxide Capture in Power Plant," 2004.

[36] F. Marechal, *Advanced energetic: Process integration techniques for improving the energy efficiency of industrial process*. Ecole polytechnique Fédérale de Lausanne, LENI.

[37] NETL. http://www.netl.doe.gov/technologies/coalpower/gasification/gasifipedia/7-advantages/7-4-1-2_sulfur.html.

[38] T. Wall, "Combustion processes for carbon capture," *Proceedings of the COmbustion Institute*, 2007.

[39] F.Emun, M.Gadalla, T.Majozi, and D.Boer, "Integrated gasification combined cycle (IGCC) Process simulation and optimization," vol. 34, no. 3, 2009.

[40] J. Gusca, I. Naroynova, and D. Blumberga, "Modelling of a carbon capture and storage system for the Latvian electricity sector," *Riga Technical University*.

[41] L.Zheng and E. Furinsky, "Comparison of Shell, Texaco, BGL and KRW gasifiers as part of IGCC plant computer simulations," vol. 46, 2004.

[42] Q.Ni and A.Williams, "A simulation study on the performance of an entrained-flow coal gasifier," 1994.

[43] C.Descamps, C.Bouallou, and M.Kanniche, "Efficiency of an Integrated Gasification Combined Cycle (IGCC) power plant including CO2 removal," vol. 33, 2006.

[44] D. Fiaschi and L. Lombardi, "Integrated Gasifier combined cylce plant with integrated CO2-H2s removal," vol. 5, no. 1, 2002.

[45] G. Martin and M. Francois, "Thermo-economic Model of a Process converting Wood to Methane," 2006.

[46] "European Technology Platform for Zero Emission Fossil Fuel Power Plant: The Costs of CO2 Capture".

Annex I: WGS model complement

The WGS reactors are modeled as described in Figure 62. ''The heat generated by the reaction is taken into account by exchanging Q_{re} with the outlet stream. This reaches the temperature T_{int}, accounting for the reaction products heat requirements inside the reactor and, in fact, contributes to the definition of the temperature profile" [28]. "The resulting composite curve approaches the real temperature profile given by the dashed line and allows for a possible energy saving that would require a more integrated reactor design" [28].

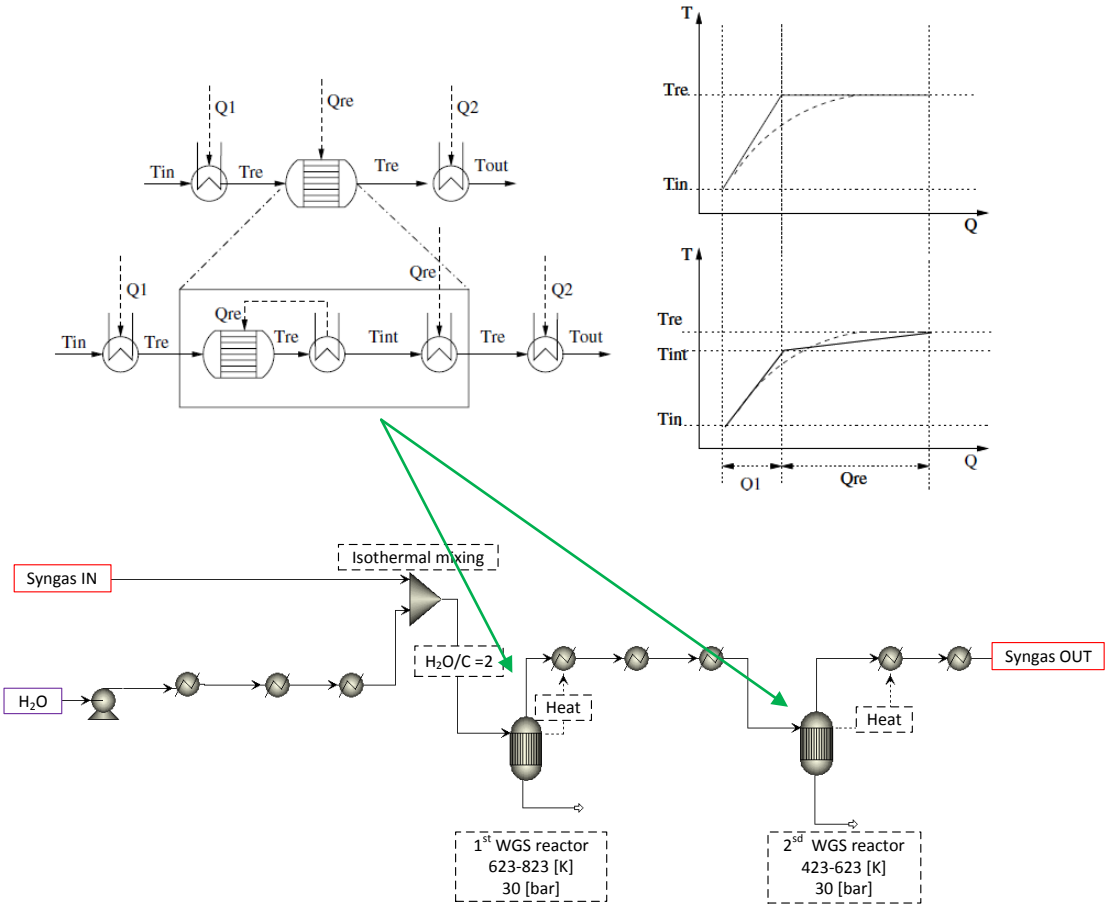

Figure 62: WGS reactor model

Annex II: MDEA absorber and stripper model

This part explains how the MDEA absorber and the stripper are modeled. The same approach is applied to the Selexol absorber and the UNO absorber and stripper.

Absorber model

Due to a high syngas mass-flow coming from the WGS unit, a ‘‘packing model’’ is more suitable than “trays model” for high liquid rate. To get the model to converge, an estimated temperature has to be established at the top of the tray. The differences between trays and packing are illustrated in Figure 63.

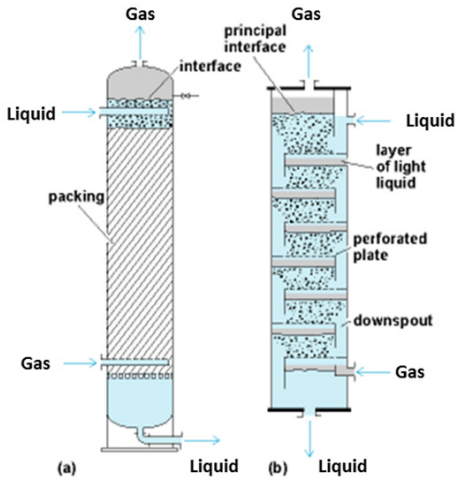

Figure 63: (a) Packed column design; (b) Tray column design

To determine the adequate number of stages for the absorber, the CO_2 vapor mole fraction and the HCO_3^- liquid fraction are calculated for each stage and allow to determine the convergence stage. Figure 65 illustrates the absorber discretization.

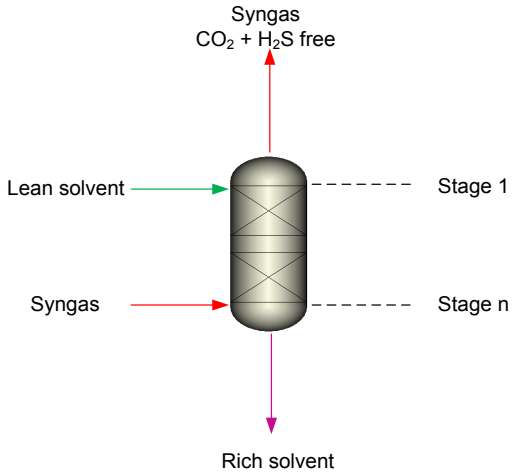

Figure 64: Absorber column with the first stage at the top.

As shown in Figure 65, the absorption process is finished after 11-12 stages but, in order to avoid unusual interface heat transfer profile, 14 stages are required.

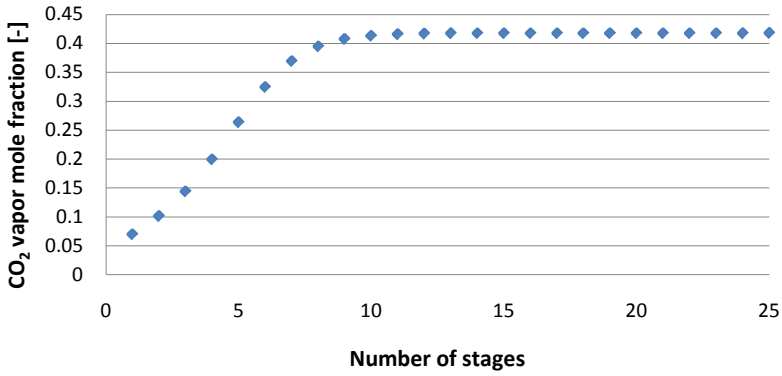

Figure 65: CO_2 vapor mole fraction absorption profile with 25 stages for each stage of the MDEA column.

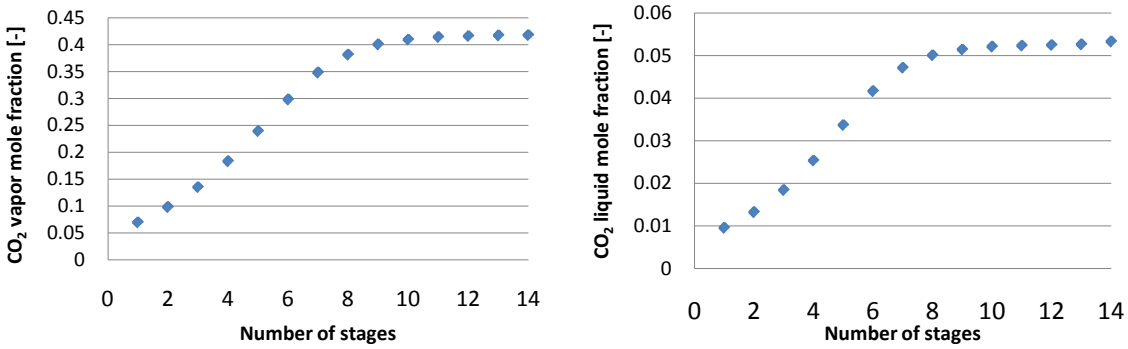

Figure 66: Absorption profile for CO_2 vapor mole fraction and HCO_3^- liquid mole fraction with 14 stages in the MDEA absorber

The dimensions of the column such as the diameter are adjusted to have a flooding around 80%. The flooding point, especially for the packing, is dominated mostly by the diameter. The main design specifications for the MDEA absorber are listed in Table 28.

MDEA absorber design parameters	
Type of calculation	Rate-based
Type of column	Packing
Number of stages	14
Diameter [m]	5.5
Height of the absorber column [m]	14
CO_2 lean loading [mole CO_2/mole amine]	0.1
Pressure [bar]	2

Table 28: MDEA absorber design parameters

Stripper model

The rate-based calculation is more accurate as it takes into account the reaction kinetics. However, at the temperature of the stripper, the kinetics do not have a large influence. For this reason, the equilibrium method constiutes a good approximation.

The same approach is used to determine the number of stages required to strip the CO_2 and the H_2S from the solvent. As presented in Figure 68, after 10 stages the CO_2 is separated from the rich solvent. The diameter is calculated by fixing the flooding at 80%. As presented in Figure 68, the number of stages required to strip the CO_2 and the H_2S is 10.

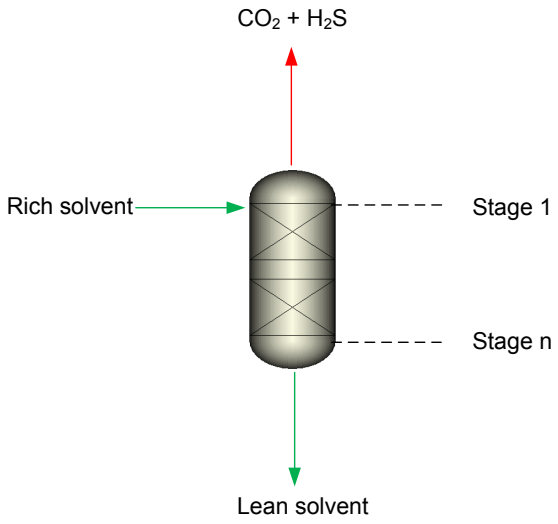

Figure 67: stripper configuration

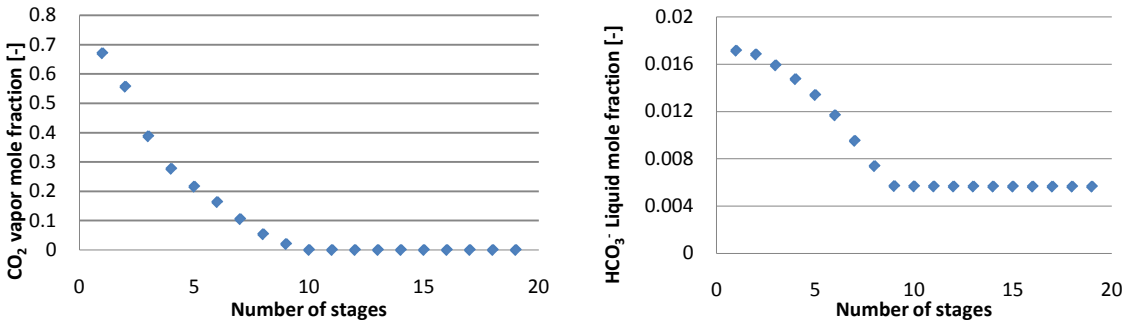

Figure 68: Desorption profile for the CO_2 vapor mole fraction and HCO_3^- liquid mole fraction profile for 20 stages in the MDEA stripper

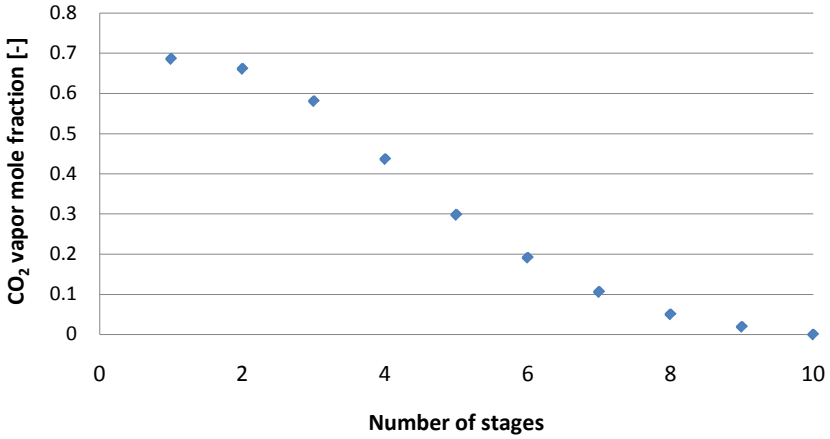

Figure 69: Desorption profile for the CO_2 vapor mole fraction for 10 stages in the MDEA stripper

An important parameter is the CO_2 loading, which leaves the stripper with the regenerated solvent. Sensitivity analyses are performed to determine the optimal CO_2 loading to have the lowest reboiler heat duty. As illustrated in Figure 70, the ideal CO_2 loading is 0.1 mole CO_2/mole amine. The CO_2 loading at the outlet of the stripper is described in eq. 38:

$$mole\ stripper\ ratio = \frac{CO_2}{MDEA} = \frac{HCO_3^-}{MDEA + MDEAH^+} \qquad \text{(eq. 38)}$$

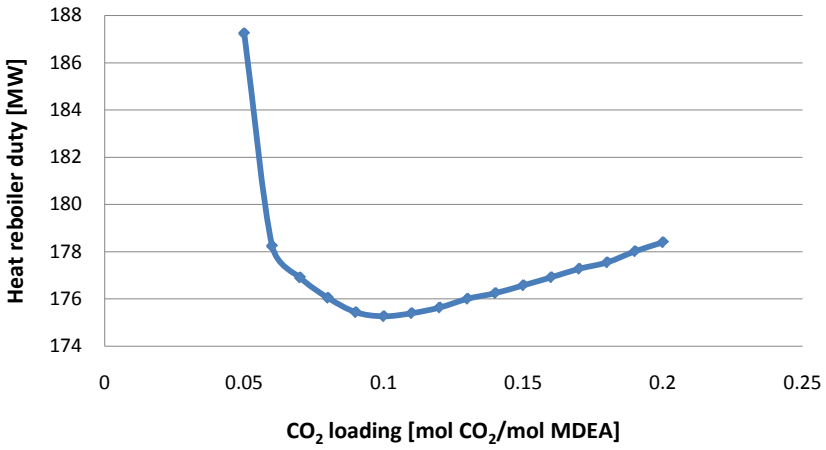

Figure 70: Sensitivity on the CO_2 loading in the stripper to determine the lowest MDEA reboiler heat duty

MDEA stripper design parameters	
Type of calculation	Equilibrium
Type of column	Packing
Number of stages	10
Diameter [m]	8.1
Height of the stripper column [m]	15
CO_2 lean loading [mole CO_2/mole amine]	0.1
Pressure [bar]	2

Table 29: MDEA stripper design parameters

Solvent with 33%- 40%-50% wt. MDEA

The percentage of MDEA in the lean solvent for CO_2 capture has an influence on the reboiler heat duty. For this reason, different MDEA wt. fractions in aqueous solution are compared. The literature gives a possible operating range between 30-50% wt. of MDEA. But with different MDEA loading, the design parameters of the absorber and the stripper have to be adapted. The same approach presented with the first configuration (33 wt. % MDEA) is used to design the two other absorbers as presented in Table 30 and Table 31.

MDEA absorber design parameters	*33% MDEA*	*40% MDEA*	*50% MDEA*
Type of calculation	Rate-based	Rate-based	Rate-based
Type of column	Packing	Packing	Packing
Number of stages	14	14	14
Diameter [m]	5.5	5.85	7.25
Height of the absorber column [m]	14	14	14
CO_2 lean loading [mole CO_2/mole amine]	0.1	0.09	0.08
Pressure [bar]	2	2	2

Table 30: MDEA absorber design parameters for different MDEA wt. fraction loading

MDEA stripper design parameters	*33% MDEA*	*40% MDEA*	*50% MDEA*
Type of calculation	Equilibrium	Equilibrium	Equilibrium
Type of column	Packing	Packing	Packing
Number of stages	10	10	10
Diameter [m]	8.1	7.75	7.3
Height of the stripper column [m]	10	10	10
CO_2 lean loading [mole CO_2/mole amine]	0.1	0.09	0.08
Pressure [bar]	2	2	2

Table 31: MDEA stripper design parameters for different MDEA wt. fraction loading

Annex III: UNO variant

Some different configurations were assessed to improve the efficiency of the UNO process. One configuration was to add two flash stages before the stripper in order to recover one part of the CO_2 in the vapor fraction at higher pressure, thus reducing the reboiler heat duty and the required compression. Unfortunately the improvement of the efficiency was less than 0.1 %. Moreover this configuration induces more costs because of the valve, the condenser and the compressor.

Another configuration was to reheat the rich solvent before the first depressurization stage as can be observed on Figure 71. The efficiency was lower than for the base case.

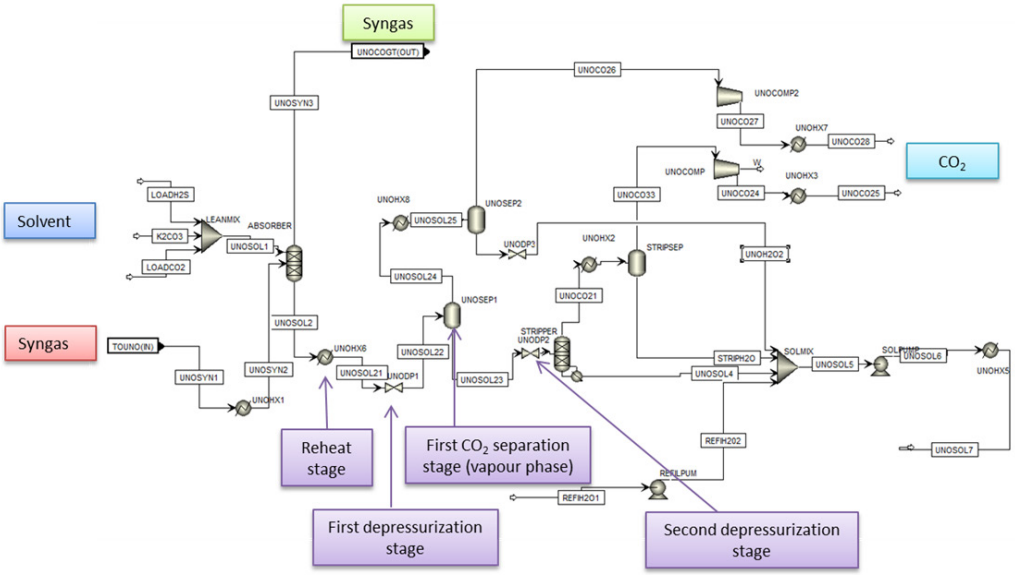

Figure 71: Configuration with two depressurization stage and reheat before the first depressurization in the UNO CO_2 capture process

Annex IV: IGCC with MDEA CO_2 capture: streams extraction

Figure 72 presents the stream extraction for the MDEA-Case 3.1.

Parent	Name	Type	Tin	Tout	DTmin_2	Load
gasif	ghx1	qt	25.639	254.105	4.000	4585.890
gasif	ghx2	qt	254.105	254.106	2.000	7247.130
gasif	ghx3	qt	254.105	400.150	8.000	1405.600
gasif	ghx4	qt	550.564	400.150	8.000	6300.990
recyquench	qhx1	qt	901.350	400.150	8.000	238516.000
recyquench	qhx2	qt	400.827	370.150	8.000	9709.160
wgs	wgshx1	qt	25.486	233.306	4.000	69562.600
wgs	wgshx2	qt	233.306	233.307	2.000	130411.000
wgs	wgshx3	qt	233.306	400.150	8.000	25936.000
wgs	wgshxin2	qt	640.716	397.022	8.000	75146.600
wgs	wgshhx4	qt	397.022	254.000	8.000	42422.600
mdea	mdeahx1	qt	277.374	44.000	8.000	160338.284
mdea	mdeahx2	qt	84.764	107.000	8.000	119393.603
mdea	mdeahx3	qt	125.595	44.000	8.000	242881.491
mdea	mdeahx5	qt	86.025	69.219	8.000	17011.489
mdea	mdeahx6	qt	69.219	40.000	8.000	17011.457
mdea	mdeahx7	qt	186.716	40.000	8.000	16794.417
mdea	mdeahx8	qt	138.549	40.000	8.000	10111.672
mdea	mdeahx9	qt	103.031	40.000	8.000	7720.104
mdea	mdeahx10	qt	86.707	40.000	8.000	8051.982
mdea	mdeahx11	qt	41.259	44.000	8.000	16.232
mdea	reboiler	qt	126.021	126.022	8.000	145091.530
gt	gthx4	qt	53.363	53.362	8.000	0.730
gt	gthx1	qt	53.738	500.150	8.000	47062.914
gt	gthx5	qt	570.018	570.017	8.000	0.000
gt	gthx3	qt	502.567	40.150	8.000	481614.888

Figure 72: IGCC with MDEA CO_2 capture stream description (temperature in °C)

Annex V: IGCC with Selexol CO_2 capture: streams extraction

Figure 73 presents the stream extraction for the MDEA-Case 3.1.

Parent	Name	Type	Tin	Tout	DTmin_2	Load
gasif	ghx1	qt	25.639	254.105	4.000	4585.890
gasif	ghx2	qt	254.105	254.106	2.000	7247.130
gasif	ghx3	qt	254.105	400.150	8.000	1405.600
gasif	ghx4	qt	550.564	400.150	8.000	6300.990
recyquench	qhx1	qt	901.350	400.150	8.000	238516.000
recyquench	qhx2	qt	400.827	370.150	8.000	9709.160
wgs	wgshx1	qt	25.486	233.306	4.000	69562.600
wgs	wgshx2	qt	233.306	233.307	2.000	130411.000
wgs	wgshx3	qt	233.306	400.150	8.000	25936.000
wgs	wgshxin2	qt	640.716	397.022	8.000	75146.600
wgs	wgshhx4	qt	397.022	254.000	8.000	42422.600
selexol	selhx1	qt	277.374	40.000	8.000	159986.978
selexol	selhx2	qt	93.003	40.000	8.000	515.465
selexol	selhx3	qt	25.582	41.078	8.000	0.124
selexol	selhx4	qt	41.078	40.000	8.000	6128.298
selexol	selhx5	qt	41.302	40.000	8.000	95.354
selexol	selhx6	qt	214.504	40.000	8.000	2423.045
selexol	selhx7	qt	185.783	40.000	8.000	13748.974
selexol	selhx8	qt	138.548	40.000	8.000	10247.373
selexol	selhx9	qt	103.042	40.000	8.000	7725.688
selexol	selhx10	qt	86.413	40.000	8.000	12721.948
gt	gthx1	qt	40.883	500.150	8.000	47559.856
gt	gthx5	qt	571.479	571.480	8.000	0.021
gt	gthx3	qt	509.533	40.150	8.000	474451.703

Figure 73: IGCC with Selexol CO_2 capture stream description (temperature in °C)

Annex VI: IGCC with UNO CO_2 capture: streams extraction

Figure 74 presents the stream extraction for the MDEA-Case 3.1.

Parent	Name	Type	Tin	Tout	DTmin_2	Load
gasif	GHX1	qt	25.639	254.105	4.000	4585.892
gasif	GHX2	qt	254.105	254.106	2.000	7247.135
gasif	GHX3	qt	254.105	400.150	8.000	1405.597
gasif	GHX4	qt	550.564	400.150	8.000	6300.985
recyquench	QHX1	qt	901.347	400.150	8.000	238516.301
recyquench	QHX2	qt	400.827	370.150	8.000	9709.161
wgs	WGSHX1	qt	25.486	233.306	4.000	69562.649
wgs	WGSHX2	qt	233.306	233.307	2.000	130411.318
wgs	WGSHX3	qt	233.306	400.150	8.000	25935.961
wgs	WGSHXIN2	qt	640.716	397.022	8.000	75146.575
wgs	WGSHX4	qt	397.022	254.000	8.000	42422.650
uno	UNOHX1	qt	277.374	122.594	8.000	112800.899
uno	UNOHX2	qt	129.399	124.409	8.000	1656.982
uno	UNOHXC1	qt	124.409	115.437	8.000	161582.630
uno	UNOHXC2	qt	115.437	40.000	8.000	161582.682
uno	UNOHXH2O	qt	40.156	141.126	4.000	45325.648
uno	UNOHXREF	qt	25.282	141.126	4.000	0.000
uno	UNOHX5	qt	141.151	155.422	4.000	66532.625
uno	UNOHX3	qt	146.068	40.000	8.000	11457.531
uno	UNOHX6	qt	137.797	40.000	8.000	10029.471
uno	UNOHX7	qt	102.634	40.000	8.000	7642.286
uno	UNOHX8	qt	86.521	40.000	8.000	8075.316
uno	REGOILER	qt	139.680	139.681	4.000	216266.663
gt	GTHX4	qt	163.531	163.530	8.000	318.115
gt	GTHX1	qt	163.993	500.150	8.000	46494.235
gt	GTHX5	qt	570.319	570.318	8.000	0.000
gt	GTHX3	qt	514.029	40.000	8.000	543640.719

Figure 74: IGCC with UNO CO_2 capture stream description (temperature in °C)

List of Figures

List of Tables